

FINAL REPORT

GTI Project Number 20754

Validation for Flaw Acceptance of Mechanical Damage to Low-Stress Natural Gas Pipelines

Submitted to:

Operations Technology Development, NFP

For:

U. S. Department of Transportation
Pipeline and Hazardous Materials Safety Administration
Office of Pipeline Safety
DOT Project No.: 257

Contract Number: DTPH56-08-T-000023

By:

Khalid Farrag, Ph.D., P.E. Gas Technology Institute Khalid.farrag@gastechnology.org 847-768-0803

and,

Robert Francini, Kiefner & Associates, Inc. www.kiefner.com 614-888-8220

Gas Technology Institute

1700 S. Mount Prospect Rd. Des Plaines, Illinois 60018 www.gastechnology.org

Legal Notice

This information was prepared by the Gas Technology Institute (GTI) for The Operations Technology Development (OTD) project sponsored by the Department of Transportation-Office of Pipeline Safety (DOT/PHMSA) Contract Number: DPTH56-08-T-000022.

Neither GTI, the members of OTD, DOT-PHMSA, nor any person acting on behalf of any of them:

- a. Makes any warranty or representation, express or implied with respect to the accuracy, completeness, or usefulness of the information contained in this report, or that the use of any information, apparatus, method, or process disclosed in this report may not infringe privately-owned rights. Inasmuch as this project is experimental in nature, the technical information, results, or conclusions cannot be predicted. Conclusions and analysis of results by GTI represent GTI's opinion based on inferences from measurements and empirical relationships, which inferences and assumptions are not infallible, and with respect to which competent specialists may differ.
- b. Assumes any liability with respect to the use of, or for any and all damages resulting from the use of, any information, apparatus, method, or process disclosed in this report; any other use of, or reliance on, this report by any third party is at the third party's sole risk.
- c. The results within this report relate only to the items tested.

Table of Contents

	Page
Table of Contents	iii
Table of Figures	V
List of Tables	vii
Executive Summary	1
Introduction	3
Current Regulations and Codes for the Repair of Pipeline Defects	4
Pipe and Operation Characteristics of Natural Gas Pipelines	8
Past Experiments on Pipelines with Mechanical Damage	18
Method 1 - Machined Notch Followed by Indentation at Zero Pressure	18
Method 2 - Indentation Followed by Machined Notching at Zero Pressure	19
Method 3 - Machined Notch Followed by Indentation at Pressure	20
Method 4 - Creating a Dent and Gouge Simultaneously in a Pressurized Pipe	20
Layout of Current Validation Experiment	21
Development of the Testing Equipment and Procedure	22
A) Dent-Gouge Loading Machine	22
B) Validation Test Matrix	26
C) Dent-Gouge Testing Procedure	28
Hydrostatic Pressure Tests on Mechanically-Damaged Pipes	35
Numerical Modeling of Pipe Damage	49
Introduction	49
Comparison of Test Results with EPRG and Plastic Collapse Models	50
Conclusion	58
Implementation of Repair Options in the Flaw Acceptance Criteria Program	60
Introduction	60
Program Data Entry	60
Evaluation of Wrinkle Bends	70

References	71
Attachment A - Results of the testing Program	72
Attachment B - Models and Experimental Studies of the Effect of Mechanical Damage	77
Attachment C - Evaluation of Wrinkle Bends	117

Table of Figures

	Page
Figure 1 - Construction Requirements of damaged pipes in 49 CFR Part 192-Subpart G	5
Figure 2 - Repair requirements of damaged pipes in 49 CFR Part 192-Subpart M	6
Figure 3 - Repair requirements of damaged pipes in ASME B31.8	7
Figure 4 - Typical indentation process associated with methods 1 and 3	19
Figure 5 - Typical indenters and re-rounding associated with methods 1 and 3	19
Figure 6 - The large-scale dent-gouge machine with a 16-inch diameter pipe	22
Figure 7 - The EPRG simplified model criterion	23
Figure 8 - The hydraulic loading system for dent-gouge applications	25
Figure 9 - Data monitoring of pipe deformation during damage application	25
Figure 10 - Results of the earlier OTD study to verify EPRG Simplified Model	26
Figure 11 - Welding of pipe caps in preparation of the pipe test sample	29
Figure 12 - Schematic of the pipe test specimen	29
Figure 13 - Shape of the applied gouge on the pipe specimen	30
Figure 14 - Application of controlled gouge on the pipe specimen	30
Figure 15 - Schematic of the rounded disc for dent application	30
Figure 16 - Application of longitudinal dent along the pipe specimen	31
Figure 17 - Measurement of dent at zero pressure (H _o)	32
Figure 18 - Measurements of dents in the pipe during and after loading	33
Figure 19 - Grinding the pipe surface for the inspection of cracks	33
Figure 20 - Inspection of cracks using magnetic particle device	34
Figure 21 - View of pipe at the completion of the burst test	34
Figure 22 - View of the Large-scale dent-gouge machine	35
Figure 23 - Applied pressure and horizontal displacement during denting	36
Figure 24 - Pipe pressure during burst tests of the 16-inch pipes in Set-A	37
Figure 25 - Pipe pressure during burst tests of the 8-inch pipes in Set-A	37
Figure 26 - View of the 8-inch pipe after burst test	38
Figure 27 - View of the 16-inch pipe after burst test	38
Figure 28 - Indentation of the 8-inch pine in Set-B	39

Figure 29 - Indentation of the 16-inch pipe in Set-B	40
Figure 30 - Pressure tests on the gouged pipes in Set-B	40
Figure 31 - Pressure tests No. 3 on the 8-inch pipe in Set-C	41
Figure 32 - View of the Test-3 8-inch pipe after Testing	42
Figure 33 - View of the Test-4 16-inch pipe after testing	42
Figure 34 - Testing parameters for test Set-D	43
Figure 35 - Results of Test 1 with 90° gouge and various dents	44
Figure 36 - Results of Test 2 with 45° gouge angle	44
Figure 37 - Results of Test 3 with rounded gouge and various dents	45
Figure 38 - Results of Test 4 with 90° gouge and various dents	45
Figure 39 - View of the backhoe tooth used in Set E	46
Figure 40 - View of the damage caused by the backhoe tooth application	47
Figure 41 - Results of pressure tests of Set F	48
Figure 42 - View of the pipe at the completion of pressure test 3	48
Figure 43 - Comparison of test results with EPRG simplified failure model	57
Figure 44 - Comparison of advanced EPRG failure prediction with actual failure pressure.	59
Figure 45 - Comparison of plastic collapse prediction with actual failure pressure	59
Figure 46 - Data entry page of the program	61
Figure 47 - Output example with operating stress larger than 40% SMYS	63
Figure 48 - Output example of damage passing EPRG criteria and not in HCA area	64
Figure 49 - Output example of damage passing EPRG criteria and in HCA area	65
Figure 50 - Output example of damage failing EPRG criteria	66
Figure 51 - Procedure for corrosion repair criteria, after ASME B31G (14)	68
Figure 52 - Example of program output of corrosion damage evaluation	69

List of Tables

F	Page
Table 1 - Nominal diameters of the steel transmission pipelines per utility	9
Table 2 - Wall thicknesses of steel transmission pipelines per utility	9
Table 3 - Range of MAOP (Maximum Allowable Operating Pressure) of steel transmission pipelines per utility	10
Table 4 - Percentage of SMYS of the transmission lines per utility	10
Table 5 - Miles of steel "transmission" rated pipeline per utility	11
Table 6 - Grade of transmission [pipes per utiity	11
Table 7 - Approximately miles of pipeline operating at various levels of %SMYS	12
Table 8 - Percentage of seamless transmission pipes per utility	13
Table 9 - Encountered damage in steel pipelines per utility	13
Table 10 - Causes of damage to steel pipelines per utility	14
Table 11 - Current procedures for dealing with damaged steel pipelines during installation, before they are put into operation	14
Table 12 - Determining if the damage is "severe enough" to warrant replacement, per utility	15
Table 13 - Current procedures for dealing with damaged steel pipelines	16
Table 14 - Average cost to replace or repair a damaged steel pipeline?	17
Table 15 - Range of pressures for hoop stresses as % SMYS in the testing program	26
Table 16 - Range of values of the testing parameters	28
Table 17 - Length of Gouge Needed for Validation Testing	31
Table 18 - The pipe and damage parameters of the test sets	35
Table 19 - Testing parameters and results of Set-A	36
Table 20 - Testing parameters and results of Set-B	39
Table 21 - Testing parameters and results of Set-C	41
Table 22 - Testing parameters and results of Set-D	43
Table 23 - Testing parameters and results of Set-E	46
Table 24 - Testing parameters and results of Set-F	47
Table 25 - Tensile test results for test pipe samples	51
Table 26 - Charpy V-notch results for test pipe samples	51
Table 27 - Results of chemical testing for test pipe samples	52

Table 28 - Comparison of pressure test results s with EPRG advanced and Plastic collapse	
models	.55
Table 29 - Comparison of final burst pressure with SMYS	.56

Executive Summary

The objective of the research project is to provide pipeline operators with a decision-making tool regarding the repair options to pipeline's mechanical damage. The research project addresses the gas pipelines operating at stress levels below 40% of their Specified Minimum Yield Strength (SMYS).

The testing program evaluated a wide range of pipes and damage characteristics using a large-scale dent-gouge machine. The tests evaluated the effects of various sizes and shapes of dents and gouges, pipe stiffness (pipe diameters/wall thickness), and pipe grades. Third-party damage was also simulated by applying a backhoe tooth on the pressurized pipes.

A review was performed on the numerical models used to characterize failures due to mechanical damage. A comparative review of the various assumptions and analysis of these models was performed and the results of the tests were implemented in the European Pipeline Research Group (EPRG) Simplified Model. The simple EPRG model was conservative and the test results showed failures at higher stresses than the ones predicted by the model. Based on the test results, the EPRG simplified model can be conservatively used to evaluate mechanical damage in low MAOP pipelines.

A web-based computer program was developed to provide a simplified procedure for pipeline operators to determine the criteria for repair needs of damaged pipelines operating below 40% SMYS. The program implemented the EPRG simple model for mechanical damages which do not cause leak or rupture of the pipeline. The program also evaluated the repair criteria for damages due to external corrosion based on the ASME B31G manual for determining the remaining strength of corroded pipelines.

An investigation of the effect of wrinkle bends on pipe stresses was performed in Task 5 of the research project. This work provides a state-of-the-art evaluation of the effects of wrinkles on buckles and bends in pressurized gas lines. The results of the investigation of the wrinkle bends incident records suggest that the vast majority of wrinkle bends do not pose a threat to pipeline safety under normal circumstances. The challenge is to use the information available to the operator to identify the small proportion of wrinkle bend installations that may pose a threat. The investigation showed that wrinkle bends with depths up to 2.5 percent of the diameter and aspect ratios (height of wrinkle over the wave length of the wrinkle) less than 0.13 are acceptable provided the following threats are not present:

- Aggressive longitudinal stress cycling of the line,
- Ground movement, i.e. mine subsidence or landslides,
- Corrosion, and stress corrosion cracking.

If it is necessary to expose a wrinkle bend or the pipe in the vicinity of a wrinkle bend, care should be taken to return the pipe to its original condition of support, soil consolidation, and restraint of the bend. Composite reinforcement of the bend shows promise for increasing the fatigue resistance of wrinkle bends.

The results of the project should provide the operators with guidelines of dealing with mechanical damages at pipelines operating at stress levels below 40% SMYS; thus increasing the safety of the operation at these stress levels.

Introduction

Mechanical damage to transmission pipelines (i.e., dents and gouges) caused by excavating equipment is one of the most common threats to pipeline integrity. The severity of these damages is affected by pipe type, grade, and operating conditions. The impact of dents and gouges on the pipe surface may not be obvious based on visual inspection alone and the damage may have various levels of impact on pressurized pipeline.

This report presents the development of a procedure for testing and evaluating the mechanical damages that affect the integrity of low pressure pipelines due to excavation impacts. The report consists of the following tasks:

- Present current regulations and codes which address the management and repair of the defects caused by mechanical damage to pipelines operating at pressures below 40% SMYS.
- 2. Survey utilities to define the specific ranges of pipeline sizes, stresses, and types of damages that are commonly encountered to help focus the testing program on current gas pipelines operating conditions and needs.
- 3. Review previous testing programs to define the testing parameters that affect the severity of the damage on the pipes.
- 4. Develop a large-scale dent-gouge testing equipment and procedure to closely simulate the application of dents and gouges on pressurized pipelines in the field.
- 5. Perform a testing program to evaluate the wide range of pipe and damage characteristics.
- Review the numerical models used to characterize failures due to mechanical damage.
 Implement the test results in the European Pipeline Research Group (EPRG) Simplified Model.
- 7. Develop guidelines for field evaluation of the severity of mechanical damage to assist operators in identifying the repair needs based on pipe characteristics, operating conditions, and the severity of damage.
- 8. Investigate the effect of wrinkle bends on pressurized gas lines. The investigation includes a review of incident records, laboratory tests, and numerical models used to predict failures in pressurized pipes with wrinkle bends.

Chapter 1

Current Regulations and Codes for the Repair of Pipeline Defects

Specific guidance for the repair of defects in non-leaking gas pipelines are provided in the following CFR 49 Part 192 requirements:

- CFR 49 Part 192-Subpart G: In this Subpart, Section 192.309 addresses the repair requirements for damaged pipe sections during construction. Figure 1 shows a flow chart of the requirements under this section.
- CFR 49 Part 192-Subpart M: Section 192.713 in this Subpart provides the maintenance requirements for non-leaking defects on steel pipelines. Figure 2 shows a flow chart of the repair options under this section.
- CFR 49 Part 192-Subpart O: In this Subpart, Section 192.903 addresses transmission pipelines which are subjected to the integrity assessment requirements in High Consequence Areas (HCA). The code assigns scheduling requirements for the repair of the damaged pipes according to the level of damage.

The ASME B31.8 standard (1) also provides various repair options to injurious dents and mechanical damages to pipelines as shown in Figure 3.

As will be seen in the following chapter, a significant number of the transmission lines owned by the gas distribution companies operate at stress levels at or below 40% SMYS. Additionally, with the new requirements for the distribution integrity management (DIM), there is a need to address the repair options for mechanical flaws of pipelines operating at and below 20% SMYS.

If flaws are discovered in pipelines that operate at these low stresses, pipeline operation and maintenance personnel need procedures to characterize the damages and identify the ones that require repair or need to be replaced for safe operation at these stress levels.

The severity of mechanical damages is affected by pipe type, grade, and operating conditions. The impact of dents or gouges on the pipe surface may not be obvious based on visual inspection alone and the damage may have different impact on low pressure pipeline. Since a large number of tests are needed to address the various pipe types and damage sizes, a survey of current utility operating conditions was performed to optimize the range of pipe parameters and damage characteristics for testing. The survey is presented in the following chapter.

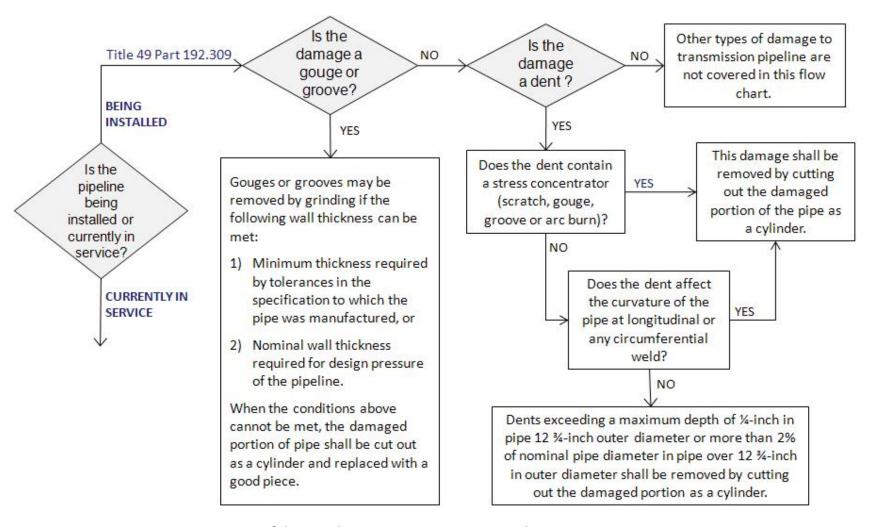


Figure 1 - Construction Requirements of damaged pipes in 49 CFR Part 192-Subpart G

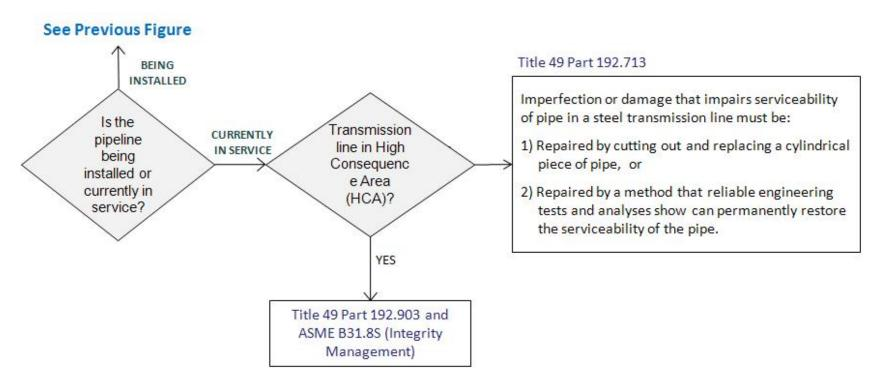


Figure 2 - Repair requirements of damaged pipes in 49 CFR Part 192-Subpart M

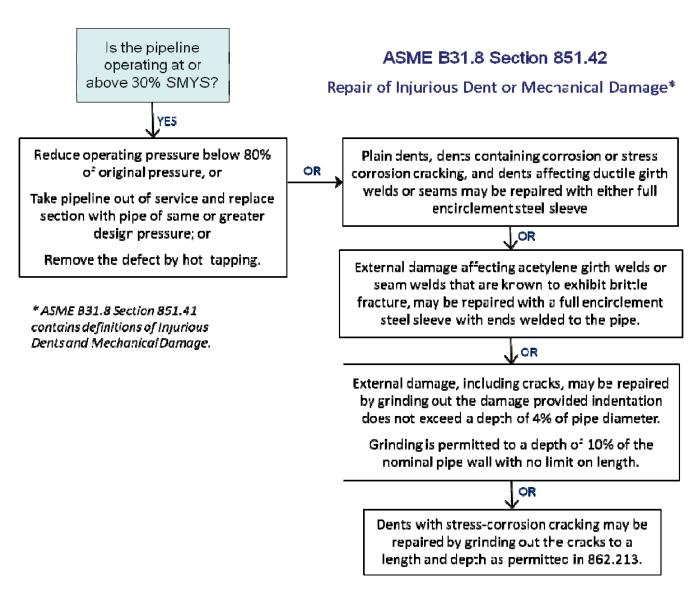


Figure 3 - Repair requirements of damaged pipes in ASME B31.8

Chapter 2

Pipe and Operation Characteristics of Natural Gas Pipelines

A significant number of gas utility companies operate transmission lines along with the gas distribution lines. As of 2005, the gas utility companies operated a total of 296 thousand miles of transmission lines along with their 1,118 thousand miles of gas distribution lines (2).

A survey of several natural gas utilities was performed by GTI to identify the specific ranges of pipeline stresses and flaw types in their gas transmission lines (3). The objectives of the survey were to determine the types of damages that are commonly encountered in transmission lines and to identify the pipeline parameters needed for the validation of mechanical damage. Emphasis was placed on determining the ranges of pipeline sizes, grades, and operating pressures that are typically used in the transmission sector of gas utilities.

The survey included 8 utilities that operate transmission lines at various regions in the United States. These utilities operated transmission lines in several states including New York, New Jersey, California, Utah, Washington, and Mississippi. The survey questionnaires and the results of the survey are presented in Table 1 to Table 14. The utilities are identified in these tables numerically from 1 to 8.

The results of the survey are summarized as follows:

- 1) Transmission pipeline sizes ranged from 4 inches to 36 inches with the majority of the pipes between 6 to 24 inches and with pipe grade X42.
- 2) Six of the eight surveyed utilities have their pipelines operating at stress levels below 40% SMYS. The other two utilities have pipelines operating up to 72% SMYS.
- 3) Third-party damage is the most common mechanical damage; causing coating flaws, scratches, gouges, and possible dents.
- 4) The common procedures for dealing with damaged steel pipelines operating at pressures below 40% SMYS are removing scratches, gouges, and grooves by grinding (provided remaining wall is sufficient for design pressure), by full encirclement sleeve, or by fully cutting and replacing the section.
- Large resources and costs are associated with identifying the damage and replacing a damaged pipeline at the low operating pressures. These operations are performed mostly by contractors.

Table 1 - Nominal diameters of the steel transmission pipelines per utility

Utility	Respond
1	From 4-30 inch for Transmission and 2-12 inch for high pressure distribution
2	6, 8, 12, 16, 20, 24, 26 and 30 inches
3	4 – 30 inch
4	3 – 24 inch IPS
5	1.3 – 36 inch OD
6	3, 4, 6, 8,10, 12 and 18 inches in diameter with 51.6 percent of the miles of transmission line with nominal diameter of 6 inches
7	6, 8, 10, 12, 16, 20 and 24 inches. The majority of the transmission lines are in the 6 to 12 inch nominal diameter range.
8	16, 20, 22.5 and 24 inches for DOT transmission lines

Table 2 - Wall thicknesses of steel transmission pipelines per utility

Utility	Respond	
1	Mostly standard wall, for transmission main to allow for 0.25 inch wall.	ns we may have used higher strength pipe
2	0.375 and 0.5 inch	
3	0.237 - 0.500 inch	
4	0.117 – 0.406 inch	
5	0.125 – 1.25 inch	
6	Ranges from 0.154 to 0.375 inches with me	ore than 50 percent less than 0.2 inches
7	Ranges from 0.188 to 0.375 inch	
	Diameter (inch)	Wall thickness (inch)
	3	0.219
	6	0.219 and 0.28
8	8 - 12	0.219
	16	0.25
	20	0.25 and 0.375
	22.5	0.25
	24	0.25 and 0.308

Table 3 - Range of MAOP (Maximum Allowable Operating Pressure) of steel transmission pipelines per utility

Utility	Respond
1	200, 450, 419 and 350 psig
_	High pressure mains at 30, 60, 99, and 124 psig
2	245 – 350 psig
3	245-800 psi
4	300 – 2000 psi
5	90 – 1440 psi
6	The MAOP Range is 230 – 1200 psi with 60 percent of the transmission lines with a
	MAOP of 500 or below
7	The utility has a range of MAOP from 400 psi to 720 psi, with the majority of the
	transmission lines having a MAOP of 400 psi.
8	250 psi and 350 psi

Table 4 - Percentage of SMYS of the transmission lines per utility

Utility	Respond
1	Ranges from 4% to 37%
2	32% or less
3	7% - 40% SMYS
4	3% - 84%
5	Less than 10% to 72%
6	Ranges from 20% to 40% with the majority less than 30%
7	Ranges from 20.1% to 62.5%
8	Ranges between 4.6% and 38.5%

Table 5 - Miles of steel "transmission" rated pipeline per utility

Utility	Respond
1	Total 212 miles
2	31 miles between 125 PSIG and 20% SMYS, 50 miles above 20% SMYS
3	73 miles
4	1442.14 miles
5	4527 miles
6	330 Miles
7	Reported 530 miles of transmission pipeline for 2003
8	148.5 miles

Table 6 - Grade of transmission [pipes per utilty

Utility	Respond
1	30,000 ft of Grade A, Grade B and X42 of a total 69 miles. Grade X46, X52, and Grade 6 of a total 126 miles. With most being either Grade B or X42
2	Various grades, including a lot of B, some A, X-42 and some others
3	Grade B and X-42
4	A25, A106, B, CL1, X42, X46, X52, X60, X65
5	All through X70
6	Grades A, B, X-42, X-46 and X-52 in transmission lines with the majority grade is X-42
7	X52 and X42 and B grade transmission lines
8	Grade B, X42 and X65

Table 7 - Approximately miles of pipeline operating at various levels of %SMYS

Utility	% SMYS	Length (miles)				
1	Less than 20%	117 miles				
	20 – 30%	180 miles				
	30-40%	15 miles				
	> 40%	None				
	Less than 20%	~31 miles				
2	20 – 30%	~35.5				
	30-40%	~15				
	> 40%	0				
	Less than 20%	10 miles				
3	20 – 30%	14				
_	30-40%	49				
	> 40%	0				
	Less than 20%	Distribution- 94.26; Transmission- 29.19				
4	20 – 30%	Transmission - 192.38				
•	30-40%	Transmission – 201.33				
	> 40%	Transmission – 1019.24				
	Less than 20%	429 Transmission miles				
5	20 – 30%	814				
J	30-40%	640				
	> 40%	2,643				
	Less than 20%	0				
6	20 – 30%	266				
Ŭ	30-40%	64				
	> 40%	0				
	Less than 20%	11,919 reported at 2003				
7	20 – 30%	206				
,	30-40%	116				
	> 40%	208				
	Less than 20%	39.4				
8	20 – 30%	91.2				
· ·	30-40%	17.9				
	> 40%	0				

Table 8 - Percentage of seamless transmission pipes per utility

Utility	Respond
1	10%
2	80%
3	Unknown
4	Less than 1%
5	183 miles = 4%
6	3%
7	None
8	Less than 5%

Table 9 - Encountered damage in steel pipelines per utility

[Not including damage due to corrosion, arc burns, or notches. If possible, please provide details regarding the damage (i.e. depth of dents or gouges, length of grooves or scratches)]

Utility	Respond
1	Third party damage is most common, it causes coating flaws, scratches possible dents. Wall loss can vary what you may want to do is set a target i.e. 10% or larger wall loss for detection
2	Dents & Gouges – at isolated spots / locations
3	Gouges and scratches
4	Gouges may range from 0 to several feet long and a depth of just removing the coating to through wall. Dents may have a similar range.
5	All conceivable except SCC
6	Dents, gouges and scratches
7	Long seam failure, or likely overstress due to ground subsidence
8	Very infrequent dents, gouges or scratches. Details not available

Table 10 - Causes of damage to steel pipelines per utility

[Not including damage due to corrosion]

Utility	Respond
1	Third party construction i.e. water companies, contractors installing or drilling
2	Third Party Damage
3	Foreign construction without company on-sight observance
4	3 rd Party, Natural Forces – Land Slide
5	Not pertinent to this study
6	Third party damages
7	Manufacturing defects, or ground movement
8	Dents and scratches

Table 11 - Current procedures for dealing with damaged steel pipelines during installation, before they are put into operation

[For pipelines running at the following %SMYS (for dents, scratches, gouges, and grooves only)]

Utility	Respond
1	New pipe must go in clean of defects and then it is pressure tested as well
2	Same as question 12
3	Dents, scratches, gouges, and grooves are full encirclement cutout. Do not operate above 40% SMYS.
4	49 CFR Part 192 subpart G.
5	Not pertinent to this study
6	For all pipelines regardless of percent SMYS, repair in accordance with CFR 192.309 as a minimum.
7	Cut out and replace damaged portion
8	Cut out and repair. N/A above 40% SMYS.

Table 12 - Determining if the damage is "severe enough" to warrant replacement, per utility

Utility	Respond
1	We use industry standards PSC code, Federal Code and ASME B31G
2	Our Gas Engineering–Major Projects section, along with our Corrosion Control Group (even though the damage may not be corrosion related) will visually conduct an on-site inspection. Pit gauges will be used if metal loss (from a gouge or scrap) has occurred.
3	Trained company personnel taking the appropriate field measurements for final evaluation by company Professional Engineer. Primary guidance material B31.8.
4	Review the Mill Test Report (MTR) for the damaged section, Caliper measurement on dent and or gouge, RSTRENG calculation.
5	Standard guidance regarding allowable dimensions of flaws provided in company standards, along with acceptable repairs. If more detailed measurements and flaw assessments are required to perhaps avoid a costly repair, or if alternative repair options are desired then Engineering is consulted by the field personnel. The large majority of anomalies are not repaired by cylinder replacement unless the line is easily removed from service and gas loss is minimal and/or the damage interferes with piggability or gas delivery. If we conclude that the gas pipeline integrity rule requires periodic assessment of repair sleeves, canopies or other repair features that cannot be assessed by pigging, then we may tend to use more cylinder replacement in the future.
6	Trained company personnel, visual and measurement equipment.
7	The utility has a standard practice to address replacing sections of pipelines due to damage. The decision is a collaborative effort by trained/experienced field personnel and senior engineers with measurement equipment.
8	All of the above listed as appropriate

Table 13 - Current procedures for dealing with damaged steel pipelines

[For pipelines running at the following %SMYS (for dents, scratches, gouges, and grooves only)]

Utility	Respond
1	No info.
2	Info on survey
3	< 20% SMYS: Scratches, gouges, and grooves are removed by grinding provided remaining wall is sufficient for design pressure, or Full encirclement sleeve, or Full cutout. 20 – 40% SMYS: Scratches, gouges, and grooves are removed by grinding provided remaining wall is sufficient for design pressure, or full encirclement sleeve, or full cutout. > 40% SMYS: Do not operate above 40%
4	Conform to the standards 49 CFR Part 192 subpart M ASTM B31-8
5	< 20% SMYS: repair clamp (<60 psig), grind & recoat, grind and restore metal using direct deposition of weld metal, Type A sleeve, Type B sleeve, Weld abandon nipple over the flaw, Cylinder replacement 20-40 % SMYS: same as above, except for clamp, grinding for repair of gouges that are not associated with denting limited to length and depth acceptable by RSTRENG (KAPA) for >30%SMYS: grinding for gouges accompanied by shallow dents limited to length and depth and dent size described in report by Rosenfeld for GTI (input for B31.8 committee) for <30% SMYS: grinding for gouge in shallow dents, length and depth limits similar to above, except maximum depth is 60%T and max length is determined using a slightly less conservative equation. >40% SMYS: same as above
6	For all pipelines regardless of percent SMYS, we repair in accordance with CFR 192.309.
7	< 20% SMYS: grind, mechanical leak clamps, boiler plugs, or Clock Spring repair. Cut out a cylindrical section containing the damage the damage is too deep for repair. 20-40 % SMYS: grind, mechanical leak clamps, or Clock Spring repair. Cut out a cylindrical section containing the damage the damage is too deep for repair. >40% SMYS: full encirclement split sleeve or cylindrical section cut out.
8	< 20% SMYS: blend out stress risers and install Clockspring or weld-over 20-40% SMYS: blend out stress risers and install Clockspring or weld-over >40% SMYS: n/a

Table 14 - Average cost to replace or repair a damaged steel pipeline?

Utility	Respond
1	Replacement could be "tens of thousands." Repair could be something like Clockspring, much less – say \$10,000
2	Replacement - ~\$400 to \$1,000 per foot, depending on pipe diameter. Repair — Much cheaper to recoat the pipe in the case of coating damage only
3	Non-Cut Outs: \$5,000 - \$15,000 depending on excavation site conditions. Cut Outs: \$30,000 - \$500,000 depending on size and location.
4	Infinitely variable based on location, pipe size and thickness, above ground or below ground installation, type and severity of damage, removal from service required,
5	\$25-\$100,000. Grinding out a minor gouge discovered during routine O&M excavations takes 5 minutes. Excavating and repairing a flaw discovered during ILI could require huge time and cost expenditures.
6	25,000 dollars.
7	\$39,000.00
8	\$1 million/mile

Chapter 3

Past Experiments on Pipelines with Mechanical Damage

Various techniques were used for laboratory simulations of the gouges and dents observed on pipelines that have been struck by excavating equipment. The most commonly used techniques are one of the following (4):

Method 1 - Machined Notch Followed by Indentation at Zero Pressure

The method was used in early studies by Battelle in the 1960s and 1970s and consisted of the following steps (5):

- 1. Machine a longitudinally oriented notch into the wall thickness of the pipe using a v-shaped cutter while the pipe is unpressurized.
- 2. Place a 12-inch-long, 1-inch-diameter round steel bar over the notch and press a dent into the pipe while it remains unpressurized.
- 3. Release the load on the round-bar indenter, and allow the indented pipe to recover. Since the pipe is usually unconfined by soil during this type of indentation, the entire cross-section of the pipe tends to ovalize in response to the indenting load. Therefore, elastic recovery includes recovery of ovalization as well as recovery of local radial indentation at the point of indentation.

A schematic drawing of the indentation process is shown in Figure 4. The indentation and rerounding process are shown in Figure 5. After the application of the damage, the pipe is pressurized and tested.

Dents formed by this method at zero internal pressure are steadily reduced as pressure is increased from zero. The re-rounding continues with increasing pressure such that unless failure occurs, the entire dent disappears. If a notch is present in the dent, a crack may grow from the notch and cause a failure before total recovery of the dent has occurred.

This type of damage application does not account for the stiffening effect of internal pressure and the method is not a valid representation of actual mechanical damage in a pressurized pipeline. However, this type of test simulates what might happen if a pipeline is damaged when depressurized, as for example, during its initial construction.

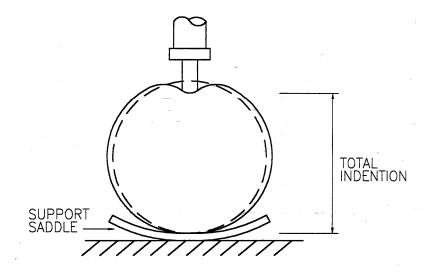


Figure 4 - Typical indentation process associated with methods 1 and 3

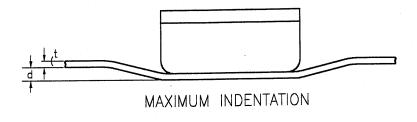




Figure 5 - Typical indenters and re-rounding associated with methods 1 and 3

Method 2 - Indentation Followed by Machined Notching at Zero Pressure

This method was first used in studies by British Gas in the 1960s and 1970's. It consisted of the following steps:

- Press a round steel bar into an undamaged pipe while it remains unpressurized.
- Release the load on the round-bar indenter, and allow the indented pipe to recover as much as its elasticity will allow.
- Machine a longitudinally oriented notch into the wall thickness of the pipe along the deepest part of the indentation using a v-shaped cutter while the pipe is unpressurized.

Upon comparisons with the results of tests of specimens created by Method 2 and Method 3, most investigators, concluded that Method 3 better simulated what actually happens during an actual mechanical-damage impact on a pipeline than Method 2. Therefore, Method 2 is seldom used (4).

Method 3 - Machined Notch Followed by Indentation at Pressure

This method was used to validate the Dent-Gouge Fracture Model (6). It was also used in studies (7) and it consists of the following steps:

- Machine a longitudinally oriented notch into the wall thickness of the pipe using a v-shaped cutter while the pipe is unpressurized.
- Pressurize the pipe to a pre-determined pressure level.
- Place a long, round steel bar over the notch, and press a dent into the pipe while it remains pressurized being careful to keep the internal pressure constant by bleeding pressure during indentation and restoring pressure as the indenter is withdrawn.
- Depressurize the pipe.

If the pipe does not fail during this process, the pipe can then be tested as desired. Usually, the test involves pressurization to failure.

Method 4 - Creating a Dent and Gouge Simultaneously in a Pressurized Pipe

The method was used in the studies described in Reference (8). In this method, the pipe specimen was supported rigidly by semi-circular plates to restrain pipe ovalization during denting; thus simulating the restraint provided by soil backfill. With the pipe pressurized, a backhoe tooth is forced into the pipe and drug along the axis of the pipe. The result provides progressively formed gouge and dent. If pipe does not fail during this process, it is hydrostatically tested to failure.

Layout of Current Validation Experiment

The review of the past experimental programs suggested the development of the testing equipment at GTI to provide the capability of performing tests using methods 3 and 4 above. The tests using these methods were used to validate the existing theoretical models; with method 4 being more realistic simulation of the mechanical damage in the field. The general procedure for tests consists of the following:

- 1. For tests using method 3, the equipment applies controlled dents on pressurized pipes which are pre-notched longitudinally into the wall thickness.
- 2. For tests using method 4, the equipment creates a gouge and dent simultaneously in each sample while it was held stationary in the test frame. The hydraulic cylinders force a backhoe tooth into the pipe while pushing it along the longitudinal axis of the pipe.
- 3. During damage application, the pipe sample is pressurized to a hoop stress level of 40% SMYS. The process was applied to reach various depths of dents and gouges in the experimental program.
- 4. All gouges were to be made in the axial direction with a minimum gouge length of about 12 inches. This minimum length is greater than the square root of 50.D.t (fifty times the diameter times the wall thickness), and therefore, it would be expected to have essentially the same effect as an infinitely long defect in the range of materials used in the tests. The damage length is then expected to drop out as a parameter affecting the results.

Chapter 4

Development of the Testing Equipment and Procedure

A) Dent-Gouge Loading Machine

In order to accommodate a wide range of pipe sizes and pressures in the testing program, a large-scale loading frame and hydraulic system were manufactured. The hydraulic system is capable of applying dents and gouges to pressurized pipes of sizes up to 22 inches in diameter. Figure 6 shows a view of the large mechanical-damage loading equipment.



Figure 6 - The large-scale dent-gouge machine with a 16-inch diameter pipe

One objective of the testing program is to confirm the validity of the European Pipeline Research Group (EPRG) Simplified Model for mechanical damage. A graphical representation of the model is shown in Figure 7. As shown in the figure, the limiting acceptance criteria for the EPRG model are at a Dent depth/Pipe diameter (Ho/D) ratio of 4 percent and a Gouge depth/Wall thickness (d/t) ratio of 18 percent.

The hydraulic system in the dent-gouge loading machine was designed to apply vertical moving load to produce dents and gouges that exceed these expected ranges of the testing program.

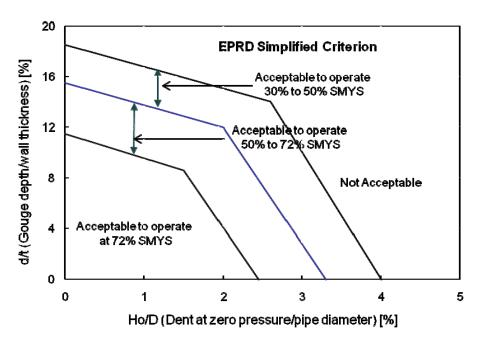


Figure 7 - The EPRG simplified model criterion

The dent-gouge loading machine was used to apply the hydrostatic pressure at 40% SMYS during indentation. Figure 8 - The hydraulic loading system for dent-gouge applications

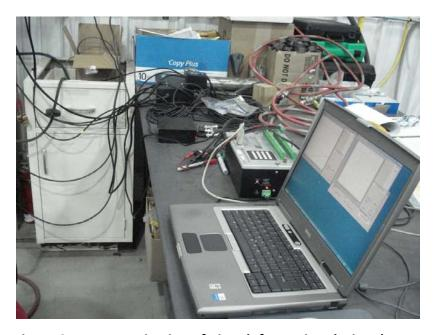


Figure 9 - Data monitoring of pipe deformation during damage application

Table 15 - Range of pressures for hoop stresses as % SMYS in the testing program

Diameter	Wall Thickness	Diameter/wall	SMYS	Pressure at 100%	Pressure at 40%	
(inch)	(inch)	thickness (D/t)	(psi)	SMYS (psig)	SMYS (psig)	
8.625	0.25	34.5	42,000	2,435	974	
8.625	0.25	34.5	52,000	3,015	1206	
8.625	0.322	26.8	42,000	3,135	1254	
16	0.25	64	42,000	1,312	525	
16	0.188	85	42,000	987	394	
16	0.25	64	60,000	1,875	750	

shows the ranges of pressures that produce stresses at 40% SMYS for various pipe sizes and grades. An external reservoir was connected to the hydraulic system to keep the pipe hydrostatic pressure constant by bleeding access pressure during indentation and restoring the pressure as the indenter is withdrawn. This process provided a constant hydrostatic pressure and simulated the field condition of dented transmission pipes with compressible gas.

The hydraulic system of the testing machine (Figure 8) was also used to apply hydrostatic pressures that exceed the 100% SMYS of the pipe specimen during bursting tests.

The data logger system (Figure 9) was used to monitor the pipe hydrostatic pressure, dent depth, and length during the application of the mechanical damage and in burst tests. This process allowed the application of accurate and consistent mechanical damages on all the pipe specimens.



Figure 8 - The hydraulic loading system for dent-gouge applications

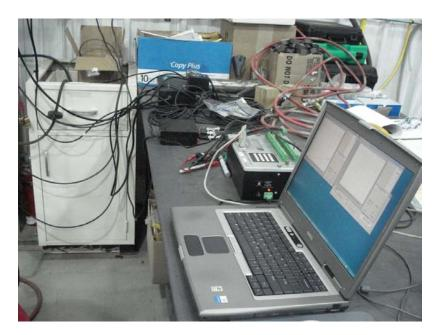


Figure 9 - Data monitoring of pipe deformation during damage application

Table 15 - Range of pressures for hoop stresses as % SMYS in the testing program

Diameter	Wall Thickness	Diameter/wall	SMYS	Pressure at 100%	Pressure at 40%	
(inch)	(inch)	thickness (D/t)	(psi)	SMYS (psig)	SMYS (psig)	
8.625	0.25	34.5	42,000	2,435	974	
8.625	0.25	34.5	52,000	3,015	1206	
8.625	0.322	26.8	42,000	3,135	1254	
16	0.25	64	42,000	1,312	525	
16	0.188	85	42,000	987	394	
16	0.25	64	60,000	1,875	750	

B) Validation Test Matrix

The results of the testing program are used to validate the EPRG Simplified Model. Earlier experiments at GTI evaluated the mechanical damages on 8-inch diameter pipes with depth to thickness (D/t) ratios from 26 to 42 (3). The results of these tests are plotted on the model diagram in Figure 10. As shown in the figure, the earlier tests were performed at high values of dents and gouges on relatively rigid pipe samples; thus resulting in very conservative failures with respect to model predictions.

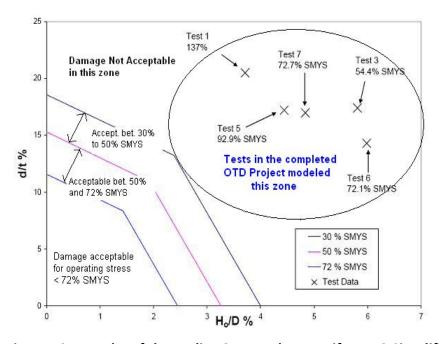


Figure 10 - Results of the earlier OTD study to verify EPRG Simplified Model

The testing parameters in the current project cover a wide range of pipe diameters from 8 to 16 inches with D/t ratios up to 64. These tests account for the increased likelihood of re-rounding in larger D/t ratios and thus the development of re-rounding cracks on the larger pipes. These re-rounding cracks, which are not always detected by visual examination, can weaken the strength of the pipe, reducing the effective minimum safe wall thickness and ultimately, causing a pipeline failure.

One of the key parameters that determine the subsequent growth and failure of the pipe during these tests is the pipe toughness. For this reason, a portion of the test matrix includes low toughness pipe material to ensure the model is valid over the whole range of pipe grades.

Most of the previous mechanical damage tests were based on machined notches applied to the pipe before or after the denting process. This approach allows for good control of the gouge depth and dent depth but may not capture all of the features of true mechanical damage. For example, the gouging process due to the mechanical contact with the pipeline results in a thin layer of highly worked material on the surface of the pipe that may initiate large numbers of small cracks. In order to capture these features in this project, the denting process will be performed on pressurized pipe. A portion of the tests will also be performed using a simulated backhoe to model field conditions. The testing matrix is shown in Table 16 and includes the following testing parameters:

- 1. Diameter and wall thickness (D/t ratio),
- 2. Yield strength and toughness,
- 3. Depth of initial indentation,
- 4. Dent depth at zero pressure /pipe diameter (Ho/D) ratio,
- 5. Gouge depth /pie wall thickness (d/t) ratio,
- 6. Pressure level during indentation (as percentage of SMYS)
- 7. Radius and shape of gouge,
- 8. Pressure level at failure.

Table 16 - Range of values of the testing parameters

Pipe Diameter/wall thickness (D/t)	Pipe Grade	Pipe toughness*	Gouge/ wall thickness (d/t)**	Dent/ diameter (Ho/D)**	Gouge Shape	Gouge Length (inch)	Field Simulation
Low (33) High (64)	X42 X52 X60	Low (12) to High (40)	< 0% (no gouge) to > 60%	< 0% (no dent) to > 20%	Rounded 45° 90°	12	Backhoe tooth at stress 20% SMYS.

^{*} Full size Charpy Energy, ft-lbs

d = gouge depth

D = Outside pipe diameter

t = pipe wall thickness

C) Dent-Gouge Testing Procedure

The testing equipment and procedure for applying pipe damages provides the capability of performing tests using methods 3 and 4 listed in the previous chapter. These methods are used to further validate the existing theoretical models; with method 4 being more realistic simulation of the mechanical damage in the field. The general procedure for tests consists of the following:

i) <u>Preparation of Pipe Test Specimen:</u>

Pipe caps and threads were welded to the pipe specimen to allow for applying hydrostatic pressure up to 150% SMYS during the bursting stage of the tests. Figure 11 shows the welding of caps on the pipe test samples.

In order to reduce the end effect of the welded caps on the location of the applied damage, the pipe sample had a minimum length of 4.5 times the pipe diameter. A sample length of 6.25 ft was used for both the 8-inch and 16-inch diameter pipes in the testing program. Figure 12 shows a schematic of the pipe test specimen.

^{**} Ho = Dent at zero internal pressure



Figure 11 - Welding of pipe caps in preparation of the pipe test sample

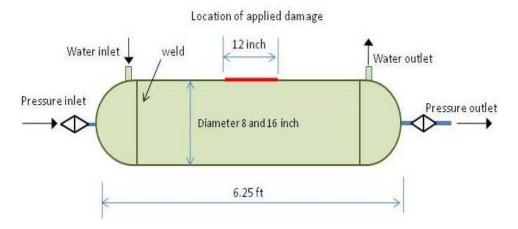


Figure 12 - Schematic of the pipe test specimen

ii) Application of Gouges:

In Method 3, described earlier in Chapter 3, a longitudinally-oriented gouge is applied into the wall of the pipe using a v-shaped cutter while the pipe is unpressurized. A schematic diagram of the controlled-gouges applied using this method is shown in Figure 13. The gouges were applied at zero internal pipe pressure at various shapes and gouge angles using a computer-controlled CNC machine as shown in Figure 14.

In Method 4, the gouges were applied along with the dents in one process using a backhoe tooth tool to introduce actual mechanical damage into a pressurized pipe.

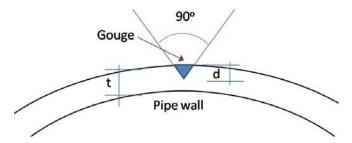


Figure 13 - Shape of the applied gouge on the pipe specimen

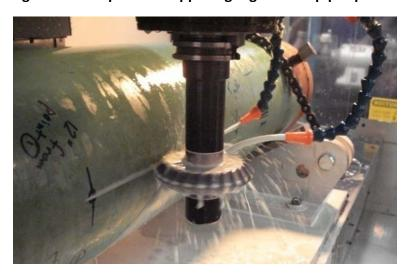


Figure 14 - Application of controlled gouge on the pipe specimen

iii) Application of Dents:

The pipes were placed in the dent/gouge loading machine and pressurized to hydrostatic pressures causing a hoop stress equals 40% SMYS. In some tests with large gouges and dents, the pipe were pressurized at 20% SMYS. A rounded disc was used to apply a vertical dent to the pipe Figure 15.

A pressure release tank is connected to the pipe during this process to accommodate the volume of water displaced from the pipe during pipe denting. The vertical pipe displacement is monitored using a data acquisition system.

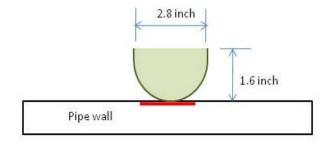


Figure 15 - Schematic of the rounded disc for dent application

Once the maximum indentation depth was achieved, the loading proceeded with applying the dent longitudinally along the pipe as shown in Figure 16, at internal pressure levels corresponding to 40% SMYS of pipe material.

The lengths of the gouges and dents were 12 inches in all the pipe specimens. Table 17 shows that the length of gouge is greater than $6\sqrt{Dt}$ for the samples in the testing program. As such, the defect can be considered to be representative of a "long" defect and the results would be similar to longer defects.



Figure 16 - Application of longitudinal dent along the pipe specimen

Table 17 - Length of Gouge Needed for Validation Testing

Pipe Diameter	Wall Thickness	Length = $6\sqrt{Dt}$
(inch)	(inch)	(inch)
8.625	0.25	8.81
8.625	0.322	9.99
16	0.25	12

iv) Measurements of Dents

In most of the tests, pipes were dented while at internal pressure equals 40% SMYS. In some tests, the pipes were dented at 20% SMYS when pipe failure was expected to occur at or below the 40% SMYS. This pressure causes the pipe surface to rebound as the dent disk is moved away. The maximum depth of indentation reached with the indenting tool present and the pipe pressurized is defined as H_{max} .

After denting, pipe pressure was released to 0 psig and the dent depth was measured using a straight edge and a depth gauge Figure 17. The dent depth after the indenting tool has been withdrawn and the pipe has been depressurized is defined as H_o as shown in Figure 18.



Figure 17 - Measurement of dent at zero pressure (H_o)

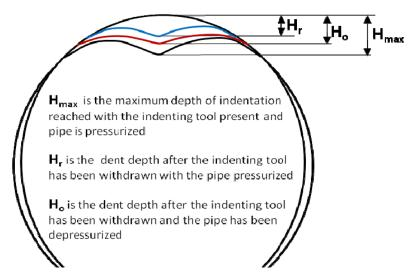


Figure 18 - Measurements of dents in the pipe during and after loading

v) Checking Pipe for Cracks

After the completion of damage application, pipe samples were investigated to check if the gouge-dent procedure causes the development of surface cracks. The procedure consisted of grinding the surface to remove pipe coating from the dented area (Figure 19) and inspecting the surface using magnetic particle test equipment (Figure 20). The pipe wall thickness was measured using an ultrasonic thickness gauge.



Figure 19 - Grinding the pipe surface for the inspection of cracks



Figure 20 - Inspection of cracks using magnetic particle device

vi) Pipe Burst Tests:

If the pipe sample did not fail during the creation of the defects, the pipe was depressurized and the depths of the dent and the gouge along the pipe length were documented.

Hydrostatic pressure was then applied to the pipe incrementally until pipe failure. Figure 21 shows a view of a 16-inch pipe sample after a burst test showing the burst failure at the dent and gouge location.



Figure 21 - View of pipe at the completion of the burst test

Chapter 5

Hydrostatic Pressure Tests on Mechanically-Damaged Pipes

Hydrostatic pressure tests were performed on pipes with various dents and gouges. Figure 22 shows the testing of an 8-inch pipe in the dent-gouge loading machine. Several test sets were performed to evaluate the failures of pipes under various testing parameters. The test sets are shown in Table 18. The details of the tests performed in each set are presented in this Chapter and the results are also summarized in Appendix A. Test Set A evaluated failure of pressurized pipes with different stiffness (i.e., pipe diameter/wall thickness) ratios. Set B evaluated pipe failures due to only gouges or dents. Test Set C had pipes dented at pressure 20% SMYS, and were tested to reach failure at 40% SMYS. Set D evaluated pipe failures with various gouge shapes. Set E simulated dents and gouges from a backhoe tooth applied to the pressurized pipes, and Set F was performed on grade X60 pipes.



Figure 22 - View of the Large-scale dent-gouge machine

Table 18 - The pipe and damage parameters of the test sets

Test Set	Pipe Grade	Diam. (inch)	D/t	Gouge (inch)	d/t (%)	Dent (inch)	Ho/D (%)
Α	X42 - X52	8 - 16	32 - 64	0.09	36	0.8 - 1.4	7.5 - 12
В	X42	8 - 16	32 - 64	0 - 0.1	0 - 40	0 - 1.4	0 - 15
С	X42	8 - 16	32 - 64	0.1 - 0.15	40 - 60	0.75 - 2.0	8 - 12
D	X42	8 - 16	32 - 64	0.1	various	0.5 - 2.0	6 - 24
Е	X42	16	64	0.06-0.1	90	1 - 1.3	6 - 8
F	X60	16	64	0.13	90	1.25	7.81

i) <u>Test Set A:</u>

The testing parameters of this set are shown in Table 19. The tests were performed on two pipe grades, namely X42 and X52. The higher grade pipes also had higher stiffness demonstrated by the low diameter/wall thickness ratio of 33.

The gouge depths in all the tests were kept constant at a (d/t) ratio of about 36 percent and the pipes were tested at various indentations as shown in the table. At these damage levels, the pipes failed at stress levels from 65% to 110% SMYS.

The dents were applied for a distance of 12 inches along the pipe surface. The vertical load was kept constant during this application and the excess pipe pressure during the denting process was collected in an external reservoir. Figure 23 shows the measured pressures during the application of horizontal dents in the 16-inch pipe tests. The results of the pressure tests on the 16-inch and 8-inch pipes are shown in Figure 24 and Figure 25, respectively.

Table 19 - Testing parameters and results of Set-A

			at piess	SMYS				
Pipe Grade	Diam.	D/t	Gouge	d/t	Dent	Ho/D	Failure Load	Failure
	(inch)		(inch)	(%)		(%)	(psig)	as (%SMYS)
X42	16	64	0.085	34	1.3	8.1	1083	82.36
X42	16	64	0.095	38	1.41	8.8	854	64.94
X42	16	64	0.09	36	1.2	7.5	1440	109.51
X52	8.625	33	0.09	36	0.82	9.5	2550	84.58
X52	8.625	33	0.091	36.4	1.1	12.8	2300	76.29
X52	8.625	33	0.089	35.6	1	11.6	2490	82.59
P	X42 X42 X42 X42 X52 X52	X42 16 X42 16 X42 16 X42 16 X52 8.625 X52 8.625	(inch) X42 16 64 X42 16 64 X42 16 64 X42 16 64 X52 8.625 33 X52 8.625 33	(inch) (inch) X42 16 64 0.085 X42 16 64 0.095 X42 16 64 0.09 X52 8.625 33 0.09 X52 8.625 33 0.091	(inch) (inch) (%) X42 16 64 0.085 34 X42 16 64 0.095 38 X42 16 64 0.09 36 X52 8.625 33 0.09 36 X52 8.625 33 0.091 36.4	(inch) (inch) (%) X42 16 64 0.085 34 1.3 X42 16 64 0.095 38 1.41 X42 16 64 0.09 36 1.2 X52 8.625 33 0.09 36 0.82 X52 8.625 33 0.091 36.4 1.1	(inch) (inch) (%) (%) X42 16 64 0.085 34 1.3 8.1 X42 16 64 0.095 38 1.41 8.8 X42 16 64 0.09 36 1.2 7.5 X52 8.625 33 0.09 36 0.82 9.5 X52 8.625 33 0.091 36.4 1.1 12.8	(inch) (inch) (%) (%) (%) (psig) X42 16 64 0.085 34 1.3 8.1 1083 X42 16 64 0.095 38 1.41 8.8 854 X42 16 64 0.09 36 1.2 7.5 1440 X52 8.625 33 0.09 36 0.82 9.5 2550 X52 8.625 33 0.091 36.4 1.1 12.8 2300

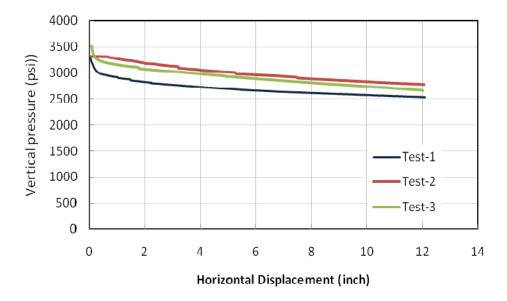


Figure 23 - Applied pressure and horizontal displacement during denting

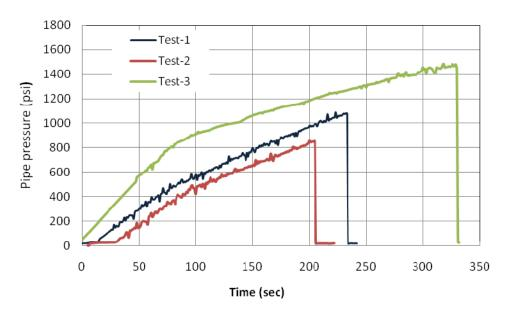


Figure 24 - Pipe pressure during burst tests of the 16-inch pipes in Set-A

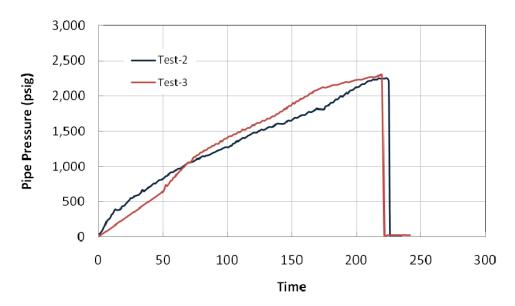


Figure 25 - Pipe pressure during burst tests of the 8-inch pipes in Set-A

Figure 26 and Figure 27 show pipe samples after the completion of the hydrostatic burst tests for the 8-inch and the 16-inch pipes, respectively.



Figure 26 - View of the 8-inch pipe after burst test



Figure 27 - View of the 16-inch pipe after burst test

ii) Test Set B:

Tests in this set evaluated pipes subjected to gouges only (i.e.; without dents) and to dents only (i.e.; without gouges). Although gouges in the field are likely to be accompanied by dents, the results of these tests provided a validation of the EPRG Simplified Model in the cases of dent-only and gouge-only damages.

The testing parameters and results of this set are shown Table 20. The 8-inch and 16-inch pipe samples after applying the dents are shown in Figure 28 and Figure 29, respectively. The indentation of the 16- inch pipes was performed was a larger denting disc. However, superficial gouges were developed on the pipe surface near the edges of the disc as shown in Figure 29.

The results of the pressure tests on pipes with gouges only are shown in Figure 30. The pipes subjected to denting only without gouge did not fail in burst tests and yielded at pressures exceeding the 100% SMYS.

Table 20 - Testing parameters and results of Set-B

Set B -	Machine Go	uges only	y & Dents	only - De	nts at pre	ssure 40% SI	MYS		
Test	Pipe Grade	Diam.	D/t	Gouge	d/t	Dent	Ho/D	Failure Load	Failure
		(inch)		(in)	(%)	(in)	(%)	(psig)	as (%SMYS)
1	X42	8.625	33	0.1	40	0	0.0	2650	108.83
2	X42	8.625	33	0	0	1.24	14.4	4000	164.27
3	X42	16	64	0.1	40	0	0.0	1400	106.46
4	X42	16	64	0	0	1.39	8.7	1720	130.80



Figure 28 - Indentation of the 8-inch pipe in Set-B



Figure 29 - Indentation of the 16-inch pipe in Set-B

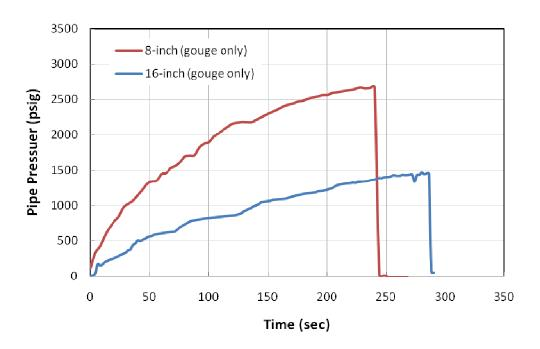


Figure 30 - Pressure tests on the gouged pipes in Set-B

iii) Test Set C

The tests of Set-C evaluated the mechanical damages which cause the pipe to fail at pressure levels of 40% SMYS. Several test trials were performed with incremental values of dents and gouges to reach failures at this level. The dents were initially applied at pipe pressures of 20% SMYS. The pressure was then incrementally increased to reach a failure at or near 40% SMYS.

The testing parameters and results of this set are shown in Table 21. Figure 31 shows the results of the burst pressure test on the 8-inch pipe in Test 3. Figure 32 and Figure 33 show the pipes after the completion of the burst tests in tests 3 and 4, respectively.

Table 21 - Testing parameters and results of Set-C

Machine go	uge - Incr	eased De	nt stepwis	se at 20%	SMYS to fail	at/below 40	% SMYS	
Pipe Grade	Diam.	D/t	Gouge	d/t	Dent	Ho/D	Failure Load	Failure
	(inch)		(in)	(%)	(in)	(%)	(psig)	as (%SMYS)
X42	8.625	33	0.15	60	1	11.6	720	29.57
X42	8.625	33	0.13	52	0.75	8.7	750	30.80
X42	8.625	33	0.1	40	1	11.6	820	33.68
X42	16	64	0.095	38	2	12.5	475	36.12
	X42 X42 X42 X42	Pipe Grade Diam. (inch) X42 8.625 X42 8.625 X42 8.625	Pipe Grade Diam. (inch) D/t X42 8.625 33 X42 8.625 33 X42 8.625 33 X42 8.625 33	Pipe Grade Diam. (inch) D/t (in) Gouge (in) X42 8.625 33 0.15 X42 8.625 33 0.13 X42 8.625 33 0.1	Pipe Grade Diam. (inch) D/t (in) Gouge (in) d/t (%) X42 8.625 33 0.15 60 X42 8.625 33 0.13 52 X42 8.625 33 0.1 40	Pipe Grade Diam. (inch) D/t (in) Gouge (in) d/t (in) Dent (in) X42 8.625 33 0.15 60 1 X42 8.625 33 0.13 52 0.75 X42 8.625 33 0.1 40 1	Pipe Grade (inch) Diam. (inch) D/t (in) Gouge (in) d/t (in) Dent (in) Ho/D (%) X42 8.625 33 0.15 60 1 11.6 X42 8.625 33 0.13 52 0.75 8.7 X42 8.625 33 0.1 40 1 11.6	(inch) (in) (%) (in) (%) (psig) X42 8.625 33 0.15 60 1 11.6 720 X42 8.625 33 0.13 52 0.75 8.7 750 X42 8.625 33 0.1 40 1 11.6 820

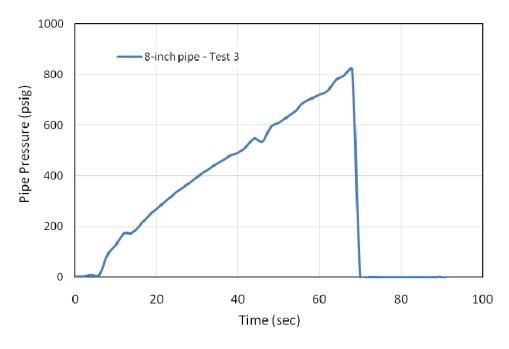


Figure 31 - Pressure tests No. 3 on the 8-inch pipe in Set-C



Figure 32 - View of the Test-3 8-inch pipe after Testing



Figure 33 - View of the Test-4 16-inch pipe after testing

iv) Test Set D

The tests in this set evaluated the effect of the gouge shape and geometry on the failure pressure. The tests were performed on pipes with constant wall thickness of 0.25 inches and gouge depth of 0.1 inches (Figure 34). The testing parameters and results of this set are shown in Table 22.

Several dents were applied to the pipe in each test. At each indentation level, the pipe was pressurized to 40% SMYS. If the pipe did not fail, higher indentation was the applied until the pipe failed at or below 40% SMYS. The results of these tests at various indentation levels are shown in Figure 35 to Figure 38.

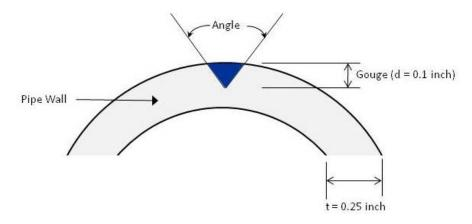


Figure 34 - Testing parameters for test Set-D

Table 22 - Testing parameters and results of Set-D

Set D	 Various Go 	uge shap	es, incre	ased dent	stepwise	to reach p	ressure to fa	ilure at or belov	v 40%
Test	Pipe Grade		D/t	gouge	Gouge	Dent	Ho/D	Failure Load	Failure
		(inch)			(angle)	(inch)	(%)	(psig)	as (%SMYS)
1	X42	8.625	33	0.1	90	1	11.6	820	33.68
2	X42	8.625	33	0.1	45	0.5	5.8	1000	41.07
3	X42	8.625	33	0.1	rounded	2	23.2	300	12.32
4	X42	16	64	0.1	90	2	12.5	475	36.12

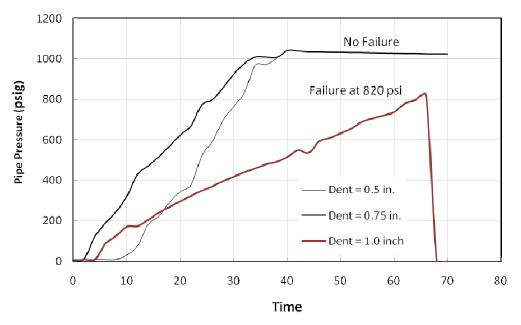


Figure 35 - Results of Test 1 with 90° gouge and various dents

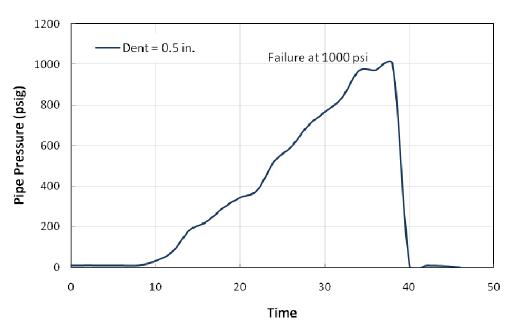


Figure 36 - Results of Test 2 with 45° gouge angle

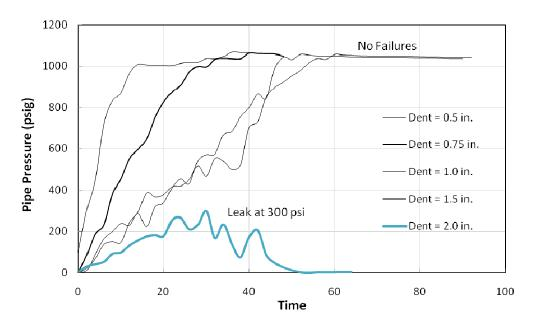


Figure 37 - Results of Test 3 with rounded gouge and various dents

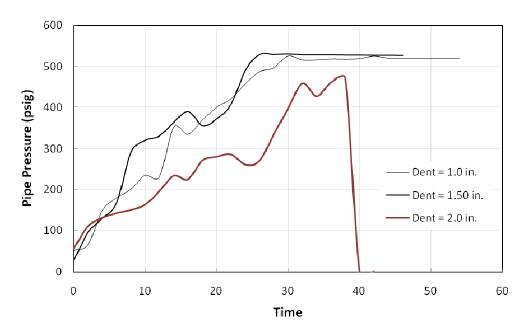


Figure 38 - Results of Test 4 with 90° gouge and various dents

v) <u>Test Set E</u>

The tests in this set simulated the application of a backhoe tooth to cause a simultaneous dent and gouge on the pipe surface. This loading condition was applied according to Method 4 listed in Chapter 3. The testing parameters and results of this set are shown in Table 23.

In contrast to the controlled machine gouges that were applied in the other test sets; the gouge depth in this set was applied with the tooth being dragged along the pipe surface using the dent-gouge machine (Figure 39). This process resulted in a varying gouge depth from 0.06 inch to 0.1 inch along the 12-inch length of the damaged area as shown in Figure 40.

Table 23 - Testing parameters and results of Set-E

Set E (5) - Pipe Grad	le X42 (Ba	ackhoe Si	mulation at	pressure 20	0% SMYS)			
Test	Pipe Grade	Diam. (inch)	D/t	Gouge (inch)	Gouge (angle)	Dent (inch)	Ho/D (%)	Failure (psig)	Failure as (%SMYS)
1	X42	16	64	0.06-0.1	90	1	6.25	815	62%
2	X42	16	64	0.06-0.1	90	1.3	8.13	550	42%
3	X42	16	64	0.06-0.1	90	1	6.25	940	72.50%



Figure 39 - View of the backhoe tooth used in Set E



Figure 40 - View of the damage caused by the backhoe tooth application

vi) Test Set F:

The testing parameters of this set are shown in Table 24. The tests were performed on 16-inch diameter pipes with grade X60 and wall thickness 0.25 inches. The gouge depths in all the tests were kept constant at a depth of about 0.13 inches and the pipes were tested at a constant dent depth of 1.25 inches. Figure 41 shows the results of the tests. The results were repeatable in tests 2 and 3. The indentations of test 1 was performed incrementally to identify the dent depth which result in a pipe failure at 40% SMYS. The incremental indentation may have caused the development of surface cracks and resulted in a pipe failure at a lower level than in tests 2 and 3.

Table 24 - Testing parameters and results of Set-F

Set F (6) - Pipe Grad	le X60 (m	achine go	ouge)					
Test	Pipe Grade	Diam.	D/t	Gouge	Gouge	Dent	Ho/D	Failure	Failure
		(inch)		(inch)	(angle)	(inch)	(%)	(psig)	as (%SMYS)
1	X60	16	64	0.13	90	1.25	7.81	750	40%
2	X60	16	64	0.135	90	1.25	7.81	890	48%
3	X60	16	64	0.13	90	1.25	7.81	980	52%

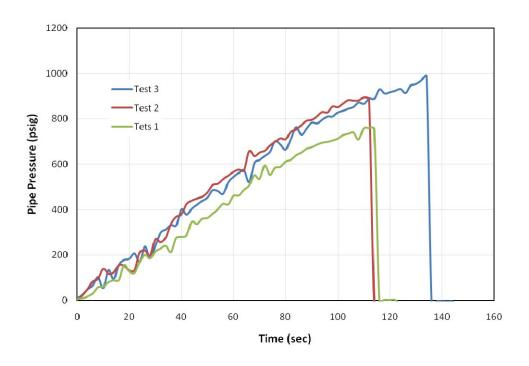


Figure 41 - Results of pressure tests of Set F



Figure 42 - View of the pipe at the completion of pressure test 3

Chapter 6

Numerical Modeling of Pipe Damage

Introduction

The impact of mechanical damage to a pipeline typically results in a gouge and dent on the pipe surface. In some cases, the pipeline may not be punctured and no release of the pressurized gas or fluid takes place. If the damage is not discovered and addressed immediately, the typically resulting gouge and dent may leave the pipeline in a significantly weakened condition such that it will later develop a leak or a rupture.

When such gouge and dent are eventually discovered, the operator of the pipeline needs to consider a response that will assure the continued serviceability of the pipeline. A helpful tool in this situation would be a reliable means for predicting the failure pressure of the pipe at the gouge-and-dent-weakened area. A reliable model or accept/reject criterion would enable the operator to decide whether or not a repair is needed. Such a model would have to account for all aspects of the pipe and the extent of the damage sufficiently well that the operator could have confidence that no failure will occur if no repair is made.

The following characteristics have significant effects on the severity of a gouge and dent in the pipes (9):

- Diameter and wall thickness of the pipe,
- Strength and strain-hardening characteristics of the pipe material,
- Toughness and tearing resistance of the material,
- Operating hoop stress level,
- Depth and length of the gouge,
- Depth of the gouge,
- Depth and length of the dent,
- Orientation of the damage with respect to the axis of the pipe.

One more factor that must be considered in the evaluation of mechanically damaged pipe is the ductile-to-brittle transition temperature of the material. The predictive models are based on the assumption that the material will behave in relatively ductile manner in response to applied tensile stress. Most line-pipe steels are capable of exhibiting ductile tearing in the presence of a crack subjected to quasi-static loading rates.

Two models were evaluated to provide the acceptance/failure criteria for the mechanical damage to low stress pipelines. These models are the Dent-Gouge Fracture Model (DGFM) and

the EPRG Simplified model. A comprehensive review of the validation of these two models is in Attachment B.

The Dent-Gouge Fracture Model

The Dent-Gouge Fracture Model (DGFM) (10) was developed by British Gas researchers with support from the European Pipeline Research Group (EPRG). It is a semi-empirical model, derived from thin-shell theory and calibrated by means of pressure tests of rings and vessels fabricated with mechanical-damage-simulating defects (11). The DGFM is meant to be applied to axially oriented damage in a ductile steel pipe consisting of an infinitely long (length not less than ½ pipe diameter based on experiments used to validate the model) "smooth" dent (radius of curvature in any direction not less than five times the wall thickness of the pipe) containing a sharp notch. While re-rounding is considered in the model, the correction of dent depth for rerounding remains an area of considerable uncertainty (9).

EPRG Simplified Model

The EPRG also has compiled a "simplified" model for screening mechanical-damage defects (10). The simplified model is based on the lower bound of all test data on mechanically damaged pipe, and it offers an attractive approach for operators of low-stress pipelines. The use of the simplified model depends on knowing only the gouge depth, the dent depth measured at the operating pressure corrected for re-rounding, the diameter of the pipe, the wall thickness of the pipe, and the operating hoop stress level. The dent and gouge are assumed to be infinitely long, and the material is assumed to behave in a ductile manner (2/3-size Charpy V-notch upper-shelf energy of at least 18 ft- lb). The simplified model is illustrated in Figure 7.

Comparison of Test Results with EPRG and Plastic Collapse Models

i) <u>Material Test Results</u>

A total of 4 materials were used for the test program, two 8-inch nominal diameter and two 16-inch diameter specimens. Table 25 lists the material properties of the test sets of the testing program. Tensile and Charpy V-notch tests were performed on all of the specimens. The tensile test orientation was in transverse directions for all of the specimens and in the longitudinal direction for two of the specimens. Finally, chemistry tests were performed on all specimens. The results of the tensile tests are summarized in Table 25. The Charpy V-notch tests were carried out at test temperatures of 68°F, 32°F and 0°F. The results of the Charpy V-notch tests are summarized in Table 26 and the results of the chemical testing are summarized in Table 27.

Table 25 - Tensile test results for test pipe samples

				Longitudina	ıl	Transverse				
Test Series	Diameter, in		Yield stress, psi	Tensile strength, psi	Elongation,	Yield stress, psi	Tensile strength, psi	Elongation,		
A	8.625	X52	57,500	73,000	41.5	51,000	71,000	42.8		
A, B, C, D, E	16	X42	50,000	68,000	45.8	48,000	68,500	45.0		
B, C, D	8.625	X42				54,000	74,000	34.6		
F	16	X60				59,000	76,000	33.5		
F*	16	X60				65,500	80,500	35.2		
* rerun of F			-							

Table 26 - Charpy V-notch results for test pipe samples

		68 F	test temperatu	ıre	32 F	test temperatu	ıre	0 F test temperature				
Test Series	Diamter, in.	Full size Charpy energy, ft- lbs	Lateral expansion, mils Shear area, %		Full size Charpy energy, ft- lbs	Lateral expansion, mils	Shear area, %	Full size Charpy energy, ft- lbs	Lateral expansion, mils	Shear area, %		
A	8.625	30	26	90	14	11	45	12	8	25		
A, B, C, D, E	16	44	35	100	40	33	95	40	33	95		
B, C, D	8.625	43.8	52	100	41.8	49	100	38.5	45	95		
F	16	149.3	82	100	145.3	64	100	140.7	72	100		

Table 27 - Results of chemical testing for test pipe samples

Grade	1D2	Sample	С	Mn3	P1	S	Si 1	Cu 5	Sn 2	Ni 2	Cr 1	Mo 2	A1 7	V 3	Nb	Zr 2	Ti 4	В1	Ca 3	Co 1
		1	0.173	1.040	0.009	0.006	0.205	0.046	0.008	0.017	0.033	0.005	0.028	0.002	0.001	0.001	0.002	0.0001	0.0000	0.003
X52	8	2	0.174	1.060	0.010	0.009	0.207	0.046	0.009	0.016	0.033	0.004	0.027	0.002	0.001	0.001	0.002	0.0001	0.0000	0.003
		ave	0.174	1.050	0.010	0.007	0.206	0.046	0.008	0.016	0.033	0.004	0.027	0.002	0.001	0.001	0.002	0.0001	0.0000	0.003
		1	0.164	0.800	0.012	0.006	0.016	0.029	0.001	0.010	0.013	0.008	0.038	0.000	0.001	,001	0.001	0.0001	0.0000	0.003
X42	16	2	0.163	0.800	0.012	0.005	0.016	0.028	0.001	0.010	0.013	0.007	0.038	0.000	0.001	0.001	0.001	0.0001	0.0000	0.003
		ave	0.163	0.800	0.012	0.006	0.016	0.029	0.001	0.010	0.013	0.007	0.038	0.000	0.001	0.001	0.001	0.0001	0.0000	0.003
		1	0.166	1.020	0.010	0.010	0.221	0.039	0.003	0.037	0.038	0.006	0.029	0.002	0.001	0.001	0.002	0.0010	0.0000	0.004
X42	8	2	0.165	1.010	0.009	0.008	0.218	0.039	0.003	0.037	0.038	0.006	0.029	0.002	0.001	0.001	0.002	0.0010	0.0000	0.004
		ave	0.166	1.015	0.010	0.009	0.220	0.039	0.003	0.037	0.038	0.006	0.029	0.002	0.001	0.001	0.002	0.0010	0.0000	0.004
		1	0.049	1.110	0.010	0.002	0.203	0.096	0.005	0.042	0.047	0.016	0.021	0.003	0.030	0.001	0.009	0.0001	0.0017	0.004
X60	16	2	0.050	1.110	0.011	0.002	0.205	0.097	0.006	0.042	0.048	0.016	0.020	0.003	0.031	0.002	0.009	0.0001	0.0016	0.003
	ĺ	ave	0.050	1.110	0.011	0.002	0.204	0.097	0.006	0.042	0.048	0.016	0.021	0.003	0.031	0.002	0.009	0.0001	0.0017	0.004

The transverse tensile results for the 8-inch, Grade X52 pipe was slightly under the yield strength requirement for Grade X52 but the longitudinal yield strength was over the requirement. The remaining specimens meet the requirements for their corresponding grades. Based on the Charpy results, the 8-inch pipe used for Test Set A has a ductile to brittle transition temperature somewhere between 32 F and 68 F whereas the remaining pipe specimens are above their transition temperature for the entire temperature range.

ii) Comparison of Burst Pressure with EPRG and Plastic Collapse Models

The material test results along with the damage test results were used with the EPRG simplified model, the EPRG advanced model and a simple plastic collapse model to predict the burst pressure of the test specimens. The results from the 6 test sets along with the predicted burst pressures from the EPRG advanced and plastic collapse models are shown in Table 28. Table 29 contains a comparison of the failure stress with the pipe SMYS. A comparison of the results with the EPRG simplified model is shown in Figure 43.

The EPRG simplified model is based on a graphical approach. The dent depth over the pipe diameter is plotted on the X-axis and the gouge depth over the pipe wall thickness is plotted on the Y-axis for the damage under consideration. These results are compared with the graphical model which is based on operating stress range. These ranges are less than 30% SMYS, 30-50% SMYS and 50-72% SMYS. If the combination normalized dent depth and normalized gouge depth falls outside a particular curve it is likely to result in a failure at pressures less than the maximum value for the curve. All of the points were well outside of the 30% SMYS curve so they would be expected to fail at pressures that resulted in stresses that were less than 30% SMYS. The actual test failure stress levels ranged from 23-128% SMYS.

Table 28 compares the results of the testing with the EPRG advanced model. The equation for the EPRG model is:

$$\frac{\sigma_{\theta}}{\overline{\sigma}} = \frac{2}{\pi} a \cos \left[\exp \left\{ -\left[113 \frac{1.5 \cdot \pi \cdot E}{\overline{\sigma}^2 \cdot A \cdot d} \left(Y_1 \cdot \left(1 - 1.18 \frac{H_0}{D} \right) + Y_2 \cdot \left(10.2 \frac{R}{t} \frac{H_0}{D} \right) \right)^{-2} \cdot \exp \left[\frac{\ln(0.738 \cdot C_V) \cdot K_1}{K_2} \right] \right] \right\} \right]$$
(1)

where

$$\overline{\sigma} = 1.15 \cdot \sigma_{Y} \cdot \left(1 - \frac{d}{t}\right) \tag{2}$$

$$Y_1 = 1.12 - 0.23 \frac{d}{t} + 10.6 \left(\frac{d}{t}\right)^2 - 21.7 \left(\frac{d}{t}\right)^3 + 30.4 \left(\frac{d}{t}\right)^4$$
(3)

$$Y_2 = 1.12 - 1.39 \frac{d}{t} + 7.32 \left(\frac{d}{t}\right)^2 - 13.1 \left(\frac{d}{t}\right)^3 + 14.0 \left(\frac{d}{t}\right)^4$$
 (4)

$$K_1 = 1.9$$
 (5)

$$K_2 = 0.57$$
 (6)

$$H_0 = 1.43H_r$$
 (7)

 σ_{θ} = predicted failure pressure, units must be consistent with $\overline{\sigma}$,

E = modulus of elasticity of the pipe, 207,000 Nmm²,

A = area of 2/3 Charpy specimen, 53.55 mm,

d = depth of gouge, mm,

D = pipe diameter, any units consistent with H_0 ,

R = D/2

t = wall thickness of pipe, any units consistent with D and d,

 $C_V = 2/3$ size Charpy energy, Joules,

 σ_{Y} = yield strength of pipe, Nmm², and

 H_r = dent depth after re-rounding, any units consistent with D.

The failure pressures predicted by this model are 22-120% of the actual failure pressure. Equation 2 is the plastic collapse solution for a plate with an infinitely long groove. The burst pressure was calculated using this equation and is shown in Table 29. The predicted pressure is 74 to 263% of the actual failure pressure.

Table 28 - Comparison of pressure test results s with EPRG advanced and Plastic collapse models

Specimen No.	Grade	Diameter, in	Wall thickness, in	Yield stress, psi	Gouge depth, in	d/t	Dent depth, in	D _{dent} /D	Denting stress/ SMYS	Burst pressure, psig	EPRG predicted burst pressure, psig	EPRG Pred/Act	Plastic collapse predicted failure pressure, psig	PC Pred/Act
A-1	X42	16	0.250	48,000	0.085	0.340	1.300	0.081	0.40	1,083	337	0.31	1,139	1.05
A-2	X42	16	0.250	48,000	0.095	0.380	1.410	0.088	0.40	854	282	0.33	1,070	1.25
A-3	X42	16	0.250	48,000	0.090	0.360	1.200	0.075	0.40	1,440	344	0.24	1,104	0.77
A-4	X52	8.625	0.250	51,000	0.090	0.360	0.820	0.095	0.40	2,550	652	0.26	2,176	0.85
A-5	X52	8.625	0.250	51,000	0.091	0.364	1.100	0.128	0.40	2,300	496	0.22	2,162	0.94
A-6	X52	8.625	0.250	51,000	0.089	0.356	1.000	0.116	0.40	2,500	552	0.22	2,190	0.88
B-1	X42	8.625	0.250	54,000	0.100	0.400	0.000	0.000	0.40	2,650	2,160	0.82	2,160	0.82
B-2	X42	8.625	0.250	54,000	0.000	0.000	1.240	0.144	0.40	4,000	3,600	0.90	3,600	0.90
B-3	X42	16	0.250	48,000	0.100	0.400	0.000	0.000	0.40	1,400	1,035	0.74	1,035	0.74
B-4	X42	16	0.250	48,000	0.000	0.000	1.390	0.087	0.40	1,720	1,725	1.00	1,725	1.00
C-1	X42	8.625	0.250	54,000	0.150	0.600	1.000	0.116	0.20	720	362	0.50	1,440	2.00
C-2	X42	8.625	0.250	54,000	0.130	0.520	0.750	0.087	0.20	750	611	0.81	1,728	2.30
C-3	X42	8.625	0.250	54,000	0.100	0.400	1.000	0.116	0.20	820	679	0.83	2,160	2.63
C-4	X42	16	0.250	48,000	0.095	0.380	2.000	0.125	0.20	475	203	0.43	1,070	2.25
D-1	X42	8.625	0.250	54,000	0.100	0.400	1.000	0.116	0.20	820	679	0.83	2,160	2.63
D-2	X42	8.625	0.250	54,000	0.100	0.400	0.500	0.058	0.20	1,000	1,196	1.20	2,160	2.16
D-3	X42	8.625	0.250	54,000	0.100	0.400	2.000	0.232	0.00	300	358	1.19	2,160	7.20
D-4	X42	16	0.250	48,000	0.100	0.400	2.000	0.125	0.20	475	193	0.41	1,035	2.18
E-1	X42	16	0.250	48,000	0.100	0.400	1.000	0.063	0.20	815	364	0.45	1,035	1.27
E-2	X42	16	0.250	48,000	0.100	0.400	1.300	0.081	0.20	550	288	0.52	1,035	1.88
E-3	X42	16	0.250	48,000	0.100	0.400	1.000	0.063	0.20	940	364	0.39	1,035	1.10
F-1	X60	16	0.250	65,500	0.130	0.520	1.250	0.078	0.20	750	583	0.78	1,130	1.51
F-2	X60	16	0.250	65,500	0.135	0.540	1.250	0.078	0.20	890	547	0.61	1,083	1.22
F-3	X60	16	0.250	65,500	0.130	0.520	1.250	0.078	0.20	980	583	0.59	1,130	1.15

Table 29 - Comparison of final burst pressure with SMYS

Specimen No.	Grade	Diameter, in	Wall thickness, in	Burst pressure, psig	Pressure at yield*, psig	Burst stress/yield stress	Burst stress/SMYS
A-1	X42	16	0.25	1,083	1,500	0.72	0.83
A-2	X42	16	0.25	854	1,500	0.57	0.65
A-3	X42	16	0.25	1,440	1,500	0.96	1.10
A-4	X52	8.625	0.25	2,550	2,957	0.86	0.85
A-5	X52	8.625	0.25	2,300	2,957	0.78	0.76
A-6	X52	8.625	0.25	2,500	2,957	0.85	0.83
B-1	X42	8.625	0.25	2,650	3,130	0.85	1.09
B-2	X42	8.625	0.25	4,000	3,130	1.28	1.64
B-3	X42	16	0.25	1,400	1,500	0.93	1.07
B-4	X42	16	0.25	1,720	1,500	1.15	1.31
C-1	X42	8.625	0.25	720	3,130	0.23	0.30
C-2	X42	8.625	0.25	750	3,130	0.24	0.31
C-3	X42	8.625	0.25	820	3,130	0.26	0.34
C-4	X42	16	0.25	475	1,500	0.32	0.36
D-1	X42	8.625	0.25	820	3,130	0.26	0.34
D-2	X42	8.625	0.25	1,000	3,130	0.32	0.41
D-3	X42	8.625	0.25	300	3,130	0.10	0.12
D-4	X42	16	0.25	475	1,500	0.32	0.36
E-1	X42	16	0.25	815	1,500	0.54	0.62
E-2	X42	16	0.25	550	1,500	0.37	0.42
E-3	X42	16	0.25	940	1,500	0.63	0.72
F-1	X60	16	0.25	750	2,047	0.37	0.40
F-2	X60	16	0.25	890	2,047	0.43	0.47
F-3	X60	16	0.25	980	2,047	0.48	0.52
* Bases on actual yield stress.							

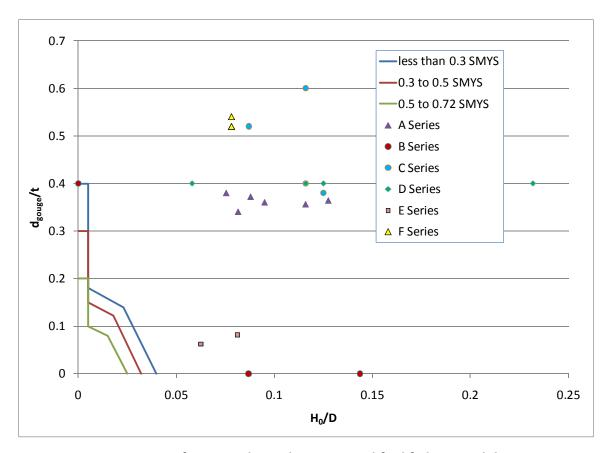


Figure 43 - Comparison of test results with EPRG simplified failure model

iii) Discussion of Test Results

The simple EPRG model on the other hand is based on a regression of the test data that was used to develop the advanced model (12). The advanced EPRG model is a fracture mechanics based model that assumes the gouge is crack-like. The advanced EPRG model also takes into account the plastic collapse of the pipe through the term in Equation 2. Both the simple and advanced EPRG models tend to give conservative results although the advanced EPRG model did produce non-conservative results in 2 cases. The basic plastic collapse solution on the other hand results in non-conservative solutions most of the time.

Figure 43 plots the normalized gouge and dent depths with respect to the simple damage criterion. Based on their locations all of these data points would be expected to fail at less than 0.30 SMYS. As can be seen in Table 29 only 2 of the tests failed at or less than 0.30 SMYS.

Figure 44 shows a comparison of the predicted failure pressure with the actual failure pressure for the advanced EPRG model. These calculations are based on the original crack size and does not account for any crack growth that may have occurred during the denting process. The

correlation coefficient for these results is 0.76. The average value of the predicted failure pressure over the actual failure pressure is 0.61 with a standard deviation of 0.30.

There were 2 cases in the Test Set-D where the predicted failure pressure was not conservative. The D Series of tests looked a different gouge shapes. Test 2 of the Set-D used a gouge angle of 45 degrees and dent depth of 5.8 percent of the pipe diameter. Test 3 of the Set-D had a rounded gouge with a dent depth of 23.2 percent of the diameter. Correlations of the advanced EPRG model with other data have shown a scatter of the test data on both sides of the 1-to-1 line (13). The conservatism in the most of the existing data may be a result of the low internal pressure when the dents were installed.

Figure 45 shows the predicted failure pressure with the actual failure pressure for the plastic collapse model based on Equation (2). The model does a fairly good job of predicting the failure pressure for Test Series A and B. The correlation coefficient for these results is 0.71. The average value of the predicted failure pressure over the actual failure pressure is 1.70 with a standard deviation of 1.33.

Conclusion

The simple EPRG model predicts that all of the test specimens would fail at less than 0.30 SMYS. In reality, only two of the specimens failed at or less than 0.30 SMYS. No failures occurred at less than the predicted pressure. Based on the test results, The EPRG simplified model can be conservatively used to evaluate mechanical damage in low MAOP pipelines.

The advanced EPRG model conservatively predicted failure in most cases. There were 2 neoconservative predictions. The model has the advantage of predicting a failure pressure as opposed to the go/no go criteria in the simplified model. If the advance model were to be used, we would recommend using a lower bound estimate of failure as is recommended in Reference 13.

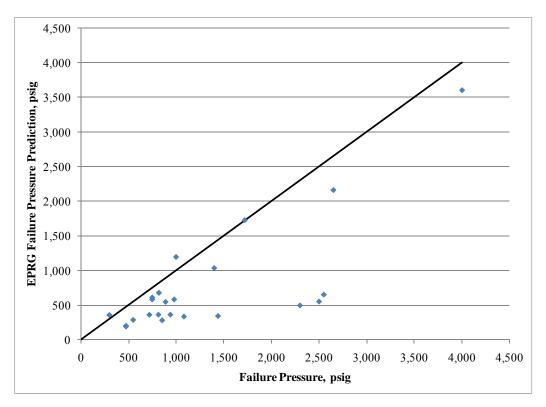


Figure 44 - Comparison of advanced EPRG failure prediction with actual failure pressure

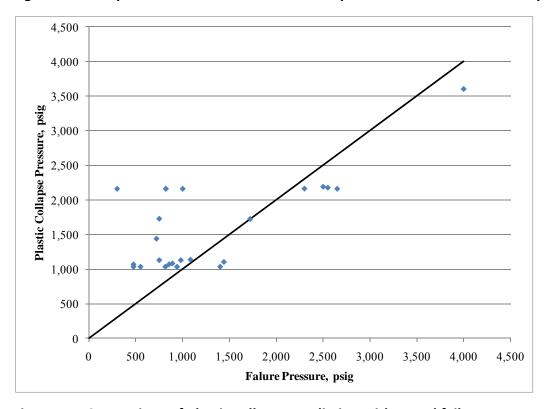


Figure 45 - Comparison of plastic collapse prediction with actual failure pressure

Chapter 7

Implementation of Repair Options in the Flaw Acceptance Criteria Program

Introduction

A web-based computer program was developed to provide a simplified procedure for pipeline operators to determine the criteria for repair needs of damaged gas pipelines operating below 40% SMYS. The program evaluates the repair criteria for damages due to:

- (a) Mechanical damage, with delayed failure mode (i.e. no leak or rupture)
- (b) External corrosion.

The evaluation of the repair needs of the pipeline due to mechanical damage is based on the 'European Pipeline Research Group (EPRG) Simplified Criterion' for flaw acceptance. This criterion was evaluated in the previous chapters and is used to determine if pipe repair by grinding and recoating, as per ASME requirements (1), is sufficient at this stress level, or other repair or replacement options are required.

The user enters pipe information, dent and gouge measurements, and operating pressure to evaluate the flaw acceptance criteria.

For the external corrosion damage, the program utilizes the equations in the ASME/ANSI B31G for the determination of the maximum allowable longitudinal extent of corrosion and the safe operating stress of the remaining pipe metal. The user enters pipe information, corrosion depth and length to obtain allowable length and safe pressure similar to the tables and charts provided in the B31G manual (14).

The program provides an approach to evaluate the mechanical and corrosion damage for repair of pipelines operating at stress levels below 40% SMYS. The program does not address the repairs of the following conditions:

- -Damage that causes leak or rupture of the pipeline,
- -Damage that affect pipeline curvature at girth welds or longitudinal seam welds,
- -Damage that causes Stress Corrosion Cracking (SCC),
- -Mechanical damage that causes flaws other than smooth dents and gouges to the external pipeline surface.

Program Data Entry

The program is located at the web address: http://apps.gastechnology.org/pipedamage

The access to the program is secured and the user may contact the e-mail address provided at the 'Log In' page to obtain the required User ID and a Password.

A view of the 'Data Entry Page' of the program is shown in Figure 46. The user selects the type of damage and pipe and damage characteristics shown in the figure.

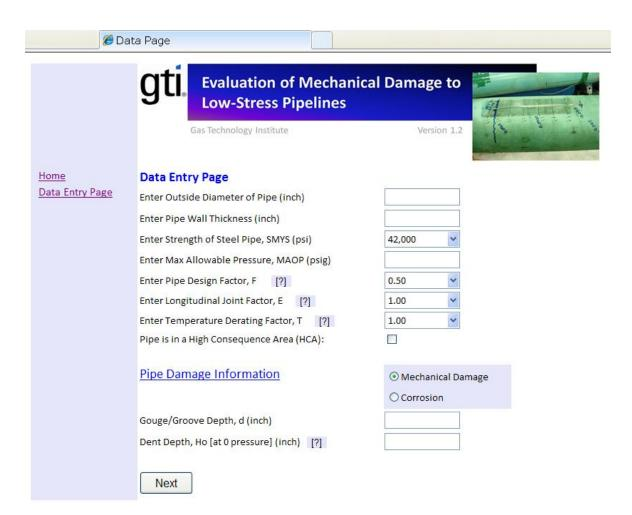


Figure 46 - Data entry page of the program

i) Evaluation of Mechanical Damage

The program first evaluates the pipe operating stress as a percentage of SMYS of the pipe material:

- At operating stress levels at or above 40% SMYS, the program recommends pipe repair by cutting and replacing the damaged part or repair by a method with reliable engineering tests according to CFR 49 Part 192.713 and ASMS/ANSI B31.8-851. Figure 47 shows an example of the output for operating stresses > 40% SMYS.
- The program applies the EPRG criteria if the operating stress level is below 40% SMYS.
 - a. The program recommends repair by grinding if the pipe passes the EPRG acceptance criteria. Further repair options are at operator's discretion and are referenced in ASME/ANSI B31.8-851. Figure 48 and Figure 49 show output examples of pipes passing the EPRG criteria.
 - b. If the pipe fails the EPRG criteria, the pipe section should be replaced or repaired by a method with reliable engineering tests as shown in the example in Figure 50.

If the pipeline is located in a High Consequence Area (HCA), the program refers to the integrity management requirements which are listed in the following references:

- Code of Federal Regulations CFR 49 Part 192, Subpart O-Integrity Management
- ASME/ANSI B31.8S Managing System Integrity of Gas Pipelines.

In HCA areas, pipeline operators should refer to the repair scheduling options listed in CFR 49 Part 192.933 and to the repair methods listed in Table 4 in ASME/ANSI B31.8S.

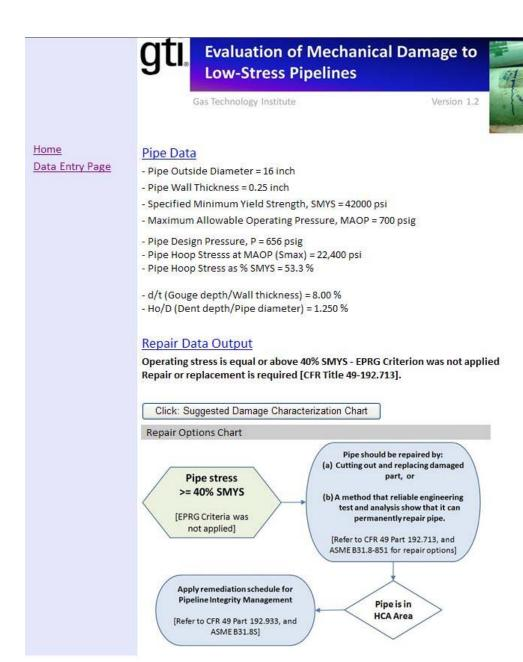


Figure 47 - Output example with operating stress larger than 40% SMYS

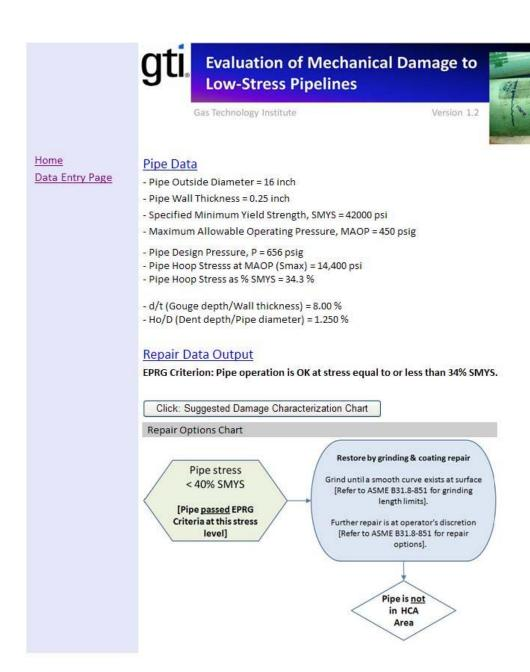


Figure 48 - Output example of damage passing EPRG criteria and not in HCA area

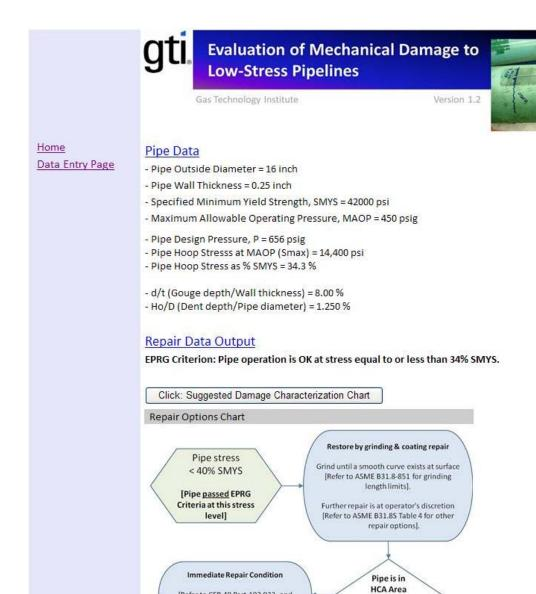


Figure 49 - Output example of damage passing EPRG criteria and in HCA area

[Refer to CFR 49 Part 192.933, and

ASME B31.8S for scheduling

remediation for integrity management]

With dents

and gouges

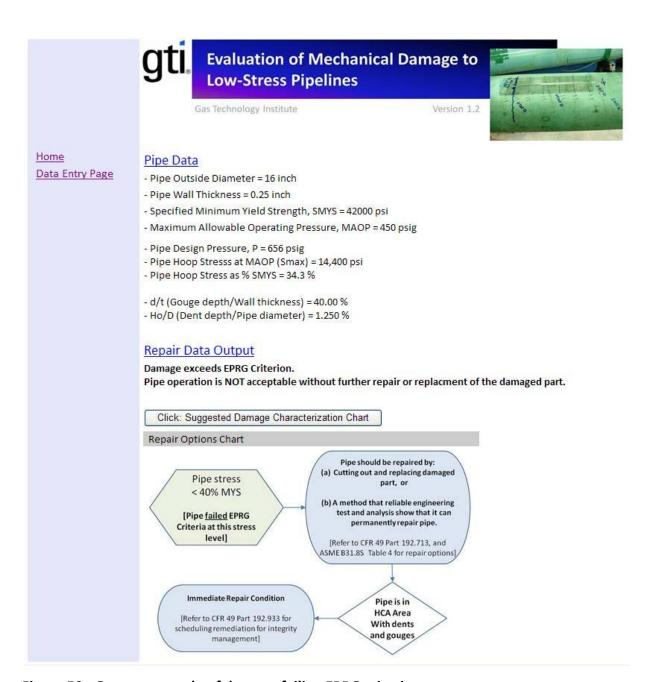


Figure 50 - Output example of damage failing EPRG criteria

ii) Evaluation of Corrosion Damage

This part of the program determines the remaining strength of corroded pipelines according to the ASME 31G-1991 Manual (14). The scope of the ASME manual includes:

- (a) External corrosion on weldable steel pipeline materials described in ASTM A53, ASTM A381, and API 5L.
- (b) The procedure does not evaluate the remaining strength of corroded girth or longitudinal welds, defects caused by mechanical damage, or defects introduced during manufacturing.
- (c) The criteria for remaining strength of corroded pipe are based on the ability of the pipe to carry its internal pressure. It should not be applied to other significant secondary stresses, such as bending.
- (d) The procedure does not apply to leaking pipes.

In the ASME procedures, corrosion length is defined as the extent of corrosion along the longitudinal axis of the pipe as shown in Figure 51.

The program calculates the maximum allowable corrosion length along the longitudinal axis of the pipe. The program also determines the safe maximum operating pressure (P') for the corroded length as entered by the user. Figure 52 shows an example of the program output for the calculation of the remaining strength of the corrosion damage.

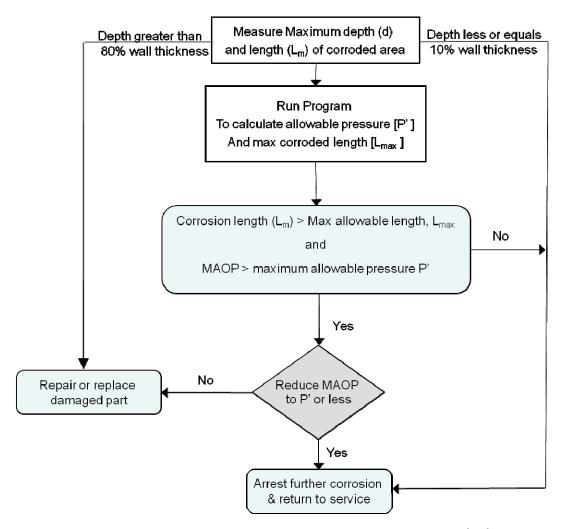


Figure 51 - Procedure for corrosion repair criteria, after ASME B31G (14)



Data Entry Page

Remaining Strength of Corroded Pipe

[See ASME B31G-1991 for scope, procedure, and limitations]

Pipe Data

- Pipe Outside Diameter = 16 inch
- Pipe Wall Thickness = 0.25 inch
- Specified Minimum Yield Strength, SMYS = 42000 psi
- Maximum Allowable Operating Pressure, MAOP = 650 psig
- Maximum Corrosion Depth (inch) = 0.1
- Length of Corroded Area (inch) = 4

Corrosion Data Output

- Design Pressure of Uncorroded Pipe, P = 656 psig
- For design pressure P, length of the corroded area should not exceed: 2.13 inch.

Safe Pressure of Corroded Pipe, P' = 609 psig MAOP exceeds safe pressure for corroded pipe. Repair or reduce MAOP to safe pressure of 609 psi.

Figure 52 - Example of program output of corrosion damage evaluation

Chapter 8

Evaluation of Wrinkle Bends

An investigation of the effect of wrinkle bends on pipe stresses was performed in Task 5 of the research project. This work was performed to provide a state-of-the art evaluation of the effects of wrinkles on buckles and bends in pressurized gas lines. Most of the current research work in this area is based on theoretical analysis and Finite Element modeling to investigate the state of strains and performance of wrinkle-damaged pipes. In most of these studies, stress concentration effects were used with suitable fatigue damage models to estimate the effect of ripple parameters on service life of the wrinkled section.

A comparative review of the various assumptions and analysis of these models was performed with the consultant: Kiefner and Associates, Inc. The report associated with this study is presented in Appendix C.

The results of the investigation of the incident record suggest that the vast majority of wrinkle bends do not pose a threat to pipeline safety under normal circumstances. The challenge is to use information available to the operator to identify the small proportion of wrinkle bend installations that ever could pose a threat. The report findings are summarized as follows:

Wrinkle bends with depths up to 2.5 percent of the diameter and aspect ratios (height of wrinkle over the wave length of the wrinkle) less than 0.13 are acceptable provided the following threats are not present:

- Aggressive longitudinal stress cycling of the line,
- Ground movement, i.e. mine subsidence or landslides,
- Corrosion, and stress corrosion cracking.

The threats stated above have not been quantified at this time. This is an area that needs further research.

It is conceivable that wrinkle bends classified as severe can remain in the pipeline if the threat level is low enough. This may be a more desirable option than exposing the bend for examination and increasing the potential threat as described below.

If it is necessary to expose a wrinkle bend or the pipe in the vicinity of a wrinkle bend care should be taken to return the pipe to its original condition of support, soil consolidation, and restraint of the bend. One method of accomplishing this is to mix cement into the soil before reburying the pipe. Composite reinforcement of the bend shows promise for increasing the fatigue resistance of wrinkle bends.

References

- 1. ASME B31.8, Gas Transmission and Distribution Piping Systems. American Society of Mechanical Engineers, 2003.
- 2. Gas Facts. American Gas Association, AGA, 2005.
- 3. Flaw Acceptance Criteria and Repair Options for Low Stress Gas Pipelines. Operation Technology Development (OTD), Gas Technology Institute, GTI Report 20053, 2007.
- 4. Kiefner, J., and Francini, R., Models and Experimental Studies of the Effect of Mechanical Damamge on the Failure Stress Levels of Pressurized Pipes. Report No. 07-52, Kiefner & Associates, for Gas Technology Institute, 2007.
- 5. Eiber, R.J., Maxey, W.A., Bert, C.W., and McClure, G.M., The Effects of Dents on the Failure Characteristics of Line Pipe. NG-18 Report No. 125, American Gas Association Catalog No. L51403, 1981.
- 6. Hopkins, P., A Study of External Damage of Pipelines. 7th NG-18/ EPRG Joint Biennial Technical Meeting on Line Pipe Research, Calgary, Alberta, Canada, 1988.
- 7. *Kiefner, J.F., and Alexander, C.R., Repair of Pipeline Dents Containing Minor Scratches.* Final Report on Contract No. PR 218-9508, PRC International,1999.
- 8. *Maxey, W.A., Outside Force Defect Behavior.* NG-18 Report No. 162, Pipeline Research Committee, American Gas Association, 1986.
- 9. Kiefner and Associates, Models and Experimental Studies of the Effect of Mechanical Damage on the Failure Stress Levels of Pressurized Steel Pipes. Report No. 07-52, Gas Technology Institute, 2007.
- 10. Roovers, P., Galli, M.R., Blood, R.J., Mareski, U., Steiner, M., and Zarea, M., EPRG Methods for Assessing the Tolerance and Resistance of Pipelines to External Damage. 3rd Pipeline International Conference, 1999.
- 11. Cosham, A. and Hopkins, P., The Pipeline Defect Assessment Manual, Proceedings of IPC'02, 4th International Pipeline Conference, Calgary, Canada, 2002.
- 12. Corder, I and Chatain, P., EPRG Recommendations for the Assessment of the Resistance of pipelines to External Damage. EPRG/PRC 10th Biennial Joint Technical Meeting on Linepipe Research, 1995.
- 13. Cosham, A and Hopkins, P, The Pipeline Defect Assessment Manual. Penspen Limited, 2003.
- 14. ASME/ANSI B31G Manual for Determining the Remaining Strength of Corroded Pipelines. 1991.

Attachment A - Results of the testing Program

SET A					
Test	Pipe Grade	Diam.	Failure Load	Failure	Picture
		(inch)	(psig)	as (%SMYS)	
1	X42	16	1083	82.36	
2	X42	16	854	64.94	
3	X42	16	1440	109.51	
4	X52	8.625	2550	84.58	No on the second
5	X52	8.625	2300	76.29	
6	X52	8.625	2490	82.59	

SET B					
Test	Pipe Grade	Diam.	Failure Load	Failure	Pictures
		(inch)	(psig)	as (%SMYS)	
1	X42	8.625	2650	108.83	
2	X42	8.625	4000	164.27	
3	X42	16	1400	106.46	
4	X42	16	1720	130.80	

SET C					
Test	Pipe Grade	Diam. (inch)	Failure Load (psig)	Failure as (%SMYS)	Pictures
1	X42	8.625	720	29.57	
2	X42	8.625	750	30.80	Set C Test2 Page-27 Gays-27
3	X42	8.625	820	33.68	
4	X42	16	475	36.12	Set (Tepty Fart-3 System Note: 35

SET D					
Test	Pipe Grade	Diam. (inch)	Failure Load (psig)	Failure as (%SMYS)	Pictures
1	X42	8.625	820	33.68	P. Con. Take
2	X42	8.625	1000	41.07	Set D Set D Set J Pro. 31 Parse of P VI'
3	X42	8.625	300	12.32	
4	X42	16	475	36.12	

SET E					
Test	Pipe Grade	Diam. (inch)	Failure (psig)	Failure as (%SMYS)	Pictures
1	X42	16	815	62%	Test Eco.
2	X42	16	550	42%	Set E(s) Test 2-5 Tes
3	X42	16	940	72.50%	5 st (5) (5) (5) (7) (7) (7) (7) (7) (7) (7) (7) (7) (7

SET F					
Test	Pipe Grade	Diam. (inch)	Failure (psig)	Failure as (%SMYS)	Pictures
1	X60	16	750	40%	Set (0) Set (0) Furt - 7 Gurt - 13
2	X60	16	890	48%	Set F(c) Test 2 12.2 12.35 10.59 myt 1.35 denot
3	X60	16	980	52%	Set F(6) Test 3 ROD. 35 cm (1) 13 mag. 13 s mag.

Models and Experimental Studies of the Effect of Mechanical Damage on the Failure Stress Levels of Pressurized Steel Pipes

Report No. 07-52

Submitted to Gas Technology Institute

By,

John F. Kiefner and Robert B. Francini Kiefner and Associates, Inc. 585 Scherers Court Worthington, Ohio 43085

EXECUTIVE SUMMARY

This report describes an investigation into models intended to assess the effects of mechanical damage on the serviceability of steel pipelines. The purposes of this investigation were to identify a satisfactory existing model for predicting the effects of mechanical damage on natural gas pipelines being operated at stress levels of 40 percent or less of the specified minimum yield strengths of the materials and to facilitate the planning of further experiments that would provide a satisfactory validation of the model in the event that the experiments conducted to date do not do so. This work was undertaken as part of a research project sponsored by the Gas Technology Institute and Operations Technology Development (GTI-OTD). The GTI-OTD project is aimed at development of a mechanical damage model that can be used with a high level of confidence by operators of low-stress natural gas pipelines comprised of low-carbon and low-alloy steels to determine appropriate repair responses when segments of mechanically damaged pipe are discovered.

One of the models investigated is referred to as the dent-gouge fracture model (DGFM), and it was developed by British Gas researchers with assistance from the European Pipeline Research Group (EPRG). The other model investigated is referred to as the empirical Q-factor model (EQFM), and it was developed by Battelle researchers with the support of the American Gas Association's Pipeline Research Committee (now Pipeline Research Council International). Both organizations and others have conducted full-scale research to examine the effects of mechanical damage on pressurized pipelines, and that research has been used by a number of investigators to validate the two models mentioned above in addition to other proprietary models not discussed in this report. It is noted that not all of the available data were used in this report. The data used were, however, reasonably representative of the types of experiments that have been conducted for the purpose of understanding mechanical damage.

Although the focus was on the two models mentioned above, the overall intent of GTI-OTD is to develop a simple go, no-go criterion, possibly based on one of these models, to permit pipeline operators to quickly and easily assess the severity of mechanical damage whenever it is discovered on an operating pipeline. The EPRG has already created a simplified version of the DGFM. Accordingly, this effort includes an assessment of the EPRG's "simplified" model developed as an adjunct to the DGFM. This EPRG simplified model is simple to use and could meet the desires of GTI-OTD for a go, no-go criterion if proven reliable.

As described herein, the initial comparisons between the model predictions and the experiments revealed that neither of the current models satisfactorily accounts for the variability of the data. It appeared that the dent-gouge fracture model is the better of the two, but the weak correlations between the model predictions and the data suggest that one or more variables are not being properly taken into account. In the case of the simplified model,

the lower-bound limits did not in fact bound some of the data. The researchers that developed both of the models were aware of the lack of strong correlation between their models and the data, and they identified two likely factors that were not adequately taken into account: rerounding of a dent by internal pressure and ductile crack extension in the mechanically damaged material during re-rounding. Fortunately, a timely new study was discovered that involved using statistically-estimated amounts of ductile crack extension in the EPRG's DGFM model to make predictions of experimental results. Using this approach, the author of the new study was able to show a significantly improved correlation between the experimental results and the improved DGFM. By extension, adding crack depth to the gouge depth for the EPRG simplified model would be expected to improve its reliability as well. Indeed, a re-comparison of appropriate data where the amount of crack extension could be taken into account did reveal that the EPRG simplified model gave reliably conservative estimates of the effects of the particular damage anomalies that were not previously well-predicted when crack extension was not included.

While it was reasonably clear from the re-comparisons where crack extension is taken into account that the EPRG simplified model is a sound approach to a simple go/no-go criterion of the type sought in this project, it was decided that additional limited experiments would be worthwhile. Accordingly, the GTI staff, with advice from Kiefner and Associates specialists, assembled a damage-creating test frame and carried out tests intended to increase confidence in the EPRG simplified model. The results of these additional tests (presented herein) added to our confidence that the EPRG simplified model does constitute a sound approach to a go/no-go criterion for deciding whether or not a given damage anomaly in a low-stress pipeline needs to be repaired. Indeed, it is the recommendation of the authors that the EPRG simplified model, accounted for any ductile cracking upon re-rounding, be adopted as the go/no-go criterion for assessing damage in low-stress natural gas pipelines.

TABLE OF CONTENTS

	Page
INTRODUCTION	80
MODELS FOR PREDICTING THE FAILURE PRESSURE LEVELS OF MECHANICALLY	
DAMAGED PIPE	88
PAST EXPERIMENTS ON PIPE CONTAINING SIMULATED MECHANICAL-DAMAGE	
DEFECTS	87
INITIAL COMPARISONS OF THE MODELS TO THE RESULTS OF EXPERIMENTS	91
DISCUSSION OF THE INITIAL COMPARISONS	100
IMPROVEMENT OF THE DENT-GOUGE FRACTURE MODEL AND RE-ASSESSMENT	
SIMPLIFIED MODEL	101
REFERENCES	103

MODELS AND EXPERIMENTAL STUDIES OF THE EFFECT OF MECHANICAL DAMAGE ON THE FAILURE STRESS LEVELS OF PRESSURIZED STEEL PIPELINES

by

John F. Kiefner and Robert B. Francini

INTRODUCTION

This report describes the nature of models and supporting experiments conducted on pressurized steel pipes to assess the effects of mechanical damage on the serviceability of pipelines. The purposes of this report are to provide validation of one or more mathematical models for predicting the effects of mechanical damage and to facilitate the planning of further experiments that would provide a satisfactory validation of the models in the event that the experiments conducted to date do not do so. This work was undertaken as part of a research project sponsored by the Gas Technology Institute and Operations Technology Development (GTI-OTD). The GTI-OTD project is aimed at development of a mechanical-damage model that can be used with a high level of confidence by operators of low-stress natural gas pipelines comprised of low-carbon and low-alloy steels to determine appropriate repair responses when segments of mechanically damaged pipe are discovered.

MODELS FOR PREDICTING THE FAILURE PRESSURE LEVELS OF MECHANICALLY DAMAGED PIPE

Factors that a Model Should Consider

Mechanical damage to a pipeline occurs when mechanical equipment strikes the pipeline. Typically, such strikes or impacts occur when excavating equipment is being used in the vicinity of a buried pipeline and either the equipment operator is not aware of the existence of the pipeline or the operator is aware of it but misjudges or is misinformed about its position. The impact typically creates a gouge and dent in the pipeline. As the result of such impacts, the pipeline may be punctured or it may fail by leaking or rupturing. When that happens, the immediate release of pressurized fluid from the pipeline assures that some type of repair will have to be made to restore the serviceability of the pipeline. In some cases, however, a pipeline may be struck and no release of the fluid in it takes place. If the damage is not

discovered and addressed immediately, the typically resulting gouge and dent may leave the pipeline in a significantly weakened condition such that it will later develop a leak or a rupture.

When any such gouge and dent are eventually discovered, the operator of the pipeline needs to consider a response that will assure the continued serviceability of the pipeline. A helpful tool in this situation would be a reliable means for predicting the failure pressure of the pipe at the gouge-and-dent-weakened area. A reliable model or accept/reject criterion would enable the operator to decide whether or not a repair is needed. Such a model would have to account for all aspects of the pipe and the extent of the damage sufficiently well that the operator could have confidence that no failure will occur if no repair is made.

It is logical to expect the factors that would determine whether or not the damage is likely to cause the pipeline to leak or rupture to include

- Diameter of the pipe
- Wall thickness of the pipe
- Strength level and strain-hardening characteristics of the pipe material
- Toughness and tearing resistance of the material
- Operating hoop stress level
- Length of the gouge
- Depth of the gouge
- Length of the dent
- Depth of the dent
- Orientation of the damage with respect to the axis of the pipe.

While the above-listed characteristics can have significant effects on the severity of a gouge and dent, less obvious attributes of the damaged pipeline are likely to determine if and when the damaged area will cause a leak or a rupture. Examinations of actual pipeline failures caused by mechanical damage indicate that mechanical impacts on pressurized pipes cause localized coldworking of the metal at the point of contact and instantaneous indentation at the point of contact, much of which is pushed back out by the internal pressure inside the pipe. The amount of "re-rounding" of the pipe in this respect is very hard (if not impossible) to determine after an impact. It depends on the elastic response of the pipe to the imposed load, the level of internal pressure present at the time, the shape of the contacting excavation tool, the force imposed by the excavator, and the constraint of pipe deformation by the surrounding soil backfill. The re-rounding stretches and often cracks the cold-worked material, significantly weakening the material in a way that is hard to measure quantitatively. The nature and amount of cold-working and subsurface cracking can be assessed only by grinding and inspecting the damaged pipe's outside surface for cracks. Thus, while the parameters in the list shown above can be objectively measured, the re-rounding/cracking phenomenon tends to be very difficult to

characterize. As will be seen in terms of the two published predictive criteria for failure stress levels for mechanical damage, this situation undoubtedly accounts for the poor predictive accuracy of the criteria.

One more factor that must be considered in the evaluation of mechanically damaged pipe is the ductile-to-brittle transition temperature of the material. The predictive models are based on the assumption that the material will behave in relatively ductile manner in response to applied tensile stress. Most line-pipe steels are capable of exhibiting ductile tearing in the presence of a crack subjected to quasi-static loading rates. However, there have been exceptions (1) where a sudden brittle failure has taken place at a relatively small mechanical-damage defect. In the case sited in Reference 1, the pipe material had an exceptionally high ductile-to-brittle transition temperature relative to the ambient temperature at the time of failure. Because this situation may be rare but not unique, the guidelines for evaluating mechanically damaged pipe that have evolved from this project include consideration of transition temperature.

The Dent-Gouge Fracture Model

The Dent-Gouge Fracture Model (DGFM) (2) as developed by British Gas researchers with support from the European Pipeline Research Group (EPRG). It is a semi-empirical model, derived from thin-shell theory and calibrated by means of pressure tests of rings and vessels fabricated with mechanical-damage-simulating defects (3,4). The DGFM is meant to be applied to axially oriented damage in a ductile steel pipe consisting of an infinitely long (length not less than ½ pipe diameter based on experiments used to validate the model) "smooth" dent (radius of curvature in any direction not less than five times the wall thickness of the pipe) containing a sharp notch. The model uses a definition of "flow" stress applicable to pipe grades of X65 and lowers although some of the validating tests were conducted on Grade X70 material. The authors of Reference 3 note that while re-rounding is considered in the model, the correction of dent depth for re-rounding "remains an area of considerable uncertainty". Also, as indicated in one of the EPRG's progress reports on the model (4), gouge depth should include the depth of any cracking at the base of the gouge. The equations that comprise the DGFM are as follows:

$$\frac{\sigma_{\theta}}{\bar{\sigma}} = \frac{2}{\pi} \cos^{-1} \left[\exp \left\{ 113 \frac{1.5\pi E}{\frac{-2}{\sigma} A d} \left[Y_1 \left(1 - 1.8 \frac{Ho}{D} \right) + Y_2 \left(10.2 \frac{R}{t} \frac{H_o}{D} \right) \right] - 2 \exp \left[\frac{\ln(0.738C_v) - K_1}{K_2} \right] \right\} \right]$$

$$\frac{\sigma}{\sigma} = 1.15\sigma_y \left(1 - \frac{d}{t} \right)$$

$$\begin{split} Y_1 &= 1.12 - 0.23 \left(\frac{d}{t}\right) + 10.6 \left(\frac{d}{t}\right)^2 - 21.7 \left(\frac{d}{t}\right)^3 + 30.4 \left(\frac{d}{t}\right)^4 \\ Y_2 &= 1.12 - 1.39 \left(\frac{d}{t}\right) + 7.32 \left(\frac{d}{t}\right)^2 - 13.1 \left(\frac{d}{t}\right)^3 + 14.0 \left(\frac{d}{t}\right)^4 \\ K_1 &= 1.9 \\ K_2 &= 0.57 \\ H_0 &= 1.43 H_r \end{split}$$

Where,

- d Depth of gouge (including crack if one exists), inch (mm)
- t Wall thickness, inch (mm)
- A Fracture area of a 2/3-size Charpy V-notch specimen, (mm²) (53.55 mm²)
- C_{ν} 2/3-size Charpy V-notch specimen upper-shelf energy, joules
- D Outside diameter of pipe, inches (mm)
- E Young's modulus (207,000 Nmm⁻²)
- H_o Dent depth measured at zero pressure, inches (mm)
- H_r Dent depth measured at pressure, inches (mm)
- R Outside radius of pipe, inches (mm)
- σ_{θ} Hoop stress at failure, psi (Nmm⁻²)
- σ_y Yield strength of the pipe material, psi (Nmm⁻²)

Note that the primary equation has built-in factors that require the use of metric units for some, but not all terms. Charpy energy, for example, must be entered in joules. It is normally given in U.S. Customary Units of ft lb in the U.S. One can multiply the value in ft lb by 1.356 to get the necessary value in joules. The area of the Charpy specimen in appropriate metric units is given above (53.55 mm 2). The value of Young's modulus must be entered as 207,000. Otherwise any quantities that appear only as ratios (i.e., d/t, H $_0$ /D, R/t) may be entered in either U.S. Customary Units or metric units because the conversion factors offset one another.

The DGFM is based on the "R6" method for assessing defects (5). This method was first put forth by the Central Electricity Generating Board of the United Kingdom in 1976. It has since been incorporated into fitness-for-service standards such as API Recommended Practice 579 and British Standard 7910, so it has gained world-wide acceptance as one means of evaluating the severity of flaws in structures. The essence of the R6 method is that a defect may reach a failure condition either through plastic collapse (ductile tearing), through fracture (sudden crack propagation), or through a combination of these two phenomena. The failure boundary for the R6 criterion is based on the Dugdale strip-yield model (6). The equation for the "failure assessment diagram" or FAD is:

$$K_{r} = S_{r} \left[\frac{8}{\pi^{2}} \ln \sec \left(\frac{\pi}{2} S_{r} \right) \right]^{-1/2}$$

$$K_r = K/K_{\text{mat}}$$

$$S_r = S/S_c$$

K is the applied stress intensity (a function of the applied stress and the square root of the crack length), and K_{mat} is the inherent toughness or resistance of the material to sudden fracture. S is the applied stress, and S_c is the yield strength of the material. The failure criterion, a plot of K_r versus S_r is shown in Figure 1. Defects will fail if S reaches S_c . Defects will fail if K reaches K_{mat} . Defects will also fail for any combination of K/K_{mat} and S/S_c that lies above the K_r curve in Figure 1. In more-recent applications of this approach such as in API RP 579, the S_r value is actually based on "flow" stress not yield strength. Flow stress is usually taken as some value between the yield strength and ultimate tensile strength of the material to account for strain hardening and/or the increase in tearing resistance with increasing crack length that occurs up to the point where a ductile crack becomes unstable. So, the K_r versus S_r curve in API RP 579 extends to an S_r value of 1.25 for carbon-manganese steels based on an empirical correction factor.

The DGFM embodies the R6 approach, though it looks much more complex. The apparent complexity results from the necessity to account for the curvature of the pipe and the depth of the dent as well as the depth of the gouge. It is recalled that the DGFM considers the dent and gouge to be axially oriented and infinitely long, so defect length and longitudinal dent curvature are not considered. The applied stress in the DGFM comes from internal pressure only, but because of the dent, the normal hoop stress, σ_{θ} , is modified and a bending stress based on the curvature of the pipe and the depth of the dent at zero pressure is calculated. If one thinks of the normalized stress intensity factor as $K/\sigma_{\theta}\sqrt{\pi d}$ where d is the depth of the gouge.

EPRG Simplified Model

It is important to note that the EPRG also has compiled a "simplified" model for screening mechanical-damage defects (2). The simplified model is based on the lower bound of all test data on mechanically damaged pipe, and it offers an attractive approach for operators of low-stress pipelines. Therefore, as will be seen, the concept is discussed herein. The use of the simplified model depends on knowing only the gouge depth, the dent depth measured at the operating pressure corrected for re-rounding, the diameter of the pipe, the wall thickness of the pipe, and the operating hoop stress level. The dent and gouge are assumed to be infinitely long, and the material is assumed to behave in a ductile manner (2/3-size Charpy V-notch upper-shelf energy of at least 18 ft- lb). The simplified model is illustrated in Figure B-2.

The Empirical Q-Factor Model

The Empirical Q-Factor Model (7, 8) was developed at Battelle with the support of the American Gas Association's Pipeline Research Committee. It is an empirical model, derived by curvefitting data from pressure tests of vessels fabricated with mechanical-damage-simulating defects. The EQFM is meant to be applied to axially oriented damage in a ductile steel pipe consisting of a dent containing a sharp notch. Unlike the DGFM, the EQFM does attempt to account for gouge length. The model uses a definition of "flow" stress applicable to pipe grades of X70 and lower. The dent depth used in the calculation is the "un-re-rounded" dent depth for a dent inflicted at a particular pressure level. An equation for calculation the un-re-rounded depth is given. The equation was derived from curve-fitting the re-rounding responses with increasing internal pressure of "long" dents inflicted at various levels of internal pressure in particular line pipe materials. Whether or not this relationship applies to a wider class of materials is not stated. The occurrence of subsurface cracking in the tests is noted, but the model does not explicitly consider any amount of cracking to be added to the gouge depth. The equations that comprise the EQFM are as follows.

$$\sigma_{\theta} / \overline{\sigma} = \frac{\left(Q - 300\right)^{0.6}}{90}$$

$$Q = \frac{CVN}{\left(\frac{H}{D}\right) \left(L\right) \left(\frac{d}{t}\right)}$$

 $\overline{\sigma} = \sigma_y + 10,000$ (U.S. Customary Units)

$$\sigma = \sigma_y + 68.95$$
 (metric units, MPa)

Where,

- d Depth of gouge (including crack if one exists), inch (mm)
- t Wall thickness, inch (mm)
- CVN 2/3-size Charpy V-notch specimen upper-shelf energy, ft lb
- D Outside diameter of pipe, inches (mm)
- Length of the gouge, inches (mm)
- H Dent depth created at zero pressure at maximum indentation, inches (mm)
- $\sigma_{\scriptscriptstyle{ heta}}$ Hoop stress at failure, psi
- σ_{v} Yield strength of the pipe material, psi

Note that the primary equation has built-in factors that require the use of U.S. Customary Units for some, but not all terms. Charpy energy, for example, must be entered in ft lb. It is normally given in U.S. Customary Units of ft lb in the U.S. If the value is given in joules, one can divide the value in joules by 1.356 to get the necessary value in ft lb. The yield strength may be entered in psi using the U.S. Customary Units equation for flow stress (σ) for calculating hoop stress at failure in psi. Alternatively, one can calculate a metric value of flow stress by the metric units equation to calculate the hoop stress level at failure in MPa. Otherwise any quantities that appear only as ratios (i.e., d/t, H/D) may be entered in either U.S. Customary Units or metric units because the conversion factors offset one another.

Other Approaches to Evaluate the Effects of Damage

In recent times researchers at Battelle have attempted to develop a sophisticated algorithm to apply to the prediction of the failure pressure of a mechanically damaged pipe (9). As one of them has noted recently (10) "the severity assessment algorithm ... offers a technically sound and comprehensive approach to severity assessment, but it is not simple to use." The discussion of the model in Reference 9 leads one to conclude that every analysis situation would require a unique solution via finite-element analysis. Since the objective of this project is to develop and validate a simple go, no-go criterion for mechanical damage, this "comprehensive" model was not reviewed or assessed as a part of this project. However, Reference 9 provides valuable insights regarding the formation and re-rounding of dents and the types of information that should be derived from future tests on mechanically damaged pipe to acquire suitable data for validating theirs or any other algorithm.

PAST EXPERIMENTS ON PIPE CONTAINING

SIMULATED MECHANICAL-DAMAGE DEFECTS

The above-described models have been validated through comparisons of model-predicted failure stresses to the actual failure stress levels of pressurized pipes containing simulated mechanical-damage defects. Various techniques were used to simulate the types of gouges and dents observed on pipelines that have been struck by excavating equipment. The most commonly used techniques were one of the following.

Method 1 - Machined Notch Followed by Indentation at Zero Pressure

The method used in the earliest studies by Battelle in the 1960s and 1970s consists of the following steps. Tests such as these were used to develop the Empirical Q-factor Model. A more recent summary of these tests is described in Reference 11.

- 1. Machine a longitudinally oriented notch into the wall thickness of the pipe using a v-shaped cutter while the pipe is unpressurized.
- 2. Place a 12-inch-long, 1-inch-diameter round steel bar over the notch, and press a dent into the pipe while it remains unpressurized.
- 3. Release the load on the round-bar indenter, and allow the indented pipe to recover as much as its elasticity will allow. Since the pipe is usually unconfined by soil during this type of indentation, the entire cross-section of the pipe tends to ovalize in response to the indenting load. Therefore, elastic recovery includes recovery of ovalization as well as recovery of local radial indentation at the point of indentation.

A schematic drawing of the indentation process is shown in Figure B-3. Typical indenters are shown in Figure B-4, the indentation and re-rounding are shown in Figure B-5, and typical specimen configurations are shown in Figure B-6. After fabrication in this manner, the pipe can then be tested as desired. Usually, the test involves pressurization to failure. The parameters of importance are thought to be

- Diameter and wall thickness,
- Yield strength,
- Toughness
- Notch length and depth,
- Indenter length,
- Depth of initial indentation,
- Shape of the indenter,
- Depth of the dent after elastic recover,

- Re-rounding during subsequent pressurization (i.e., change in depth of dent as pipe is pressurized),
- Pressure level at failure.

As will become apparent in the discussions of data acquired from such tests, dents formed at zero internal pressure are steadily reduced in size and extent as the level of internal pressure is increased from zero. The re-rounding continues with increasing pressure such that unless failure occurs, the entire dent, if it is not accompanied by any localized kinking, will disappear. Of course if a notch is present in the dent, a crack may grow from the notch and cause a failure before total recovery of the dent has occurred. In some cases, when a notch was present in such a test, crack growth occurred upon re-rounding, leading to a failure at a pressure level well below the expected burst pressure level of a sound piece of pipe. Such behavior appears to mimic the observed experiences in real pipelines that mechanical damage can have a significant impact on the integrity of a pressurized pipe. However, this kind of experiment does not account for the stiffening effect of internal pressure. The latter tends to result in more gouging, less denting, and more tendencies to form a localized kink, and it cannot be assumed that Method-1 tests are a valid representation of actual mechanical damage in a pressurized pipeline. At best this type of test can only simulate what might happen if a pipeline is damaged when depressurized, as for example, during its initial construction.

Method 2 - Indentation Followed by Machined Notching Both at Zero Pressure

This method was first used in studies by British Gas in the 1960s and 1970's. It consists of the following steps.

- 1. Press a round steel bar into an undamaged pipe while it remains unpressurized.
- 2. Release the load on the round-bar indenter, and allow the indented pipe to recover as much as its elasticity will allow.
- 3. Machine a longitudinally oriented notch into the wall thickness of the pipe along the deepest part of the indentation using a v-shaped cutter while the pipe is unpressurized.

The pipe can then be tested as desired. Usually, the test involves pressurization to failure. The parameters of importance are thought to be the same as those listed above, namely

- Diameter and wall thickness,
- Yield strength,
- Toughness,

- Notch length and depth,
- Indenter length,
- Depth of initial indentation,
- Radius of the indenter,
- Depth of the dent after elastic recovery,
- Re-rounding during subsequent pressurization (i.e., change in depth of dent as pipe is pressurized),
- Pressure level at failure.

Upon comparisons with the results of tests of specimens created by Method 1 and Method 3, most investigators, while recognizing that none of these methods may correctly simulate actual damage, concluded that Method 3 better simulated what actually happens during an actual mechanical-damage impact on a pipeline than Method 2. Therefore, Method 2 is seldom used.

Method 3 - Machined Notch Followed by Indentation at a Significant Level of Pressure

Tests such as these were used to validate the Dent-Gouge Fracture Model (4). This method was also used in studies by Kiefner & Associates, Inc. and Stress Engineering Services Inc. (12) in the 1990s, and it consists of the following steps. The latter experimental programs were aimed at either evaluating the fatigue lives of dents or evaluating grinding out of gouges as a means to repair mechanically damaged pipe.

- 1. Machine a longitudinally oriented notch into the wall thickness of the pipe using a v-shaped cutter while the pipe is unpressurized.
- 2. Pressurize the pipe to a pre-determined pressure level.
- 3. Place a long, round steel bar over the notch, and press a dent into the pipe while it remains pressurized being careful to keep the internal pressure constant by bleeding pressure during indentation and restoring pressure as the indenter is withdrawn.
- 4. Depressurize the pipe.

If the pipe does not fail during this process, the pipe can then be tested as desired. Usually, the test involves pressurization to failure. The parameters of importance are thought to be

- Diameter and wall thickness,
- Yield strength,
- Toughness,
- Notch length and depth,
- Indenter length,
- Pressure level during indentation,

- Depth of initial indentation,
- Radius of the indenter,
- Depth of the dent after withdrawal of indenter, measured after depressurization.
- Re-rounding during subsequent pressurization (i.e., change in depth of dent as pipe is pressurized),
- Pressure level at failure.

Method 4 - Creating a Dent and Gouge Simultaneously in a Pressurized Pipe

In the mid-1980s Battelle researchers designed and constructed a machine to introduce actual mechanical damage into a pressurized pipe. The machine was comprised of a large structural frame for holding a piece of pipe and a hydraulically activated, tooth-like tool. The pipe specimen was supported rather rigidly by closely spaced plates having semi-circular cut-outs as bearing points. This system undoubtedly prevented ovalization to a large degree. On the other hand, it may have tended to simulate to a degree, the restraint provided by soil backfill. With the pipe pressurized, the tooth was force into the pipe while being drug along the axis of the pipe. The result was a progressively formed gouge and dent. In some cases the progressively lengthening defect caused the pipe to fail. In other cases, the motion of the tooth was terminated before a failure took place, leaving a gouge and dent. The method was used in the studies described in Reference 8.

The parameters of importance are thought to be:

- Diameter and wall thickness,
- Yield strength,
- Toughness,
- Notch length and depth,
- Indenter length,
- Depth of initial indentation,
- Radius of the indenter,
- Depth of the dent after recovery,
- Re-rounding during subsequent pressurization ,
- Pressure level at failure.

Tests such as these were used to validate both the Empirical Q-factor Model (7) and the Dent-Gouge Fracture Model (4).

INITIAL COMPARISONS OF THE MODELS TO THE RESULTS OF EXPERIMENTS

The experiments used in this report to assess the two candidate models fall into three classes: Method-1 Tests, Method-3 Tests, and Method-4 Tests. As will become apparent, it is essential to compare the models to each of these three sets of data separately.

Comparisons with Method-1 Data

General Points about the Method-1 Tests

Data from 30 full-scale experiments conducted at Battelle (7, 8) are used in the comparisons. All the data, except two, were true Method 1 tests in which the pre-notched pipe was indented a zero internal pressure. The dent depth was measured after the indenter had been withdrawn and before the notched and indented pipe was subjected to any internal pressure. The maximum indentation required to make the dents was not given in any of the references in which these data appeared. Whether or not the maximum indentation was recorded prior to release of the indenter load is not known. So, the dent depth in every case is the residual inelastic deformation measured after elastic recovery. It is also not entirely clear whether the dent depth given is an average value or an individual value. As one can see in Figure B-5, the depth of this type of dent (long-narrow indenter) is not uniform. The end points typically do not re-round much because the ends of the indenter cause localized kinking. It appears from some of the discussion in the references that the dent depth given is an average value not including the extreme depths at the kinked ends.

The comparisons are summarized in Figures B-7, B-8, and B-9. The DGFM-predicted failure pressures are compared to the actual failure pressures in Figure B-7, and the EQFM-predicted failure pressures are compared to the actual failure pressures in Figure B-8. A comparison between the data and the limits imposed by the EPRG's simplified model are shown in Figure B-9. The comparisons are analyzed below. A perfect model would predict the actual failure pressure exactly for every experiment, so "perfect" comparisons in Figure B-7 and B-8 would lie on the diagonal line. The degree of scatter of the points indicates the accuracy of each model with respect to the data. Values that lie above the line correspond to tests in which the model over-predicted the failure pressure, an unsafe situation. Values the lie below the line correspond to tests in which the model under-predicted the failure pressure.

Comparisons between the Data and the DGFM for Method-1 Tests

In the case of Figure B-7, a plot of DGFM-predicted failure pressures versus actually observed failure pressures, the compared values lie on both sides of the line in a pattern that suggests no discernable correlation between the model predictions and the test results. It does not necessarily follow, however, that the DGFM is inadequate because it appears not to be predicting the results of the Method-1 tests.

The first thing that needs to be considered before one concludes that the DGFM does not work, is that it is not clear how one should use the DGFM to predict these results. For one thing, the meaning of dent depth at zero pressure in the tests is not the same as the meaning of dent depth at zero pressure as defined by the creators of the DGFM. The researchers who conducted the Method-1 tests took depth-at-zero-pressure to mean the residual inelastic deformation after a dent has been pressed into a pipe with zero internal pressure and after all indenting force has been removed, allowing the pipe to recovery all elastic deformation. In contrast, the creators of the DGFM took depth-at-zero-pressure to mean the depth of a dent that has been created in a pressurized pipeline where it is re-rounded by internal pressure as well as by elastic recovery of the pipe; the measurement being made only after a pipe soindented has been depressurized. Only the depths given for Tests 1 and 2 fit this latter definition, and it is probably significant, as seen in Figure B-8, that the results of Tests 1 and 2 would have been conservatively predicted by the model. In contrast, the result of the only experiment that is very un-conservatively predicted, Test 22 (see Figure B-7), probably cannot be legitimately represented by its depth measured at zero pressure. For one thing, the specimen failed at 200 psig when subjected to internal pressure (corresponding to 11 percent of SMYS). Therefore, it is highly unlikely that a pipeline comprised of the same pipe could have survived while operating at any reasonable operating pressure, the degree of damage represented by the defect created by notching and indenting at zero pressure. Secondly, the relative length of the notch (as denoted by the parameter, $\frac{L}{(Dt)^2}$) was the longest of all 30

tests. Therefore, one could expect that it re-rounded more completely than any of the other tests. In so doing, the notch may actually have extended by ductile tearing and, if so, the d/t value given in the table would understate its severity. For these reasons, it seems likely that at least the result from Experiment 22 does not provide a valid basis for evaluating the DGFM. Aside from this one case, the model does not seem to have made any highly un-conservative predictions.

Comparisons between the Data and the EQFM for Method-1 Tests

In the case of Figure B-8, a plot of EQFM-predicted failure pressures versus actually observed failure pressures, the compared values lie on both sides of the line in a pattern that suggests a poorly fitting curve-fitting relationship. The standard deviation of the Predicted/Actual values is 0.38 with an average of 1.04. The R² value of 0.58 where 1.0 is a perfect fit is indicative of a weak correlation at best. It is recalled that the Q-factor was empirically derived from these data, but the authors of Reference 7 warn that the Q-factor probably does not adequately account for the mechanical-damage factors. Therefore, a good fit would have been a surprise. Nevertheless, one can see that the Q-factor is at least accounting for some of the variability in the factors. Note that the one value that seems to lie on the x-axis (~zero predicted failure pressure) has a Q-value of about 300, and the predicted failure pressure for Q less than 300 is undefined because of the nature of the equation for failure stress.

Comparisons between the Data and the EPRG's Simplified Model

A comparison between the Method-1 tests and the EPRG's simplified model is presented in Figure B-9. As can be seen, two of the comparisons correspond to non-conservative predictions. In Experiment 14 the failure occurred at 55 percent of SMYS about where the criterion would have indicated an acceptable defect for that operating stress level. In Experiment 26 the failure occurred at 45 percent of SMYS. This point lies on the non-conservative side of the "acceptable" criterion line for 50 percent of SMYS operating stress. It is possible that either or both of the notches in these experiments had been extended by ductile tearing. If so, they were, in effect, deeper defects than indicated by their nominal d/t values. The phenomenon of ductile crack extension of machined and indented notches was recognized in nearly all of the experimental work (7, 8, 12, and 13). However, the amount of such crack extension was usually not measured and, therefore, unfortunately, cannot be taken into account in the predictions.

Comparisons with Method-3 Data

General Points about the Method-3 Tests

The Method-3 test results included data from 25 full-scale experiments. These data are extracted from Reference 13 (Tests 1-8) and Reference 12 (Tests 9-25). For each Method-3 test, a pre-notched pipe was indented at an internal pressure level within the range of 62 to 69 percent of SMYS. In some cases a failure occurred during indentation or during withdrawal of the indenter. If this did not occur, the pipe was completely depressurized and dent depth was measured. The pipe was then pressurized to failure.

The comparisons are summarized in Figures B-10, B-11, B-12, and B-13. The DGFM-predicted failure pressures are compared to the actual failure pressures in Figure B-10 using the re-rounded dent depth at zero pressure to predict failure pressure in the manner prescribed and in Figure B-11 using the maximum indentation to predict failure pressure. The EQFM-predicted failure pressures are compared to the actual failure pressures in Figure B-12. A comparison between the data and the limits imposed by the EPRG's simplified model are shown in Figure B-13. The comparisons are analyzed below. A perfect model would predict the actual failure pressure exactly for every experiment, so "perfect" comparisons in Figure B-10, B-11, and B-12 would lie on the diagonal line. The degree of scatter of the points indicates the accuracy of each model with respect to the data. Values that lie above the line correspond to tests in which the model over-predicted the failure pressure, an unsafe situation. Values the lie below the line correspond to tests in which the model under-predicted the failure pressure.

Comparisons between the Data and the DGFM for Method-3 Tests

In the case of Figure B-10, a plot of DGFM-predicted failure pressures versus actually observed failure pressures using the re-rounded dent depth at zero pressure, the compared values lie on both sides of the line but in a pattern that suggests a rough correlation between the model predictions and the test results. The experiments accounting for the two most outlying non-conservative points are Experiment B2-15N from Reference 12 and Experiment V10 from Reference 13. The prediction based on Experiment B2-15N is suspect because the gouge depth given for this test in Reference 12 is suspect. The reason is that this specimen failed at a pressure level below the intended indentation pressure level. The likely explanation is that the original notch had been extended significantly by ductile tearing. Therefore, the machined notch depth used in the calculation likely causes the prediction to be artificially high. A similar situation may account for the outlying data point based on Experiment V10 as well. It is noted in Reference 13 that some of the other defects in the specimens that did not fail exhibited

ductile crack extensions ranging from one to 11 percent of the wall thicknesses. The author of Reference 13 recommends that the crack depth be added to the notch depth for the purpose of the model predictions. Unfortunately, the ductile crack depths, if they existed, were not recorded for either set of experiments. It should also be noted that Tests 1 through 7 from Reference 5 (the triangular symbols in Figure B-12) resulted in failures of the specimens either during indentation or during withdrawal of the indenter. Therefore, the dent depths at zero pressure could not be actually measured and are in fact estimates.

In Figure B-11 the DGFM-predicted failure pressures are modified by using the maximum dent depth (maximum amount of indentation with the indenter present). Except for the same two outliers discussed above, the DGFM gives conservative predictions.

Comparisons between the Data and the EQFM for Method-3 Tests

In the case of Figure B-12, a plot of EQFM-predicted failure pressures versus actually observed failure pressures, the compared values, except for one, are conservative. However, the scatter is such that no correlation is recognizable. It is would appear that the Q-factor does not adequately account for the mechanical-damage factors for the Method-3 tests.

Comparisons between the Data and the EPRG Simplified Model

A comparison between the Method-3 tests and the EPRG simplified model is presented in Figure B-13. As can be seen, one of the comparisons corresponds to non-conservative predictions. In the suspect experiment from Reference 12 (Experiment B2-15N), the failure occurred at 58 percent of SMYS. This point lies well on the non-conservative side of the "acceptable" criterion line for 72 percent of SMYS operating stress. Because it is a "suspect" data point, possibly because of undisclosed ductile tearing, one can take the position that it does not refute the validity of the simplified model.

Re-rounding of Dents in the Method-3 Tests

One of the most important aspects of mechanical-damage behavior is the re-rounding of dents. Indentation of a piece of supported pipe requires the imposition of radially oriented force that must be increased with increasing indentation. As the indenting force is withdrawn, the pipe recovers some of its initial curvature as the result of at least one of the following: elastic recovery of elastic deformation in response to the force (both indentation and ovalization) and

pressure-induced re-rounding. Pressure-induced re-rounding occurs only when the pipe is pressurized. One part of pressure-induced re-rounding comes from the "stiffening" of the pipe by pressure. This portion of re-rounding comes and goes as pressure is applied and removed. As a result the dent will be deeper at zero pressure than when the pipe is pressurized. Another part of pressure-induced re-rounding is the one-time inelastic (non-recoverable) re-rounding that results in a final dent at pressure being considerably less deep than the initial indentation while the indenting device is still present. The process in terms of indenting force versus displacement is illustrated in Figure B-14. The depth of dent at Point B is usually referred to as the maximum depth or initial dent depth (IDD). The dent depth at Point C while the pipe is still pressurized is referred to as H_r in the DGFM. The final depth at Point D after removal of the indenting force and after the pipe is depressurized is sometimes referred to as the residual dent depth (RDD) or to H_o in the DGFM. The depth will go back to Point C if pressure is restored, but the re-rounding from B to C cannot be reversed.

One of the main points of confusion regarding re-rounding is that some authors (9, 13) focus on the re-rounding as defined by the movement between Points C and D in Figure B-14. In fact, the re-rounding equation that is part of the DGFM addresses only this aspect of rerounding, that is, re-rounding resulting solely from pressure-stiffening. The rationale is that a person using the criterion likely will be measuring the depth of a dent while the pipeline is under pressure. The model, however, is based on the depth of the dent at zero pressure. Hence, a linear correction factor was derived through EPRG research (13), namely, that H_0 = 1.43H_r. It is not that the authors of Reference 9 or developers of the DGFM ignored the movement of the dent as represented by the path from Point B to Point C. It is just that they did not propose a way to deal with the consequences of such re-rounding even though they recognized that it could cause ductile tearing at a gouge. In contrast, the Battelle work (8, 11) focused on the re-rounding characterized by the difference between maximum indentation and the re-rounded depth measured after depressurization, in other words the difference between Point B and D in Figure B-14 without considering that the Point C-depth might be considerably different from the Point D-depth. In reality, both aspects of re-rounding need to be considered so that one is certain of the definition of dent depth under a given set of circumstances. There is little question, however, that the component of re-rounding that is most difficult to characterize is the re-rounding that occurs between Points B and C in Figure B-14. The latter component of re-rounding is almost certainly a significant factor in determining whether or not ductile crack extension of the gouge takes place. Future experimental work must address measuring this re-rounding accurately as well as the re-rounding that occurs between zero pressure and some level of pressure as the result of pressure-stiffening.

IDD and RDD were measured in the Method 3 tests, and the hoop stress at indentation relative to the flow stress of the material is plotted as a function of RDD/IDD in Figure B-15 for

the results. The data lie almost on the same horizontal line because the tests were conducted at a hoop stress level with the range of 62 to 69 percent of SMYS. As can be seen the RDD/IDD values derived from the tests described in Reference 12 are clustered between about 0.03 and 0.30. The values from the tests described in Reference 13 range from about 0.35 to about 0.75. It must be recalled, however that seven of the eight tests described in Reference 13 failed during indentation or indenter withdrawal, so the RDD values where that happened are not representative. For the one test where failure was produced on re-pressurization after indentation, Test 8, the RDD/IDD value is about 0.45 and should be a legitimate value. The smooth curve on Figure B-15 comes from an empirical relationship fit to another set of data by Maxey in Reference 8. The source of that relationship is described subsequently herein. It is expressed by the following equation.

$$\sigma/\overline{\sigma} = e^{-x/22}$$

Where,

 σ is the level of hoop stress at the time of indentation, psi

 $\sigma\,$ is the flow stress of the material (yield strength plus 10,000 psi), psi

x is the ratio RDD/IDD.

Comparisons with Method-4 Data

General Points about the Method-4 Tests

The Method-4 test results had data from 17 full-scale experiments. The indentation and gouging was accomplished simultaneously by a simulated backhoe tooth forced into and along a pressurized pipe at a constant load by means of a hydraulically driven head mounted on the track of the framework holding the pipe. The dent depth (IDD) was measured instantaneously as the tool was moved along the pipe. In all 17 of the tests, the gouge/dent length was steadily increased until a failure occurred. Because a failure occurred in every Method-4 test, the final dent depth, RDD, was not available. Therefore, to be able to make predictions of the results using the DGFM, it was necessary to calculate the RDD, and Maxey's relationship shown previously was used for that purpose.

The DGFM and EQFM comparisons are summarized in Figures B-16 through B-19. The DGFM-predicted failure pressures using a calculated dent depth at zero after re-rounding are compared to the actual failure pressures in Figure B-16, and the DGFM-predicted failure pressures using the measured maximum dent depth during simultaneous gouging and denting are compared to the actual failure pressures in Figure B-17. The EQFM-predicted failure pressures are compared to the actual failure pressures in Figure B-18. A comparison between the data and the limits imposed by the EPRG's simplified model are shown in Figure B-19. The comparisons are analyzed below.

Comparisons between the Data and the DGFM for Method-4 Tests

A comparison of DGFM-predicted failure pressures versus actually observed failure pressures using a calculated re-rounded dent depth at zero pressure is presented in Figure B-16. The re-rounded dent depths at zero are based on Maxey's empirical re-rounding equation. Ho as defined by EPRG is the re-rounded dent depth at zero pressure, and it is the same as RDD in Maxey's equation. Hence, $H_o = -22 \ln \frac{\sigma}{\sigma}$. In 15 of the 17 comparisons shown in Figure B-16, the failure pressures predicted using Ho calculated in this manner values lay above the line of perfect agreement. The pattern of the comparisons suggests a weak correlation at best between the model predictions and the test results. When the predictions are recalculated using the maximum dent depth, IDD, instead of RDD, the predicted failure pressures are much lower and in all but two cases, they lie below the perfect fit line as shown in Figure B-17. The scatter associated with Figure B-17 (R² = 0.339) is only slightly better than that associated with Figure B-16 (R² = 0.249). So, it would seem that the DGFM is not accounting very well for the

variability in the data. One likely partial explanation is that the visible gouges had been extended significantly by ductile tearing. Therefore, the gouge depths used in the calculations likely caused the predictions to be artificially high. It is recalled that the author of Reference 13 recommends that the crack depth be added to the notch depth for the purpose of the model predictions. Unfortunately, the ductile crack depths, if they existed, could not be recorded for these experiments because each one resulted in a failure at some point during the lengthening of the gouge/dent defect.

Comparisons between the Data and the EQFM for Method-4 Tests

In the case of Figure B-18, a plot of EQFM-predicted failure pressures versus actually observed failure pressures, the compared values, except for one, are conservative. However, the scatter is such that no correlation is recognizable. It would appear that the Q-factor does not adequately account for the mechanical-damage factors for the Method 4 tests.

Comparisons between the Data and the EPRG Simplified Model

A comparison between the Method-4 tests and the EPRG simplified model is presented in Figure B-19. As can be seen, at least four of the comparisons correspond to non-conservative predictions. These points lie well on the non-conservative side of the appropriate "acceptable" criteria for the particular operating stresses. Because of possible undisclosed ductile tearing, one can take the position that these data do not necessarily refute the validity of the simplified model. It is clear, however, that in future validating tests, measurement of the amount of ductile tearing will be essential.

Re-rounding of Dents in the Method-4 Tests

Maxey's empirical equation was derived from the results of a 60 tests described in Reference 8. These tests were carried out in a manner quite similar to that of the Method-4 tests. The only difference is that none of the 60 special Method-4 tests resulted in failures. In all cases the gouging and denting was stopped short of the length required to produce a failure. This allowed the researchers to measure not only IDD but RDD as well. A plot of hoop stress of the data for these 60 tests divided by flow stress versus RDD/IDD is shown in Figure B-20. Although one of the results is an outlier, most seem to fit Maxey's equation. How Maxey developed the equation is not known. There is certainly a fair amount of scatter, though Maxey's curve appears to provide a rough estimate of the amount of re-rounding one can expect over a fairly wide range of materials and stress levels.

DISCUSSION OF THE INITIAL COMPARISONS

The comparisons between the model predictions and the three sets of experiments reveal that neither the DGFM nor the EQFM satisfactorily accounts for the variability of the data. Of the two it appears that the DGFM is somewhat better than the EQFM, but the weak correlations between the model predictions and the data suggest that one or more variables are not being properly taken into account. The same can be said for the EPRG's simplified model based on the DGFM. In the case of the simplified model, the lower-bound limits did not in fact bound some of the data. The researchers that developed both the DGFM and the EQFM were aware of the lack of strong correlation between the models and the data, and they identified two likely factors that were not adequately taken into account: re-rounding and ductile crack extension of the machined notches. Unfortunately, these parameters were not measured in the validating experiments. The amounts of re-rounding and cracking were, in some cases, assessed by means of ancillary experiments, but such experiments were generally not continued to the point of failure where the failure pressures would have been known. So, the effects of re-rounding and cracking on failure pressure were not documented. The knowledge generated in the experiments does, however, suggest ways in which future experimentation can be conducted so as to measure more of the critical parameters. If that is done, it is possible that one or both of the existing models will be capable of adequately predicting the results. More importantly from the standpoint of the desire to have a simple go, no-go criterion, it turns out that the EPRG's simplified model can be used with confidence if one can either verify that there is no ductile crack extension beyond the visible gouge or measure and account for the amount of ductile crack extension.

IMPROVEMENT OF THE DENT-GOUGE FRACTURE MODEL AND RE-ASSESSMENT

OF THE EPRG SIMPLIFIED MODEL

A significant amount of support for the use of the EPRG simplified model as a go/no-go criterion for accepting or rejecting mechanical damage defects in low-stress natural gas pipelines comes from a newly published report entitled "A New Limit State Function for the Instantaneous Failure of a Dent Containing a Gouge in a Pressurized Pipeline" (14). This report describes a limit-state approach to improving the Dent-Gouge Fracture Model (DGFM) (2). The improved model reduces some of the scatter in comparisons between predicted failure pressures and experimentally-determined failure pressures that has long been recognized as a weakness of the model. The improvements to the DGFM included a modified equation for calculating fracture toughness from Charpy energy, a factor by which to include the effects of residual stress in a dent, a factor by which to include the effect of the radius of curvature of the gouge, and, most importantly, a factor by which to include the effects of a crack at the base of the gouge. Although reference 14 does not reveal exactly how the improved model was applied, the concepts of the modifications are adequately described. Of these modifications, the one involving the effects of a crack is the most significant. The author of the new study re-analyzed the full-scale test results, some of which are the same data presented herein, using a statistical technique to predict the amount of ductile crack extension from re-rounding of the dents in the experiments. The data were then re-compared to the DGFM predictions using actual gouge depths plus estimated amounts of crack extension. The comparisons were significantly better than those depending only on actual gouge depths. The results strongly suggest that the DGFM is a valid model for predicting gouge and dent behavior. By extension, it is logical to assume that the simplified EPRG model will work well if crack extension is added to gouge depth for the purpose of screening a particular damage defect. In order for the simplified model to be used as the go/no-go criterion, consideration of crack extension is the one improvement that we need to consider.

In both the Battelle research (8) and the EPRG-sponsored research (13), the importance of ductile cracks that formed during re-rounding of dents was recognized. Neither the Empirical Q-factor Model (EQFM) nor the original DGFM accounted for the effect because it was felt at the time that crack depth could not be reliably measured by non-destructive means. However, both groups of researchers recognized and suggested that if crack depth were to be included, the predictive models might give improved predictions. As indicated in previous sections of this report, neither model when applied without considering crack depths consistently predicted

the observed failure pressures. Moreover, our review indicated that the EPRG simplified model occasionally gave non-conservative predictions of failure pressures. This fact is most clearly shown by Figure B-13 where visible gouge depth only not including any ductile crack extension was use to calculate d/t.

As seen in Figure B-13, even if one discounts the "suspect" data point, one of the specimens failed at a stress level corresponding to 86 percent of SMYS whereas based on the dimensions of the anomaly (d/t and H_o/D) the simplified model implies that it would be okay to leave such an anomaly in a pipeline being operated at a stress level of 72 percent of SMYS. Traditionally, fitness-for-service criteria used by the pipeline industry such as ASME B31G anticipate that anomalies to be left unprepared in a pipeline being operated at 72 percent of SMYS should have a minimum predicted failure stress level not less than 100 percent of SMYS. If crack depth had been taken into account (assuming a crack existed), it is possible that the model would not have given the anomaly a pass for being left in a pipeline to be operated at 72 percent of SMYS.

In an attempt to show what the impact of an unaccounted-for crack might have on the predictions of the simplified model, we did a further review of the research (12) that produced the data represented by the squares in Figure B-13. The major objective of the research described in Reference 12 was to show that grinding the cracks out of a gouged and dented pipe would restore its serviceability provided that grinding out the crack completely did not require the removal of an excessive amount of material. The data taken from this work are represented by the squares in Figure B-13, and they represent the set of experiments on samples of notched and indented pipe that consisted of pressurization to failure in the unprepared that is ungrounded, condition. In each case a companion test was conducted, and a repair was affected by grinding out any cracks that had been created at the base of the notch. These cracks were ductile tears that had occurred as the dent re-rounded at constant pressure as the load on the indenter was relaxed. In most cases the amount of material removed to completely, but just barely, remove the cracks was measured. We assumed that the depth of material removed was exactly the depth of the crack that had been created. If we also assume that the companion test that was pressurized to failure without being repaired had exactly the same amount of cracking, we can add that crack depth to the depth of the gouge for each specimen where a crack depth was measured on the "repaired" companion specimen. When the total depth including gouge depth plus presumed crack depth is used to represent "d" in the d/t value, the data where crack depth is added change position as shown in Figure B-21. The original data plotted on the basis of gouge depth only are represented by "x" in Figure B-21. The effect of adding crack depth is seen in terms of the repositioned squares. Only eight satisfactory companion test results were available, so cases where no data were available on crack depth remain where they were in Figure B-13 and are shown in Figure B-21 as an "x"

inside a square. It is likely that cracks existed in these latter specimens as well, but no valid measurement of the crack was available to facilitate repositioning.

The repositioning based on the inclusion of the assumed crack depths moves the data into positions that represent adequately conservative predictions. The net result is that we are confident that when the d/t term of the EPRG simplified model includes crack depth, the model can be used with a high degree of confidence as a go/no-go criterion for assessing damage in pipelines being operated at stress levels at or below 40 percent of SMYS.

Attachment B - REFERENCES

- Texas Eastern Transmission Corporation Natural Gas Pipeline Explosion and Fire Edison, New Jersey, March 23, 1994, National Transportation Safety Board Report Number PAR-95-01, adopted on January 18, 1995.
- 2. Roovers, P., Galli, M.R., Blood, R.J., Mareski, U., Steiner, M., and Zarea, M., "EPRG Methods for Assessing the Tolerance and Resistance of Pipelines to External Damage (Part 1)", 3R International (October 11, 1999).
- 3. Cosham, A. and Hopkins, P., "The Pipeline Defect Assessment Manual", *Proceedings of IPC'02*, 4th *International Pipeline Conference*, Calgary, Alberta, Canada, Paper No. IPC2002-27067, ASME (September 29-October 3, 2002).
- 4. Hopkins, P., "A Study of External Damage of Pipelines", 7th NG-18/EPRG Joint Biennial Technical Meeting on Line Pipe Research", Calgary, Alberta, Canada (August 29 September 1, 1988).
- 5. Harrison, R.P., Loosemore, K., and Milne, I "Assessment of the Integrity of Structures Containing Defects", CEGB Report R/H/R6, Central Electricity Generating Board, United Kingdom, 1976.
- 6. Dugdale, D.S., "Yielding of Steel Sheets Containing Slits", *Journal of the Mechanics and Physics of Solids*, 8, 1960, P. 100.
- 7. Mayfield, M.E., Maxey, W.A., and Eiber, R.J., "Fracture Initiation Tolerance of Line Pipe", Sixth Symposium on Line Pipe Research, American Gas Association, Catalog Number L30175 (1979).
- 8. Maxey, W.A., "Outside Force Defect Behavior", *NG-18 Report No. 162*, Pipeline Research Committee, American Gas Association (August 15, 1986).
- 9. Leis, B.N. and Francini, R.B., "Line Pipe Resistance to Outside Force, Volume Two, Assessing Serviceability of Mechanical Damage" Final Report on Project PR 3-9305, Pipeline Research Council International, Inc. (November 1999).

- 10. Leis, B.N., Forte, T.P., and Zhu, X.K., "Integrity Analysis for Dents in Pipelines", *Proceedings of IPC 2004, International Pipeline Conference,* Calgary, Alberta, Canada, Paper No. IPC04-0061, ASME (October 4 8, 2004).
- 11. Eiber, R.J., Maxey, W.A., Bert, C.W., and McClure, G.M., "The Effects of Dents on the Failure Characteristics of Line Pipe", NG-18 Report No. 125, American Gas Association Catalog No. L51403 (May 8, 1981).
- 12. Kiefner, J.F., and Alexander, C.R., "Repair of Pipeline Dents Containing Minor Scratches", Final Report on Contract No. PR 218-9508, PRC International, (March 18, 1999).
- 13. Hopkins, P., "The Significance of Mechanical Damage in Gas Transmission Pipelines", EPRG/NG-18 Eighth Biennial Joint Technical Meeting on Line Pipe Research", Paris, France (May 14-17, 1991).
- 14. Francis, Andrew, "A New Limit State Function for the Instantaneous Failure of a Dent Containing a Gouge in a Pressurized Pipeline", Confidential report to Adventism, August 23, 2004.

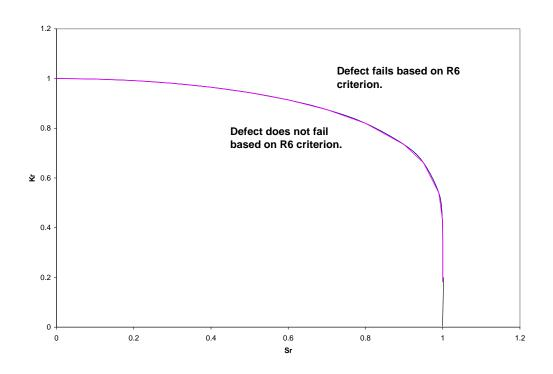


Figure B-1. Failure Assessment Diagram

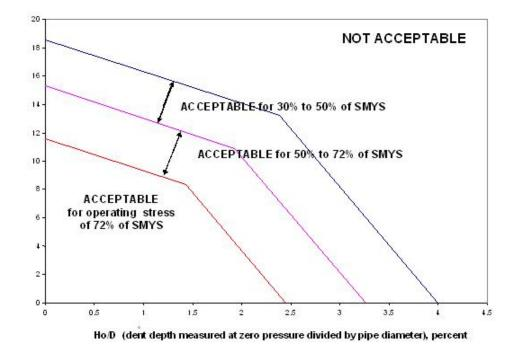


Figure B-2. The EPRG Simplified Model

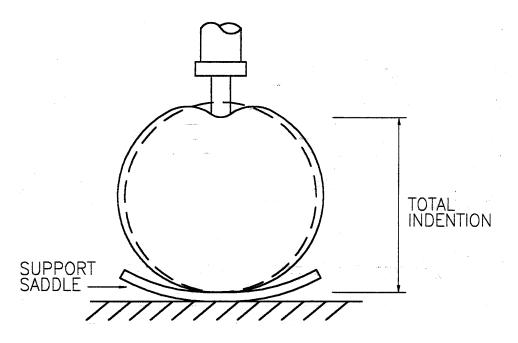


Figure B-3. Typical Indentation Process Associated with Methods 1 and 3

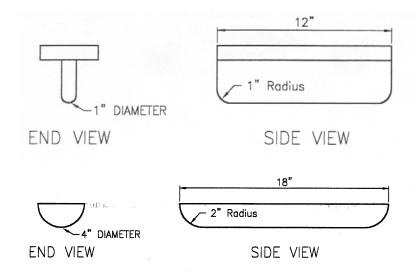


Figure B-4. Typical Indenters Associated with Methods 1 and.3

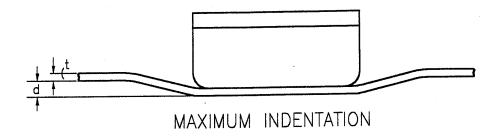




Figure B-5. Typical Indentation and Re-rounding Associated with Methods 1 and 3

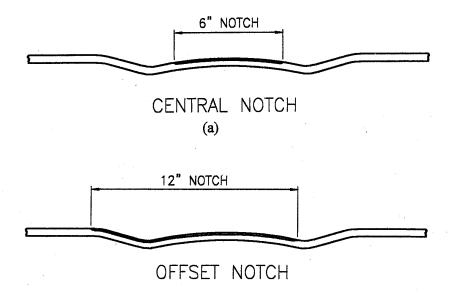


Figure B-6. Typical Locations of Notches Associated with Methods 1 and 3

(Note that notches shown here after indentation were created prior to indentation and thus were exposed to the indentation and re-rounding process.)

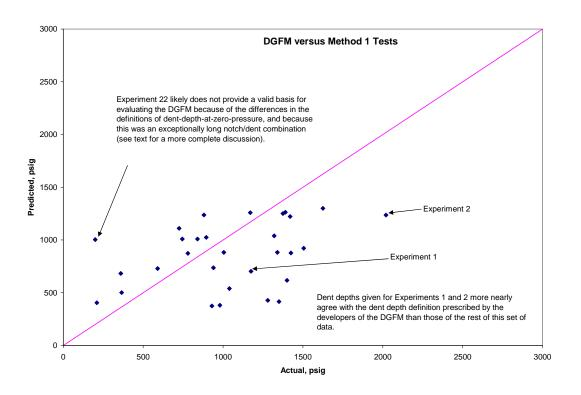


Figure B-7. Comparison between DGFM Predictions and Method-1 Test Data

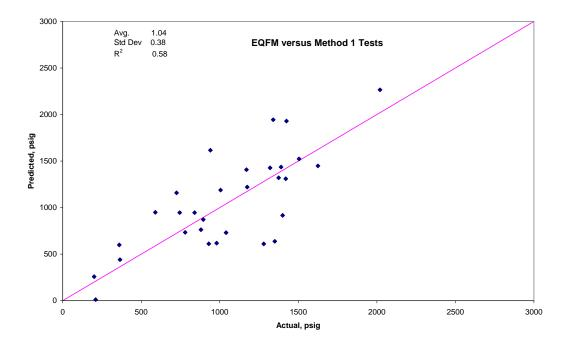


Figure B-8. Comparison between EQFM Predictions and Method-1 Test Data

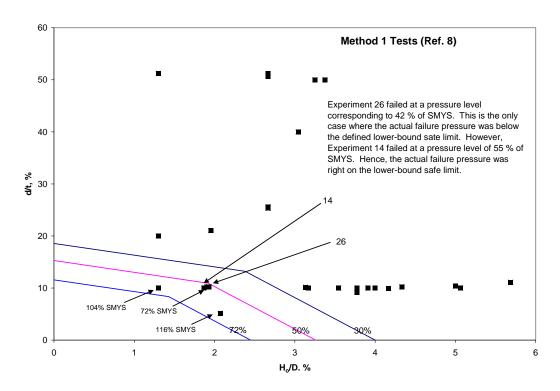


Figure B-9. Comparison between DGFM Simplified Criterion and Method-1 Test Data

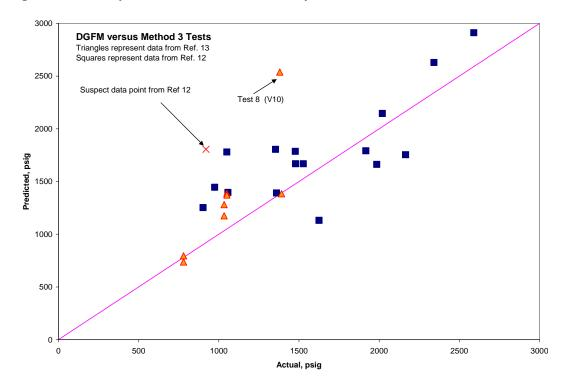


Figure B-10. Comparison between DGFM Predictions Based on Dent Depth at Zero Pressure and Method-3 Test Data

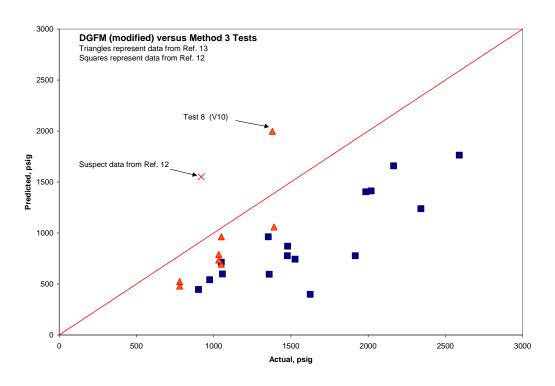


Figure B-11. Comparison between DGFM Predictions Based on Maximum Dent Depth and Method-3 Test

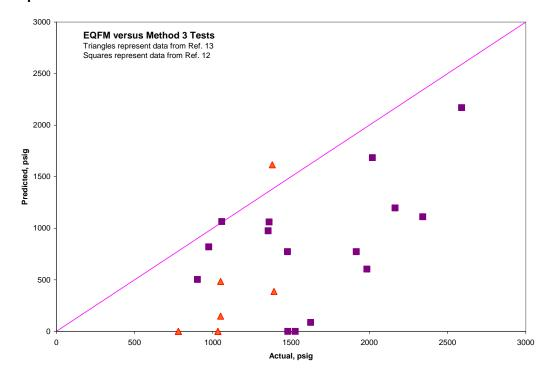


Figure B-12. Comparison between EQFM Predictions and Method-3 Test Data

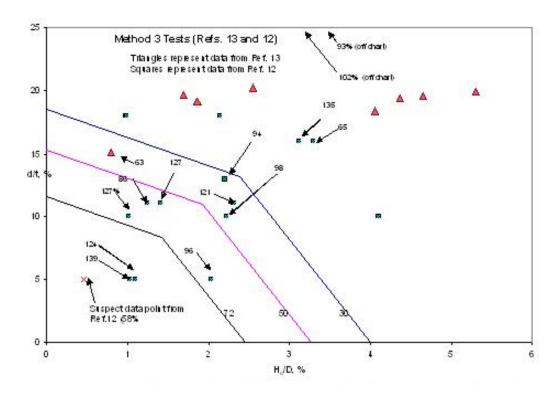


Figure B-13. Comparison between DGFM Simplified Criterion and Method-3 Test Data

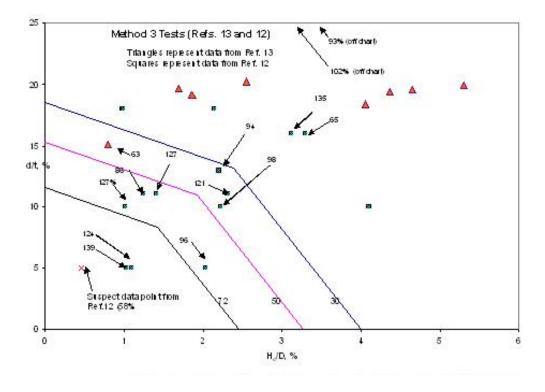


Figure B-14. Characteristic of Dent Formation in Pressurized Pipe

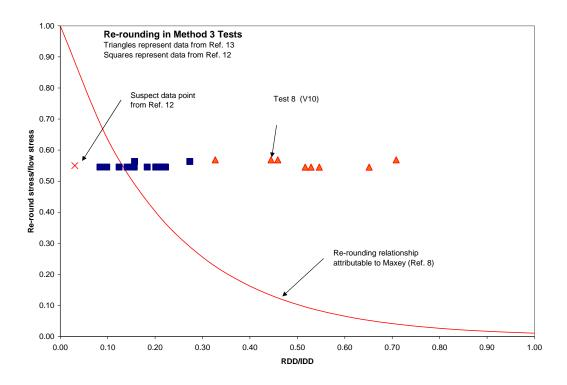


Figure B-15. Re-rounding at Pressure

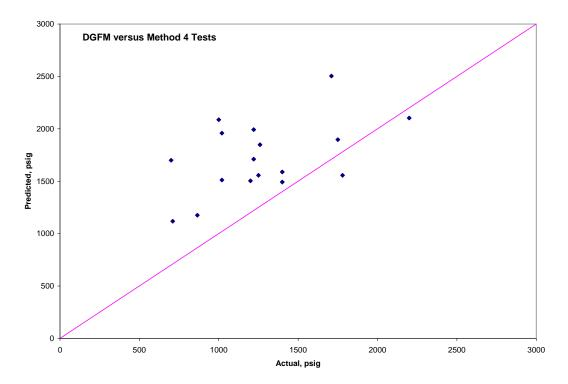


Figure B-16. Comparison between DGFM Predictions Based on Dent Depth at Zero Pressure and Method-4 Test Data

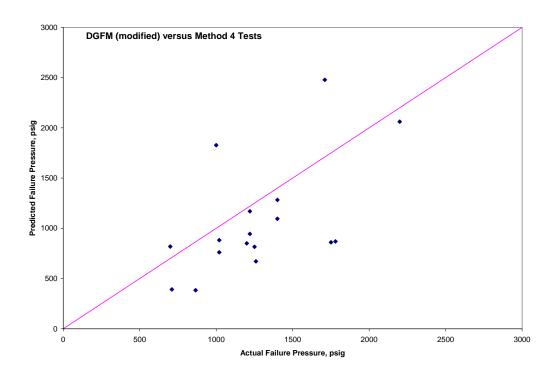


Figure B-17. Comparison between DGFM Predictions Based on Maximum Dent Depth and Method-4 Test Data

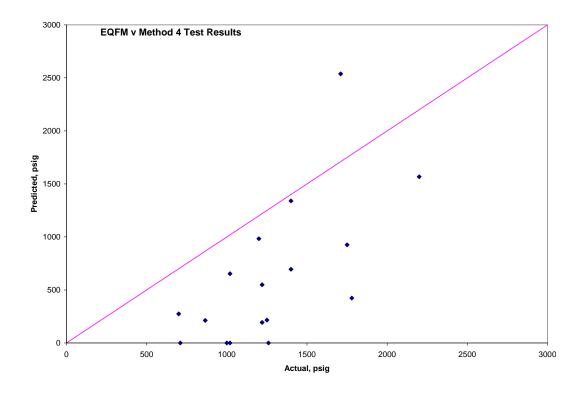


Figure B-18. Comparison between EQFM Predictions and Method-4 Test Data

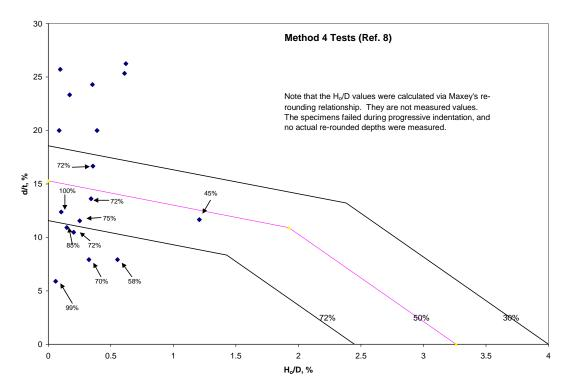


Figure B-19. Comparison between DGFM Simplified Criterion and Method-4 Tests

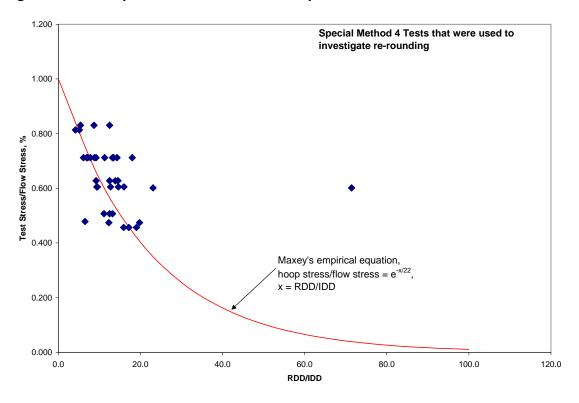


Figure B-20. Special Method-4 Tests that Show Characteristics of Re-rounding

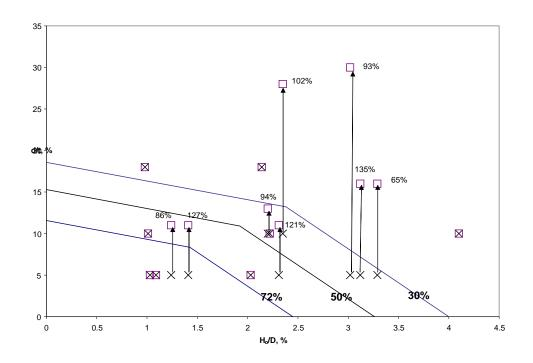


Figure B-21. Repositioned data from Figure 13 with crack depth included

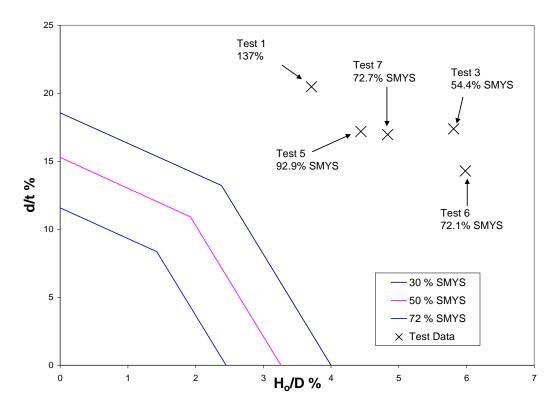


Figure B-22. EPRG simplified model compared to GTI's test data

Final Report No. 10-048

Evaluation of the Effects of Wrinkle Bends on PipelineIntegrity

for

Gas Technology Institute

and

Operations Technology Development

by

Robert B. Francini

Kiefner and Associates, Inc. 585 Scherers Court Worthington, Ohio 43085

August, 2010

0394-0801

Table of Contents

Introduction	. 118
Summary and Conclusions	. 118
Background	. 119
Integrity Issues Related to Wrinkle Bends	. 121
Wrinkle Bend Fatigue Models	. 125
Experimental Testing of Wrinkle Bends	. 130
Discussion and Recommendations	. 135
References	137

Introduction

The objective of this task is to investigation the effect of wrinkle bends on pipeline integrity. Integrity concerns have been expressed about the formation of wrinkle bends as far back as the early 1950's (1). At that time there were conflicting views as to whether wrinkle bends were an acceptable method for forming pipe bends. Although concerns have been expressed over the years, the fact of the matter is that wrinkle bends account for a small percentage of pipeline incidents since 1970 (1). Current research on wrinkle bends is based on theoretical analysis and Finite Element (FEA) modeling to investigate the state of strain in and performance of wrinkled pipes. In most of these studies, stress concentration effects were used with suitable fatigue damage models to estimate the effect of ripple parameters on service life of the wrinkled section. A comparative review of the various assumptions and analysis of these models has been performed. A verification of these models was investigated based on the existing available experimental results on full scale test sections.

For the purpose of this report we draw the distinction between wrinkle bends which were formed using common field practice up until the early 1950's and incidental minor ripples which can occur in modern bending machine-made cold bends. Although there may be some overlap in terms of deformation characteristics, modern field bending practice does not allow the use of pipe with ripples of the magnitude that were allowed in the past. This report also does not address buckle deformations that occur due to uncontrolled or accidental loadings on a buried pipeline.

Summary and Conclusions

- The incident record suggests that the vast majority of wrinkle bends do not pose a threat to pipeline safety under normal circumstances. The challenge is to use information available to the operator to identify the small proportion of wrinkle bend installations that ever could pose a threat.
- Wrinkle bends with depths up to 2.5 percent of the diameter and aspect ratios (height of wrinkle over the wave length of the wrinkle) less than 0.13 are acceptable provided the following threats are not present:
 - 1. Aggressive longitudinal stress cycling of the line,
 - 2. Ground movement, i.e. mine subsidence or landslides,
 - 3. Corrosion, and
 - 4. Stress corrosion cracking.

- The threats stated above have not been quantified at this time. This is an area that needs further research.
- It is conceivable that even wrinkle bends classified as severe can remain in the pipeline if the threat level is low enough. This may be a more desirable option than exposing the bend for examination and increasing the potential threat as described below.
- If it is necessary to expose a wrinkle bend or the pipe in the vicinity of a wrinkle bend care should be taken to return the pipe to its original condition of support, soil consolidation, and restraint of the bend. One method of accomplishing this is to mix cement into the soil before reburying the pipe. Composite reinforcement of the bend shows promise for increasing the fatigue resistance of wrinkle bends.

Background

Reference (1) contains a short history of wrinkle bend practice. The term wrinkle bend is used to describe bends made by intentionally creating local buckles on the intrados of the pipe bend in order to foreshorten the inside arclength. This process was used from the advent of welded pipe construction through the latter part of the 1950's. The practice went out of favor with the introduction of field bending machines in the 1940's. The two methods of forming wrinkle bends were hot bending and cold bending. As the names imply, hot bends were formed by heating the steel before bending and cold bends were formed by bending the pipe at ambient temperature. The formation of a cold bend required much larger forces than hot bends and usually required the use of fixtures. Hot bends on the other hand required considerably less force and, in many cases, only the weight of the pipe was required to form the bend. The quality of these bends could vary considerably from project to project and across spreads within a project. This leads to the conclusion that the quality of the bends reflects the craft and practices of contractor or crew rather the period when the bend was made. Figures C-1a and C-1b taken from Reference (1) illustrate the range in quality in wrinkle bends. These figures show that wrinkle bends can range from an internally bulging diamond-shaped buckle as shown in Figure C-1a to smooth external bulges shown in Figure C-1b. In addition, the temperatures used to form hot bends could affect the strength of the steel, particularly where the pipe was mechanically expanded, resulting in grain coarsening and decarburization local to the wrinkle, and burnt metal defects.



Figure C-1a. Hot formed bend with diamond shaped buckle from Reference (1)



Figure C-1b. Cold formed wrinkle bend from Reference (1)

Integrity Issues Related to Wrinkle Bends

Pipeline incident data indicate that the actual number of wrinkle bends that have failed in service is small. Table C-1 taken from Reference (1) and updated with current information shows the number of wrinkle bend incidents from the Federal Power Commission (FPC) and US Department of Transportation (DOT) Office of Pipeline Safety (OPS) and Pipeline and Hazardous Materials Safety Administration (PHMSA) databases. Overall, wrinkle bends account for 0.3 percent of the reported incidents since 1950. Pipelines that were constructed in the 1950's and earlier account for 36.5 percent of hazardous liquid pipelines and 35.8 percent of natural gas transmission pipelines by mileage according to the 2008 DOT annual report. Given that wrinkle bending of pipe was a common practice in pipeline construction as late as the 1950's it is safe to assume that a large number of wrinkle bends exist in these pipelines. The incident record suggests that the vast majority of wrinkle bends do not pose a threat to pipeline safety under normal circumstances. The challenge is to use information available to the operator to identify the small proportion of wrinkle bend installations that could pose a threat.

An important consideration when evaluating the integrity of wrinkle bends is that they are a longitudinal stress-driven integrity issue. The stresses that result in the failure of wrinkle bends are typically longitudinal stresses, not hoop stresses due to internal pressure. For a buried pipe these longitudinal stresses arise from the soil restraint on the longitudinal contraction of the pipe when it is pressurized, thermal expansion, and external forces such as soil movement. The interaction between the soil and pipe is an important part of these forces. For instance, a pipe bend that is not restrained by soil will tend to open under internal pressure whereas a buried pipe will have a reduced stress because it will not be able to flex as much. The importance of restraint is the basis for the conclusion that rehabilitation (involving excavation of the bend) may relax the restraint around wrinkle bends and result in loading that otherwise would not be present (2).

Precise determination of the longitudinal stress on a pipe requires detailed knowledge of the pipe, the pipe coating, soil mechanical properties, temperature when the pipe was tied in, thermal history of the pipe, and historic geophysical data such as soil slip and earth movement. In most cases the analyst is forced to make conservative assumptions due to a lack of knowledge of the real stress state of the pipe.

By far the largest integrity concern with regard to wrinkle bends is the reduction in the fatigue life of the pipe. This is followed by the reduction of longitudinal load capacity of the bend in areas where earth movement might occur. Secondary issues are the concern that corrosion will affect both the fatigue and longitudinal capacity of the pipe and the possibility that the residual stress in the wrinkle provide sites for the initiation of stress corrosion cracking (SCC) under the right conditions.

Table C-1. Number of wrinkle bend incidents from FPC/DOT databases

Description	Time Period	Number of Incidents		
		Total	Wrinkle bend total/%	
FPC	January, 1950 - June, 1965	1067	26	2.44
DOT/OPS	1970 - mid 1984	7864	4	0.05
DOT/OPS	mid 1984 - mid 2002	1455	7	0.48
DOT/PHMSA	2002 - present	3951	5	0.10

It is necessary to discuss the detection and physical evaluation of wrinkle bends before moving on to specific integrity issues. Reference (3) discusses the ability of in-line inspection (ILI) tools to evaluate metal loss in wrinkle bends. Much of what is discussed concerning metal loss assessment also holds for the physical measurement of the shape of a wrinkle bend. Almost all of the current ILI tools can detect the presence of wrinkle bends either directly in the case of a caliper tool or indirectly through the loss of signal due to bounce in the case of a magnetic flux leakage tool. The Baker report states that ILI tools perform reasonably well in detecting metal loss in areas of relatively smooth deformation but not in areas of severe deformation. In areas of severe deformation the sensors will not conform properly to the surface. "Thus, it is possible that severity of metal loss can be accurately reported in pipe containing mild ripples. However, since wrinkles and buckles are more severely deformed than ripples and tend to exhibit areas of extreme pipe wall curvature, the probability of one of the metal loss tools being able to perform well within these discontinuities is relatively low." The same holds true for deformation tools. If the bend is exposed the evaluation is relatively straightforward but may result in relaxing the restraint around the pipe which, as discussed above, could prove detrimental to the integrity of the pipe.

<u>Fatigue</u>

The primary integrity concern with regard to wrinkle bends is the possibility of fatigue failure due to cyclic loads (1, 4, 5, and 6). The wrinkle acts as a stress concentrator for externally applied loads. Also, depending on the strain that went into forming the wrinkle, the process of wrinkling can use up a portion of the strain life of the pipe.

The science of fatigue life prediction has been used extensively in the machinery, automotive, and aerospace industries (7), as well as facility piping and pressure vessel design. These methods center on determining crack initiation life and/or fatigue crack growth life. The crack initiation method is what has been used extensively with regard to wrinkle bends. This method assumes that failure occurs when a crack initiates in the pipe. This approach is conservative. In

the case of high-strain low-cycle fatigue, it may be overly conservative because the time spent initiating and growing the crack is the same order of magnitude (4). Approaches that are used to determine crack initiation are based on stress, strain and damage mechanics. All three approaches have been used to analyze wrinkle bends.

The fatigue analyses of wrinkle bends center on determining a stress/strain concentration factor for the wrinkle and the appropriate model for the fatigue life of the wrinkled pipe. In most cases the stress/strain concentration factor is estimated based on finite element analysis (FEA) and some simplifying scheme used to reduce the FEA results to a closed form. Dinovitzer (4) bases the entire analysis on FEA whereas Olsen estimates a strain concentration factor based on the solution developed by Bilston (8). All of these models do a pretty good job of predicting laboratory test results where the loading is well defined. These laboratory tests do not have the restraint that is typical of a buried pipeline. Also, as described above, the determination of longitudinal loading on an in service pipe is difficult. This is especially true for older pipelines where much of the early history is unknown.

Loss of Longitudinal Load Capacity

We have not been able to find any research into the longitudinal load-carrying capacity of wrinkle bends as defined in the introduction. There has been work done on modern cold field bend pipes (9, 10, and 11). This work notes that the buckle passes through a state that is reminiscent of old wrinkle bends during the process of buckling. Figure C-2 shows a moment-displacement diagram taken from a pipe bending test from Reference (11). The arrow in Figure C-2 points to an unloading and reloading during the test. The important thing to note is that even though the buckle has progressed well past the peak load, the specimen still has significant load capacity. The major concern is that the local strains not exceed the strain capacity of the material so that the pressure integrity is maintained.

Corrosion and Stress Corrosion Cracking

If the coating over the wrinkle is damaged or the pipe is not fully cathodically protected there is the possibility that corrosion will occur on a wrinkle. The Baker Pipe Wrinkle Study (3) suggests evaluating the pressure capacity of corrosion in a wrinkle bend using standard evaluation techniques for corrosion in cylindrical pipe. Their reasoning is that the plastic strains in the wrinkle will tend to "wash out" at the large strains associated with the burst pressure. The Baker report mentions proprietary burst tests on wrinkled pipe specimens that support their approach. The effect of corrosion on the fatigue of a wrinkle is not known but the Baker report makes the statement "Based on the combined experience of the project team and upon

discussions with industry experts, pipeline failures due to fatigue in corroded ripples, wrinkles or buckles could not be identified."

Given the potential for high residual stress in a wrinkle bend it is conceivable that stress corrosion cracking (SCC) could occur in the wrinkle under the proper conditions. The author has not been able to find any references to this in the literature that was reviewed for this project but knows of one case where wrinkle bends were included in the criteria for selecting SCC digs.

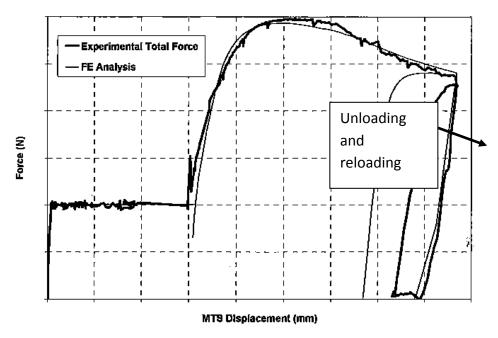


Figure C-2. Moment-displacement diagram from a displacement controlled pipe buckling test taken from Reference (11)

Wrinkle Bend Fatigue Models

Since fatigue is a primary concern with wrinkle bends, this review of prior work was focused on models that have been developed to determine the fatigue life of wrinkle bend pipe. As mentioned previously, the science of determining the fatigue life is well developed. The key to successfully predicting the remaining life of a wrinkle bend is to determine the local stress/strain/damage parameter for the wrinkle and to determine the appropriate fatigue life curve.

A) Olson, Bilston and Murray (6, 8)

The Pipeline Research Council International (PRCI) funded project carried out by Olson was oriented toward developing an acceptance criterion for the ripples that developed in modern high strength pipe during field bending. The project involved the cyclic bend testing of 2 wrinkle specimens and a theoretical model for the fatigue analysis of a wrinkle. The testing will be described in the next section. The analytical effort was based on a load-local strain model for cold field bends developed by Bilston. Bilston's model predicts the strain as a function of the ripple geometry and ripple "shortening" under bending. The strain model was compared to the results of the 2 tests and was found to give reasonably good estimates of the strain in the dent. The stress in the ripple was then determined from the stress strain curve for the pipe and an estimation of the spring-back in the pipe during wrinkle formation. The resulting stress and strain along with the applied stress were used in a damage-life model to determine the fatigue life of the wrinkle. The damage-life model required some modification to explain the results of the two tests. The final model was then used to estimate the damage-life of ripples for a range of pipe geometries and grades. All of the ripples had a height of 1.5 times the wall thickness and a range of length-to-height ratios between 8.2 and 12.8. Olson developed an acceptance criterion for ripples based on this modeling. The ripple is acceptable if it meets the following conditions:

- There is no evidence of cracking.
- There are no creases or sharp features in the ripple, i.e. has a smooth contour.
- Independent of specified minimum yield stress, ripples can be up to 1-1/2 wall thicknesses in height, so long as the wave length-to-height ratio is above 12.
- On a case specific basis, ripples up to 1-1/2 wall thicknesses in height can have a length-to-height ratio less than 12.

No attempt was made to look at ripple heights greater than 1-1/2 wall thicknesses. The stress range used for these analyses was probably much higher than most pipelines would experience (30% specified minimum yield strength and a 60° F temperature change) so the results are conservative. Even with these conditions the minimum predicted life for Grade X52 pipe was

greater than 180,000 cycles. Although the model developed by Olson was for the cold bending of modern high-strength line pipe, the analysis included Grade X52 which incorporates much vintage line pipe with wrinkle bends.

B) Rosenfeld, Hart and Zulfigar (5)

The work performed by Rosenfeld et al. was also oriented toward the field bends in modern high-strength, high diameter/thickness ratio pipe. This project developed an expression for the stress concentration factor (SCF) in a wrinkle based on the ratios of the diameter to wall thickness (D/t), wrinkle height to diameter (d/D), wrinkle wavelength to height (L/d) and wrinkle arc length to circumference (a/C). The equations for the SCF's were based on the regression of a parametric FEA analysis of a range of the ratios described above. The FEA was based on a linear model with a predefined wrinkle built into the mesh. The linear model was used on the assumption that the wrinkle would "shake down" to linear behavior after a few cycles. These analyses cover a much larger range of wrinkle geometries than the Olson study. Separate expressions were developed for wrinkles subject to internal pressure and subject to external bending moments. Since these expressions are simple and could be useful for the evaluation of wrinkle bends in the field, they are given below. The equation for the stress concentration factor for a ripple in a pipe with internal pressure is:

$$SCF_{pressure} = 0.123 \cdot \left(\frac{D}{t}\right)^{1.639} \cdot \left(\frac{d}{D}\right)^{1.910} \cdot \left(\frac{L}{d}\right)^{-0.041} \cdot \left(\frac{a}{C}\right)^{-2.971} \tag{1}$$

The equation for the SCF for a ripple in a pipe that is subject to an external bending moment is:

$$SCF_{bending} = 0.165 \cdot \left(\frac{D}{t}\right)^{1.200} \cdot \left(\frac{d}{D}\right)^{0.810} \cdot \left(\frac{L}{d}\right)^{-0.504} \cdot \left(\frac{a}{C}\right)^{-1.657}$$
(2)

A nonlinear soil spring FEA was utilized to develop an expression for the thermal SCF. This SCF also depends on the bend radius (R) and the bend angle of the wrinkle bend (A) given in degrees of arc. The thermal SCF is:

$$SCF_{thermal} = 92.5 \cdot \left(\frac{D}{R}\right)^{0.637} \cdot \left(\frac{D}{t}\right)^{-0.215} \cdot (A)^{-0.368}$$
 (3)

The stress in the wrinkle is determined by multiplying the nominal applied stress (i.e. longitudinal stress due to pressure for the case of applied pressure) by the SCF. It should be noted that the objective of the project was to develop a criterion for the ripples that form during cold field bending of pipe and that the range of d/L used for the FEA was between 0.067 and 0.111. This may be why this report concludes that the SCF is only weakly dependent on d/L but other authors (2, 12) have found it to be highly dependent on this parameter.

Rosenfeld uses the stress-life curve developed by Markl for whole pipe tests (13). The equation developed by Markl is:

$$0.5 \cdot S \cdot N^{0.2} = C \tag{4}$$

Where,

S is the elastically calculated stress amplitude (i.e. half of the stress range), ksi,

N is the number of cycles until failure, and

C is a constant that equals 245,000 for displacement controlled stresses and equals 163,000 for load controlled stresses.

Equations 1 through 4 were used to predict the results of 3 full scale tests performed under API funding (14) and the two Olson tests described in the last section. The predictions were good except for the second Olson test which was under predicted in terms of fatigue life by a factor of 8, indicating that stresses were over-predicted by a factor of 1.5. Rosenfeld explains this discrepancy by noting that the wrinkle geometries were measured prior to hydrostatic testing; the second specimen exhibited a nonlinear pressure-volume plot well before achieving the maximum pressure, suggesting that the resulting plastic deformation in the wrinkle could have reduced the depth of the wrinkle and therefore the actual cyclical stresses.

Using the analysis procedure Rosenfeld concludes that the following allowances would not be expected to be harmful in pipelines operating under conditions normally encountered in transportation industry:

- shallow ripples having crest-to-trough dimensions up to 1 percent of the pipe OD for gas pipelines operating at hoop stress levels in excess of 47 ksi, increasing to 2 percent of the OD for gas pipelines operating at less than 37 ksi; and
- shallow ripples having crest-to-trough dimensions up to 0.5 percent of the pipe OD for hazardous liquid pipelines operating at hoop stress levels in excess of 47 ksi, increasing to 2 percent of the OD for hazardous liquid pipelines operating at less than 20 ksi.

If the wrinkle geometry is known and the stress levels applied to the pipe can be estimated then Equations 1-4 can be used to directly estimate the life of the wrinkle bend.

It should be noted that Reference (3) uses the same approach for fatigue analysis of wrinkle bends.

C. Leis, Zhu and Clark (1, 2)

The work by Leis et al. is the only one that deals specifically with the integrity management of wrinkle bends in vintage pipe. The fatigue life model is based on a damage parameter given by:

$$D = \frac{\sigma_{\text{max}} \cdot \Delta \varepsilon^{\text{t}}}{2} \tag{5}$$

Where.

D is an energy-based damage parameter,

 σ_{max} is the maximum critical location stress and

 $\Delta \varepsilon^{t}$ is total strain.

The reports use FEA to express the damage parameter D in terms of the ratio of the height to wavelength of the wrinkle (d/L). Specific damage parameters are developed for cycling between pressure levels, pipe diameters to thickness ratios, pipe grades, and operating pressure ranges. This damage parameter is used in conjunction with the following damage-life equation:

$$D_f = 273 \cdot (2N_f)^{-1.02} + 2.1 \cdot (2N_f)^{-0.28}$$
(6)

Where,

D_f is the accumulated damage at failure, and

N_f is the number of half cycles to failure.

Although the basic concept is simple, the use of this approach is hampered by the large number of separate equations for D_f. Also, it is not clear how the different damage parameters should be combined for the many conditions outlined in the report.

Leis et al. draw the following conclusions based on their model:

- wrinkle shape characterized by H/L has been successfully related to fatigue resistance and criteria developed meeting the objectives of this project including the effects of grade, line pipe geometry, and service loading;
- consideration has been given to the effect of service at 72-percent of SMYS as well as to cases where the maximum stress could be as high as 80-percent SMYS, as can occur for some grandfathered lines: depending on the wrinkle's severity and other conditions, operation at the higher stress reduced the service life by as much as a factor of two, all else being equal;
- pitting corrosion can significantly reduce the life of a wrinkle bend, with possible lifereduction indicated up to a factor of about thirty;
- the criteria were validated through successful prediction of full-scale pressure cycling of wrinkle bends and through its successful prediction of the response of ripple-bends produced in modern bending machines reported independently;
- the criteria also were validated through successful prediction of a range of wrinkle bend scenarios from an in-service guillotine rupture through several wrinkles whose severity covered severe through benign, and included the effects of corrosion based on bends removed from service for a variety of reasons;

- the validated criterion can be implemented using data available from field and in-line measurements to characterize d/L, supplemented by file data addressing pipeline design and line pipe properties, wrinkle-bending practices, as well as its construction, operation, and maintenance; where data are uncertain, conservative fallbacks were provided;
- the criteria are simple to use and applicable on a case-specific basis if desired by the user in applications to single wrinkles; multiple wrinkles were independently found to be less severe than otherwise identical single wrinkles; and finally
- the criteria is generic in terms of pressure history, so it can be used for liquid as well as gas pipelines be reference to differences in service.

D) Dinovitzer, Fredji, Lazor and Doblanko (4)

The work by Dinovitzer et al. was oriented toward the formation of buckles and wrinkles that develop in service but the methodology can easily be extended to wrinkle bends. Reference (4) uses an FEA model to simulate the wrinkle and then applies loading to the wrinkled pipe to determine the cyclic strains. The remaining life of the wrinkled pipe is then determined through a strain-life model. It is unlikely that this approach would be used except in rare cases for the evaluation of wrinkle bends but it does serve to illustrate the full spectrum of approaches to the fatigue of wrinkle bends.

Alexander and Kulkarni (12)

Alexander and Kulkarni report using FEA to develop stress concentration factors (SCF) for wrinkle bends. An axisymmetric model was used for the analysis. Although the paper does not specifically state it, the SCF's appear to be based on a linear FEA with the wrinkle built into the initial model. These SCF are given in terms of the pipe diameter to wall thickness (D/t) and the severity ratio (d/L). The equation for the SCF is:

$$SCF_{axial} = 13.497 \cdot \frac{d}{L} + \left[4.975 \cdot \frac{d}{L} - 0.05 \right] \cdot \left[\frac{D_{t}}{50} - 1 \right]$$
 (7)

This stress concentration factor was developed for pressure only. The fatigue life is then estimated using the nominal stress range with the SCF in a fatigue in a stress life fatigue model similar to the Markl model described above.

Experimental Testing of Wrinkle Bends

A) Olson (6)

Olson reports on the testing of 2 wrinkle specimens which were selected from a group of four pipes that were bent during a joint Australian Pipeline Industry Association (APIA)/Line Pipe Research Supervisory Committee (LPRSC) project (6). The first of the two test specimens, labeled Specimen A, was 30-inch diameter, 0.300-inch wall thickness Grade X70 pipe with a 2 shallow, 3 mild and 1 large ripples. The large ripple had a depth of 0.44 inch with a peak-to-peak wavelength of 4.86 inches resulting in an aspect ratio (d/L) of 0.09. The second specimen labeled Specimen B was 36-inch diameter, 0.385-inch wall thickness Grade X65 pipe with a large ripple that was 0.61 inch deep and had a peak-to-peak wavelength of 6 inches resulting in an aspect ratio of 0.10.

The two specimens were pressure tested to simulate a hydrotest and then cyclically loaded in four-point-bending until they failed. Specimen A was hydrotested to 100 percent SMYS and Specimen B was hydrotested to 108 percent SMYS. The two specimens were cyclically loaded in four-point bending. The cyclic loading for Specimens A and B are shown in Table C-2. The strain at the peak of selected wrinkles were measured with strain gauges and compared with the predictions of the Olson model. The comparisons are shown in Table C-3.

B) Kiefner and Alexander (14)

Kiefner and Alexander performed cyclic pressure testing on 3 specimens with buckles that were 1.7, 3.7 and 6.9 percent of the pipe diameter. The aspect ratios for these wrinkles were not reported. The samples were fabricated by cold bending 36-inch diameter, 0.281-inch wall thickness, Grade X52 pipe. The pressure was cycled between 100 psig and 684 psig which results in a nominal stress range of 37,400 psi. The sample with the 6.9 percent buckle failed after 1,086 cycles, the sample with the 3.7 percent buckle failed after 2,791 cycles and the sample with the 1.7 percent buckle did not fail after 44,541 cycles.

C) Leis, Zhu and Clark (2)

Leis et al. report tests that were performed by Columbia Gas on 20-inch diameter, 0.250-inch wall thickness, nominal Grade B and X42 pipe. The report notes that actual test results were more typical of Grade X60 for the Grade B specimens and of Grade X52 for the Grade X42 specimens. The specimens were cycled between 150 and 1,100 psig which resulted in a nominal longitudinal stress range of 3,000 to 22,000 psi. The aspect ratio (d/L) for the wrinkles ranged from 0.229 to 0.766. Figure C-3 shows the results of these tests. The report does not present a table with the actual values for the fatigue lives of the specimens. Based on the test results, these wrinkles can be classified as severe.

Table C-2. Olson wrinkle test specimen cycling stress and number of cycles applied

Specimen	Wrinkle	Maximum stress, psi	Minimum stress, psi	Cycles		
	2-B,2-C and 2-D	57,600	31,250	75,864		
A	Large	49,300	29,525			
	2-B,2-C and 2-D	63,000	31,250	9,133		
	Large	59,300	29,525	, 2,233		
В	Single wrinkle	48,125	27,000	75,000		
	Jingle Willine	56,675 27,000		67,726*		
* Did not fail in wrinkle, girth weld leak at ends of pups						

Table C-3. Comparison of measured strain with predicted strain from Olson tests

			Ripple Peak Strain Range		Ripple Valley Strain Ran	
Ripple	Wave Height	Wavelength	Prediction $\mu\epsilon$	Experiment με	Prediction με	Experiment με
2-D	1.83 mm (0.072 in)	63.8 mm (2.51 in)	+ 486	+468	+1279	+1524
2-4	11.3 mm (0.444 in)	123,4 mm (4.86 in)	-100	-95	+ 1887	+2087
Specimen B	15.5 mm (0.611 in)	152.1 mm (5.99 in)	+33	+115	+ 1444	+1890

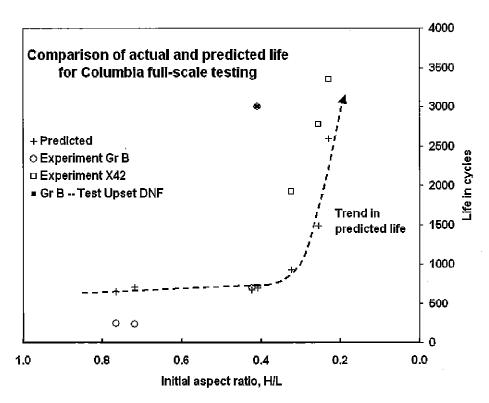


Figure C-3. Columbia Gas wrinkle bend test results

D) Alexander and Kulkarni (12)

Alexander and Kulkarni are the only authors that report tests on actual wrinkle bends pulled from service. Sample EP22 was 22-inch diameter, 0.312-inch wall thickness, Grade X42 pipe that went into service in 1947. Sample EP30 was 30-inch diameter, 0.312-inch wall thickness, Grade X52 pipe that went into service in 1948. A total of 6 specimens were fabricated from the two pipe samples. Half of these specimens were repaired using a composite wrap and the remaining specimens were left as is. The two specimens made from EP30 had 40 percent deep simulated corrosion machined into the specimens. The aspect ratio (d/L) of the wrinkles ranged from 0.093 to 0.132. Table C-4 contains the details on the wrinkles in each specimen. The EP22 specimens were cycled between 100 and 858 psig resulting in a nominal longitudinal stress range of 1,763 to 15,125 psi. The EP30 specimens were cycled between 100 and 779 psig resulting in a nominal longitudinal stress range of 2,885 to 22,471 psi. The upper pressure levels represent 72 percent SMYS. Strain gauges were placed at the peak of each ripple and at 1.5, 3 and 6 inches from the peak. The strain results are shown in Table C-5. The cycles to failure are shown in Table C-6.

Table C-4. Wrinkle measurements for Alexander and Kulkarni tests

Sample	Pipe properties	Wrinkle height (d),	Wrinkle length (L),	d/L	Notes
no.		in.	in		
EP30-1A	30-in. D, 0.312 in. t,	0.662	5	0.132	40%
EP30-1B	X52	0.736	6	0.123	corrosion
EP22-1A	22 in D 0 212 in +	0.558	6	0.093	
EP22-1B	22-in. D, 0.312 in. t, X42	0.728	6	0.121	
EP22-2A		0.570	6	0.095	
EP22-2B		0.712	6	0.119	

Table C-5. Strain measurements from Alexander and Kulkarni tests

Sample	Condition		Wrinkle ial)	3 inches from Wrinkle (Axial)		
•		Δε (με)	$ riangle\sigma$ (ksi)	Δε (με)	∆σ (ksi)	
EP22-1A (unrepaired)	Wrinkle in seam weld	1190	36	979	29	
EP22-1B (repaired)	Wrinkle in seam weld	820 25		703	21	
	reduction composite	31.1 p	ercent	28.2 percent		
EP22-2A (unrepaired)		954	29	1096	33	
EP22-2B (repaired)		757	23	868	26	
	Percent reduction due to composite		20.6 percent		20.8 percent	
EP30-1A (unrepaired)	40 percent corrosion	1960	59	1321	40	
EP30-1B (repaired)	40 percent corrosion	1259	38	1213	36	
	Percent reduction due to composite		35.8 percent 8.2 percent		ercent	

- Notes:

 1. Sample EP22-1 fabricated from 22-in x 0.312-in, Grade X42 pipe
 2. Sample EP22-2 fabricated from 22-in x 0.312-in, Grade X42 pipe
 3. Sample EP30-1 fabricated from 30-in x 0.312-in, Grade X52 pipe

Table C-6. Fatigue test results from Alexander and Kulkarni tests

Sample Number	Pipe Geometry	Grade	Condition	ΔP (psi) (min to max)	Cycles	Notes
EP30-1A	30-inch x 0.312-inch	X52	Unrepaired (40% corrosion)	100-779	19,252	Crack developed in center of wrinkle
EP30-1B	30-inch x 0.312-inch	X52	Repaired (40% corrosion)	100-779	41,171	Crack developed beneath APPW repair
EP22-1A (weld)	22-inch x 0.312-inch	X42	Unrepaired	100-858	42,818	Crack developed in center of wrinkle
EP22-1B (weld)	22-inch x 0.312-inch	X42	Repaired	100-858	55,371	Longitudinal crack developed outside of repair
EP22-2A	22-inch x 0.312-inch	X42	Unrepaired	100-858	93,135	Crack developed in bosset weld (test aborted)
EP22-2B	22-inch x 0.312-inch	X42	Repaired	100-858	93,135	Crack developed in bosset weld (test aborted)

Discussion and Recommendations

The Summary and Conclusions section of Reference (1) contains many good observations with regard to wrinkle bends some of which will be repeated here before beginning our discussion:

- Early field practices evolved significantly from the 1930's through the 1950's. Important
 dates include 1942, when "smooth bending" machines were first used and the early 1950's,
 when track-mounted integral "vertical bending" machines are fund in commercial service;
- Wrinkle bend quality and uniformity varied considerably even when essentially equivalent methods were being applied, which was likely due to several factors including the wide variety of wrinkle-bending methods used, material stability and limited process control when hot bending, and perhaps most importantly quality control imposed by the pipeline contractor and/or operator;
- Because wrinkle bend practices and quality control varied, some showed uniform wrinkle geometries spaced at regular intervals while others were essentially complex shaped buckles that significantly deformed the local pipe geometry;
- Although wrinkle bends were phased out in the early 1950's, many pipeline systems still contain wrinkle bends so it is important to understand failure incidence and their causes. Incident experience indicates the rate is dropping, a trend typical of other material and construction related incidents, whereas when incidents have occurred they have done so where pressure cycling and local soil stability were major causative factors;
- Wrinkle shape and size were indicated to be critical parameters in characterizing wrinkle bend integrity, with shape being important because it relates to curvature, which in turn relates to strain, while parameters defining size. The wrinkle length (pitch) and height (amplitude) of the wrinkle were found to act as surrogates for curvature at the crown (apex) of the wrinkle;
- Strains at and around the crown of the wrinkle increase as pressure increases, with endfixity (restraint imposed on bends by the soil) being important, suggesting rehabilitation that significantly relaxes the restraint can cause potentially worsen circumstances;
- Cyclic loading including the effects of pressure and thermal variations is the major causative factor in field failures. Corrosion pitting can significantly reduce the serviceable life where it occurs whereas secondary loading due to soil/support stability can also be a factor.

Since the use of wrinkle bends was a common practice up through the 1950's and many miles of 1950's vintage pipe are still in service, it is safe to say that a large number of wrinkle-bent pipe joints are still in service. This is problematic in several respects. First, the quality of these

bends varies greatly. As discussed in Reference (1) the quality of these bends most likely vary on a spread to spread basis. Second, current ILI technology cannot accurately evaluate these bends (3). The presence of wrinkle bends can be inferred from an ILI log but its use to evaluate the quality of the wrinkle is limited. ILI can be used to measure relatively smooth wrinkle but the more severe the wrinkle the less likely ILI will be able to accurately determine its shape and depth due to sensor lift off. Finally, the act of digging up a wrinkle bend to evaluate it can actually do more harm than good because of the change in the constraint around the bend. The reduction in constraint can result in larger stress cycles than were occurring before the excavation which in turn will affect the fatigue life of the bend.

Leis discussed the possibility that digging up a wrinkle bend can result in a reduction of the restraint around the bend which in turn can increase its susceptibility to cyclic loading in Reference (2). As a result of Leis' observation, our recommendation is to not disturb existing wrinkle bends unless a specific threat is identified. These threats are:

- 1. Aggressive longitudinal cycling of the line,
- 2. Ground movement, i.e. mine subsidence or landslides,
- 3. Corrosion and
- 4. Stress corrosion cracking.

The levels at which each of these threats become a concern needs to be quantified. At the most basic level, there will also have to be an upper bound to the wrinkle severity in the threat quantification. If the bend is disturbed (i.e. dug up) then care should be taken to make sure that the restraint conditions are returned to the original conditions before the bend was excavated. This can be done by immobilizing the bend in the soil environment, for example by mixing cement in with the soil before backfilling or by the use of a flowable fill, or by making the bend itself more rigid by installing repair sleeves over the wrinkles. The Alexander and Kulkarni report investigated the use of composite sleeves to improve the fatigue resistance of wrinkle bends (12).

There seems to be a general consensus that a small amount of wrinkling is acceptable. Rosenfeld (5) finds wrinkles up to 2 percent of the diameter acceptable with restrictions on the maximum nominal hoop stress. The results of the Alexander and Kulkarni (12) testing suggest that this could be as high as 2.5 percent with the restriction that the aspect ratio is less than 0.13. This range of depths and aspect ratios should be measurable by a caliper tool. The acceptable limits will require some restrictions on the longitudinal stress. ASME B31.8-2007 allows longitudinal loads as high as 90 percent SMYS and ASME B31.4-2006 allows longitudinal loads as high as 64.8 percent SMYS on restrained pipe (15, 16). These loads are a combination of pressure, thermal expansion and additional bending and axial loads. The B31 levels will most

likely be unacceptable if the stress concentration in the wrinkle is taken into account. For this reason we recommend that a load cycle analysis should per performed as part of any wrinkle integrity management plan. There also needs to be some means of classifying the severity of the load cycles in order to determine if stress cycling is an integrity threat. An expansion on the limits set by Rosenfeld could be used as a starting point for this classification.

Appendix C - References

- 1. Zhu, XK, Leis, BN and Clark, EP. Integrity Management for Wrinkle bends and Buckles. s.l.: US DOT PHMSA Contract No. DTRS56-05-T-003, Project No. G005189, December 2007.
- 2. Leis, BN, Zhu, XK and Clark, EB. Criteria to Assess Wrinkle bend Severity For Use in Pipeline Integrity Management. s.l.: PRCI, August 2007.
- 3. Michael Baker Jr., Inc. TTO Number 11, Integrity Management Program Delivery Order DTRS56-02-D-70036, Pipe Wrinkle Study. s.l.: Department of Transportation Research and Special Programs Administration, October, 2004.
- Development and Validation of a Pipeline Buckle and Wrinkle Assessment Model.
 Dinovitzer, A, Fredj, A, Lazor, R, Doblanko, R. Calgary, Alberta, Canada: ASME, IPC2004.
 IPC04-0254.
- 5. Rosenfeld, MJ, Hart, JD and Zulfiqar, N. Acceptance Criteria for Mild Ripples in Pipeline Field Bends. s.l.: PRCI, 2008. L51994.
- 6. Olson, RJ. Evaluation of the Structural Integrity of Cold Field-Bent Line Pipe. s.l.: PRCI, 1996. L51740.
- 7. Society of Automotive Engineers. Fatigue Design Handbook. Warrendale, Pa. : SAE, 1988. ISBN 0-89883-011-7.
- 8. Bilston, P and Murray, N. The Role of Cold Field Bending in Pipeline Construction. Houston, Texas: PRCI, September 26-29, 1993. L51680.
- 9. Full-Scale Testing of Cold Bend Pipes. Sen, M, Cheng, JJR, Murray, DW, Zhou, J, Adams, K, Yoshizaki, K, Fukuda, N, Como, M and Cerelli, E. Calgary, Alberta, Canada: ASME, 2004. IPC04-0743.
- 10. Simulation of Cold Bends by Finite element Method. Behbahanifard, M, Cheng, JJR, Murray, DW, Zhou, J, Adams, K, Yoshizaki, K, Fukuda, N, Como, M, and Cerelli, E,. Calgary, Alberta, Canada: ASME, 2004. IPC04-0744.

- 11. Development of a Pipeline Wrinkle Material Ultimate Limit State-Full Scale Modeling. Semiga, V, Tiku, S, Dinovitzer, Aaron, Zhou, J, Sen, M. Calgary, Alberta, Canada: ASME, IPC2008. IPC2008-64620.
- 12. Evaluating the Effects of Wrinkle Bends on Pipeline Integrity. Alexander, C and Kulkarni, S. Calgary, Alberta, Canada: IPC2008 ASME, September 29-October 3, 2008. Paper no. IPC2008-64039.
- 13. Markl, ARC. Fatigue Tests of Piping Components. Transactions. 1952, Paper No. 51, PET-21.
- 14. Kiefner, JF and Alexander, CR. Effects of Smooth and Rock Dents on Liquid Petroleum Pipelines, Phase 2. s.l.: Addendum to API Publication 1156, September 3, 1999.
- 15. American Society for Mechanical Engineers. ASME B31.8 Gas Transmission and Distribution Piping Systems. New York: ASME, 2007.
- 16. American Society of Mechanical Engineers. ASME B31.4 Pipeline Transportation Systems for Liquid Hydrocarbons and Other Liquids. New York, NY: ASME, 2006.
- 17. Development and Validation of a Pipeline Buckle and Wrinkle Assessment Model. Dinovitzer, A, Fredj, A, Lazor, R and Doblanko, R. Calgary, Alberta, Canada: s.n., 2004. IPC04-0254.

[END OF REPORT]